



# LUND UNIVERSITY

## Co-assembly of proteins and lipids

### From lipodiscs to amyloid aggregates

Frankel Willén, Rebecca

2021

*Document Version:*

Publisher's PDF, also known as Version of record

[Link to publication](#)

*Citation for published version (APA):*

Frankel Willén, R. (2021). *Co-assembly of proteins and lipids: From lipodiscs to amyloid aggregates*. Lund University, Faculty of Science, Department of Chemistry.

*Total number of authors:*

1

#### General rights

Unless other specific re-use rights are stated the following general rights apply:

Copyright and moral rights for the publications made accessible in the public portal are retained by the authors and/or other copyright owners and it is a condition of accessing publications that users recognise and abide by the legal requirements associated with these rights.

- Users may download and print one copy of any publication from the public portal for the purpose of private study or research.
- You may not further distribute the material or use it for any profit-making activity or commercial gain
- You may freely distribute the URL identifying the publication in the public portal

Read more about Creative commons licenses: <https://creativecommons.org/licenses/>

#### Take down policy

If you believe that this document breaches copyright please contact us providing details, and we will remove access to the work immediately and investigate your claim.

LUND UNIVERSITY

PO Box 117  
221 00 Lund  
+46 46-222 00 00

The background of the slide is a black field filled with numerous small, semi-transparent circles. These circles are arranged in several distinct, roughly parallel diagonal bands that run from the top-left towards the bottom-right. Each band is composed of circles of a single color, and the colors transition through a rainbow spectrum from top-left to bottom-right: red, orange, yellow, green, cyan, blue, and magenta. The circles are slightly offset from each other, creating a sense of depth and movement.

# Co-assembly of proteins and lipids

## From lipodiscs to amyloid aggregates

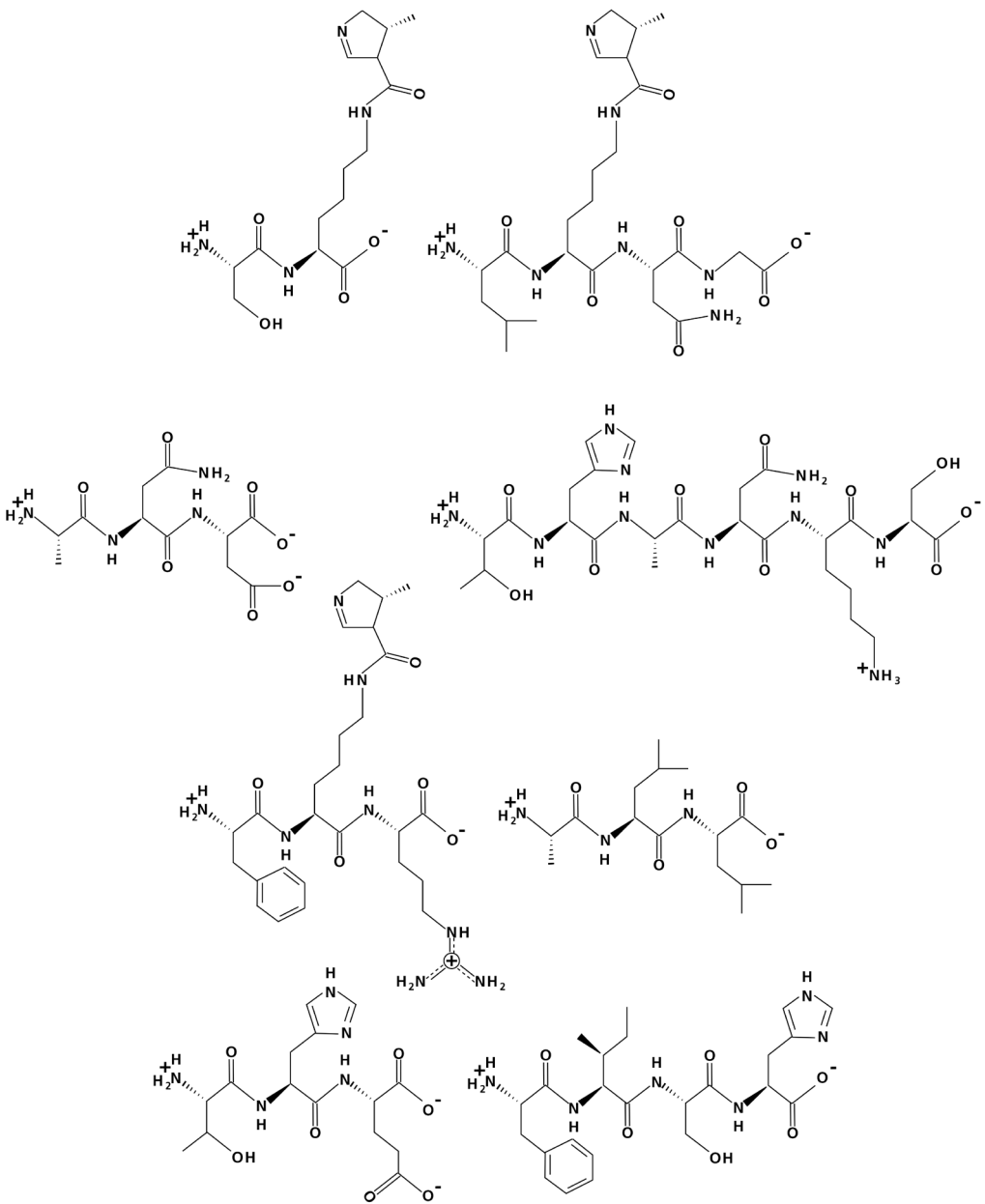
REBECCA FRANKEL WILLÉN | DEPARTMENT OF CHEMISTRY | LUND UNIVERSITY





ISBN: 978-91-7422-842-7

Physical Chemistry  
 Faculty of Science  
 Lund University



# Co-assembly of proteins and lipids

From lipodiscs to amyloid aggregates

by Rebecca Frankel Willén



**LUND**  
UNIVERSITY

Thesis for the degree of Doctor of Philosophy

To be presented, with the permission of the Faculty of Science of Lund University, for public criticism  
in lecture hall KC:A on Friday, 2021-11-12 at 09:15.

Thesis advisors:

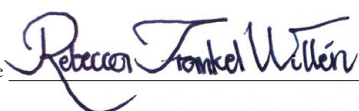
Prof. Sara Linse  
Prof. Emma Sparr

Faculty opponent:

Assoc. Prof. Elin Esbjörner Winters

<b>Organization</b> <b>LUND UNIVERSITY</b> Division of Physical Chemistry Box 124 SE-221 00 LUND Sweden		<b>Document name</b> <b>DOCTORAL DISSERTATION</b>	
		<b>Date of disputation</b> 2021-11-12	
<b>Author(s)</b> Rebecca Frankel Willén		<b>Sponsoring organization</b>	
<b>Title and subtitle</b> Co-assembly of proteins and lipids: From lipodiscs to amyloid aggregates			
<b>Abstract</b> <p>Assemblies of different molecules is a prevalent phenomenon in nature, and crucial in biological life. Most of the biological assemblies are co-assembled composites, made up from several different components, either of the same biomolecular type or a combination of different ones. Knowledge regarding amyloid fibril structure and the mechanism behind it has been elucidated through the development of protocols rendering reproducible kinetic data in buffer systems. The vast majority of these studies have been focused on the self-assembly of the peptides. However, peptide aggregation <i>in vivo</i> typically occurs in a more complex environment, surrounded by either different proteins or lipids, or both.</p> <p>In this thesis, different systems of self- and co-assembly has been studied. We use both top-down and bottom-up approaches to explore the aggregation of the A<math>\beta</math> peptide involved in Alzheimer's disease. In an <i>in vivo</i>-like environment (cerebrospinal fluid, CSF), we find that A<math>\beta</math>42 fibrillisation is retarded, but occurring through the same mechanism as inferred for A<math>\beta</math> in a buffer system, including the secondary nucleation mechanism. We further investigated the possible effectors of CSF and the minimum component requirement to replicate the effect from this environment through the creation of HDL-like particles. This was achieved through the development of methodology for the expression and purification of ApoA-I from a CSF-free host. Further, the effect of A<math>\beta</math> in the presence of both lipids and other proteins was investigated. We find that we can replicate the effect seen in CSF by the HDL-like particles, in that we see a retarding effect, more pronounced when ApoA-I is added in lipid-free form. We also find that ApoA-I will readily aggregate, and the morphology of the aggregates depend on both extrinsic and intrinsic factors. Finally, we investigated if the inhibiting effect of DNAJB6 on A<math>\beta</math> fibril formation could be reproduced by an isolated chaperone domain. We found that the C-terminal domain of DNAJB6 – suggested to be involved in peptide binding after dimerization – will inhibit the secondary nucleation of A<math>\beta</math> fibril formation as opposed to the intact protein which inhibits the primary nucleation.</p>			
<b>Key words</b> amyloid, A $\beta$ 42, apolipoprotein A-I, aggregation, high-density lipoprotein, DNAJB6, Alzheimer's disease, protein-lipid interactions			
<b>Classification system and/or index terms (if any)</b>			
<b>Supplementary bibliographical information</b>		<b>Language</b> English	
<b>ISSN and key title</b>		<b>ISBN</b> 978-91-7422-842-7 (print) 978-91-7422-843-4 (pdf)	
<b>Recipient's notes</b>		<b>Number of pages</b> 218	<b>Price</b>
		<b>Security classification</b>	

I, the undersigned, being the copyright owner of the abstract of the above-mentioned dissertation, hereby grant to all reference sources the permission to publish and disseminate the abstract of the above-mentioned dissertation.

Signature 

Date 2021-10-04

# Co-assembly of proteins and lipids

From lipodiscs to amyloid aggregates

by Rebecca Frankel Willén



**LUND**  
UNIVERSITY



**Author photo:** Picture by Daniel Frankel Willén

**Cover illustration front:** By author. ThT fluorescence curves of A $\beta$ 42 in CSF (**paper I**)

**Cover illustration back:** Picture by author. Thank you, Douglas Adams.

Quote: C. Buck, J. Lee. Frozen 2. Walt Disney Studios Motion Pictures, 2019

Paper I © 2019 The Authors. Published by Springer Nature.

Paper II © 2021 The Authors. Published by Elsevier Inc.

Paper III © by the Authors (Manuscript unpublished)

Paper IV © by the Authors (Manuscript unpublished)

Paper V © by the Authors (Manuscript unpublished)

Pages I-73 © Rebecca Frankel Willén 2021

Faculty of Science, Division of Physical Chemistry

ISBN: 978-91-7422-842-7 (print)

ISBN: 978-91-7422-843-4 (pdf)

Printed in Sweden by Media-Tryck, Lund University, Lund 2021



Media-Tryck is an environmentally certified and ISO 14001:2015 certified provider of printed material. Read more about our environmental work at [www.mediatryck.lu.se](http://www.mediatryck.lu.se)

**MADE IN SWEDEN** 

*One day when I'm old and wise  
I'll think back and realise  
That these were all completely normal events*

# Contents

List of publications	viii
My contribution to the papers	x
Acknowledgements	xii
Populärvetenskaplig sammanfattning på svenska	xiv
<b>1 Introduction</b>	<b>1</b>
<b>2 Studied biomolecules</b>	<b>5</b>
2.1 Proteins and peptides . . . . .	5
2.2 Lipids . . . . .	8
2.3 Cerebrospinal fluid . . . . .	9
<b>3 Biomolecular assemblies</b>	<b>11</b>
3.1 Protein assembly . . . . .	12
3.2 Lipid assembly . . . . .	19
3.3 Co-assembly of proteins and lipids . . . . .	20
<b>4 Misfolding diseases</b>	<b>23</b>
4.1 Amyloidosis . . . . .	23
4.2 Alzheimer's Disease . . . . .	24
<b>5 Methodologies and experimental techniques</b>	<b>27</b>
5.1 Top down versus bottom up . . . . .	27
5.2 Protein expression and preparation . . . . .	28
5.3 Chromatographic methods . . . . .	28
5.4 Sodium Dodecyl Sulphate – PolyacrylAmide Gel Electrophoresis (SDS-PAGE) . . . . .	31
5.5 Mass spectrometry (MS) . . . . .	31
5.6 Dynamic Light Scattering (DLS) . . . . .	32
5.7 Circular Dichroism (CD) spectroscopy . . . . .	33
5.8 Fluorescence spectroscopy . . . . .	35
5.9 Kinetic analysis . . . . .	36
5.10 Cryogenic-transmission electron microscopy (cryo-EM) . . . . .	37

<b>6</b>	<b>Summary of thesis work</b>	<b>39</b>
6.1	Paper I . . . . .	40
6.2	Paper II . . . . .	42
6.3	Paper III . . . . .	44
6.4	Paper IV . . . . .	46
6.5	Paper V . . . . .	48
<b>7</b>	<b>Concluding remarks</b>	<b>51</b>
7.1	Outlook . . . . .	52
	<b>References</b>	<b>53</b>
	<b>Scientific publications</b>	<b>75</b>
	Paper I: Autocatalytic amplification of Alzheimer-associated A $\beta$ 42 peptide aggregation in human cerebrospinal fluid . . . . .	77
	Paper II: Purification and HDL-like particle formation of apolipoprotein A-I after co-expression with the EDDIE mutant of N <sup>pro</sup> autoprotease	101
	Paper III: Retardation of A $\beta$ 42 fibril formation by apolipoprotein A-I and recombinant HDL particles . . . . .	125
	Paper IV: On the aggregation of apolipoprotein A-I . . . . .	147
	Paper V: Effects on aggregation kinetics and interactions with A $\beta$ 42 of the functionally important C-terminal region of the anti-amyloid chap- erone DNAJB6 . . . . .	167

# List of publications

This thesis is based on the following publications, referred to by their Roman numerals:

- I **Autocatalytic amplification of Alzheimer-associated A $\beta$ 42 peptide aggregation in human cerebrospinal fluid**  
R. Frankel\*, M. Törnquist\*, G. Meisl, O. Hansson, U. Andreasson, H. Zetterberg, K. Blennow, B. Frohm, T. Cedervall, T.P.J. Knowles, T. Leiding, S. Linse  
*Commun. Biol.*, 2019, 2, 365
- II **Purification and HDL-like particle formation of apolipoprotein A-I after co-expression with the EDDIE mutant of N<sup>Pro</sup> autoprotease**  
R. Frankel, K. Bernfur, E. Sparr, S. Linse  
*Protein Expr. Purif.*, 2021, 187, 105946
- III **Retardation of A $\beta$ 42 fibril formation by apolipoprotein A-I and recombinant HDL particles**  
R. Frankel, E. Sparr, S. Linse  
*Manuscript*
- IV **On the aggregation of apolipoprotein A-I**  
R. Frankel, E. Sparr, S. Linse  
*Manuscript*
- V **Effects on aggregation kinetics and interactions with A $\beta$ 42 of the functionally important C-terminal region of the anti-amyloid chaperone DNAJB6**  
N. Österlund, R. Frankel, A. Carlsson, D. Thacker, M. Karlsson, V. Matus, C. Emanuelsson, S. Linse  
*Manuscript*

\*These authors contributed equally to the article.

All papers are reproduced with permission of their respective publishers.

## List of publications not included in thesis

- I    Controlled protein mediated aggregation of polystyrene nanoplastics does not reduce toxicity towards *Daphnia magna*  
R. Frankel, M.T. Ekvall, E. Kelpsiene, L.-A. Hansson, T. Cedervall  
*Environ. Sci. Nano*, 2020, 7(5), 1518-1524

## **My contribution to the papers**

### **Paper I: Autocatalytic amplification of Alzheimer-associated A $\beta$ 42 peptide aggregation in human cerebrospinal fluid**

I participated in the planning of all experiments. I performed the experiments following kinetics at different CSF concentrations, and participated in those at constant CSF concentrations. I participated in the testing of the automated dispenser. I participated in the seeding experiments. I participated in data analysis of all experiments. I wrote first draft of the manuscript – as well as edited according to co-authors' and reviewers' comments – with MT and SL.

### **Paper II: Purification and HDL-like particle formation of Apolipoprotein A-I after co-expression with the EDDIE mutant of N<sup>pro</sup> autoprotease**

I planned the experiments. I performed all the expression and purification experiments, as well as the DLS measurements. I participated in the mass spectrometry and cryo-EM experiments. I analysed the data with co-authors. I wrote the first draft of the manuscript and edited it according to co-authors' comments.

### **Paper III: Retardation of A $\beta$ 42 fibril formation by apolipoprotein A-I and recombinant HDL particles**

I planned the experiments with ES and SL. I performed all the experiments, with technical support for the NMR and cryo-EM experiments. I analysed all data with co-authors. I wrote the first draft of the manuscript, and edited it together with ES and SL.

### **Paper IV: On the aggregation of apolipoprotein A-I**

I planned the experiments with ES and SL. I did all the sample preparation. I performed all experiments, with technical support for the cryo-EM experiments. I analysed all data with co-authors. I wrote the first draft of the manuscript, and edited it together with ES and SL.

**Paper V: Effects on aggregation kinetics and interactions with A $\beta$ 42 of the functionally important C-terminal region of the anti-amyloid chaperone DNAJB6**

I prepared the A $\beta$ 42 samples for some of the experiments. I participated in discussions regarding the data analysis. I participated in writing the manuscript with co-authors.

# Acknowledgements

I wish I had the eloquence needed to express how I feel about the amazing people I have had the great pleasure of meeting during my studies. Alas, I do not, so please enjoy my inelegant rambling:

First and foremost, I would like to thank my supervisors **Sara** and **Emma**. You are truly the best supervisors I could have asked for (if I'd known what to ask for) and if someday I am half the researcher you two are, I would consider myself lucky. **Sara**, special thanks for keeping me around, first as a master student and then as a PhD student, and for being an inspiration daily. **Emma**, for our weekly meetings, your insights, and for being there throughout my time here (especially for trying to ensure I preserved some sort of sanity while writing this thesis).

Thanks to all past and present members - and members by extension - of SSLRGLU. **Andreas**, thank you for the images of DNAJB6 constructs; **Birgitta**, for the A $\beta$ , and all the talks about Vittsjö; **Caroline**, for making our group meetings a little more entertaining; **Christin**, for all your energy; **Dev**, for always answering my questions with a lot of patience, and for our awesome gingerbread house; **Egle**, for being a great office- and teaching-mate; **Eimantas**, for all the help around the lab; **Emil** and **Max**, for bringing new energy and ideas into the group; **Kalyani**, for your wonderful tips both in cooking and in the lab (but not both at the same time); **Karin Åkerfeldt**, for being such a wonderful companion whenever you visited our lab; **Katja**, for your positive energy, and always helpful hand; **Lei**, for the interesting conversations in the lab, both related and unrelated to the work being done; **Martin**, for everything you do around the lab, and all the inventory we did together; **Mattias**, I guess everything (for the collaboration on the CSF paper, for all the coffee, all our talks, and your weird and excellent humour); **Tanja**, for the A $\beta$ , and for returning to us (or at least to the premises); **Thom**, for keeping the instruments running, and for inventing competitions to try to keep our collective energy going through the dark months of the pandemic; **Tinna**, for being a wonderful office-mate, and a wonderful friend; **Veronica**, for the times we've shared a cubicle and laughter.

Further gratitude to all co-authors and collaborators, including the COLIBRI-group **Alexandra, Daniel T., Kasia, Marija, Peter J., Simon E., Ulf O.** Thanks to **Cecilia, Maja, Nicklas, and Vanessa**, for the work with DNAJB6, and to our collaborations in Cambridge, Gothenburg, and Lund for the CSF paper. Thank you, **Anna Stadner** for your work as institution representative, **Maria Lövgren** for all your administrative work, and **Paula** for your help with the thesis.

To the past and present people at CMPS for the nice time since I started here. 6 years passed remarkably fast. Thanks should be given to many, for making the divisions run somewhat smoothly, and for making the coffee breaks so very enjoyable. An honorary mention to **Camille, Filip, Helin, Lovisa, Mads, Mathias, Mikael, Simon, Susanna, Sven, Tommy, Veronika, Magnus, and Maryam**, for all our conversations and for trying to make the workplace as great as possible. A special shout-out to **Bella**, for the lovely times in the sunshine; **CJ**, for the mutual criticism; **Samuel**, for being my ally down in the course lab; and **Olof**, for keeping my caffeine levels and mood elevated.

To the **DnD group** – both permanent and visiting members – for your company, your weird and clever (and not so clever) ideas, and for constantly keeping me on my toes.

To my amazing family: my parents – **Lotta and Krister** –, my siblings – **Simone, Sandra, Natali, Jonatan, Ronja** – and my nephew – **Vide**. You are the best family one could ever hope for, flaws and all. I love you incredibly. My grandparents – **Antje and Fredrik** – for your immense support. My family in-law, **Olle, Maria, Malin and Anders**. I'm so happy to know you all.

To my dear **Momo**, for choosing me... every single night. There's no rest for the wicked. **Daniel**, my incredible husband, for simultaneously keeping me afloat and down to earth; for doing your PhD at the same time as I, so we always knew what the other was going through; for being your awesome self. Du är bäst.

Slutligen skulle jag skulle vilja tacka **mig själv**, för visad hänsyn.

# Populärvetenskaplig sammanfattning på svenska

Kroppen består av flera olika sorters molekyler, vars samverkan är ansvarig för så gott som alla livsnödvändiga funktioner. Fetter – eller lipider – är en av dessa sorter, som bland annat ansvarar för cellstrukturer, värmeisolering, och energireserver. En annan typ av biomolekyler är proteiner, som bland annat ansvarar för funktioner såsom muskelupbyggnad, katalys, transport av andra molekyler, etc.

För att proteiner ska fungera har de specifika strukturer som hjälper till att upprätthålla deras funktioner. Kroppen har olika sätt att säkerställa att strukturerna är de rätta; dock händer det att dessa felsökande system misslyckas. Flera sjukdomar bottenar i felveckningar av protein, eller visar i vart fall symtom där felveckade proteiner upptäcks. Ett par exempel av dessa är Alzheimers sjukdom, vår tids vanligaste demenssjukdom, samt amyloidos som innebär proteininlagring i olika delar av kroppen. Gemensamt för dessa sjukdomar är just bildandet av *amyloider*, som består av proteiner som har gått samman för att skapa långa trådar – eller fibrer – som bland annat kan leda till att celler och vävnader i kroppen förstörs.

I min avhandling har jag studerat hur olika biomolekyler påverkar bildandet av fibrerna från ett visst protein, nämligen amyloid- $\beta$  ( $A\beta$ ), som är involverad i Alzheimers sjukdom. Även om man inte har kunnat säkerställa exakt vad som händer i kroppen vid felveckningen och det som startar Alzheimers sjukdom, så har man genom att studera proteinet i laboratoriemiljö kunnat komma fram till hur det bildar fibrerna, om den enbart får reagera med sig själv. Därför har vi nu studerat vad som händer när man tillsätter andra molekyler som den kan reagera med – vilka delar av processen kommer de att påverka?

För att göra detta har vi använt oss av två tillvägagångssätt, som kallas *top-down* och *bottom-up*. I det första så man blandningen av molekyler som är av intresse, tillsätter proteinet, och studerar vad som händer. Således får man reda på vilken effekt blandningen har; däremot är det svårt att urskilja vilken av alla sorters molekyler som är

ansvarig för effekten. Då kommer bottom-up till användning: i detta tillvägagångssätt tillsätter man istället en molekylsort i taget, och på så sätt ser man vilken påverkan dessa har var för sig. Det tar lite längre tid, och leder inte till det exakta förhållandet som sker i den komplexa miljö som kroppen består av, men det är fortfarande framgångsrikt för att kunna förstå samverkan mellan olika molekyler.

En av dessa komponenter som vi har studerat kallas ”det goda kolesterolet”, eller *high density lipoprotein*-partiklar, som består av en skara proteiner och lipider. Vi har studerat hur enskilda komponenter av HDL-partiklarna kan påverka A $\beta$  fibrillisering, för att undersöka huruvida dessa kan vara ansvariga för den effekt vi såg i ett mer komplext system.

Slutligen har vi även undersökt ett annat protein – DNAJB6 – som har visat sig vara oerhört effektiv på att förhindra bildandet av just A $\beta$  fibrer. Även här använder vi ett bottom-up tillvägagångssätt, då vi är intresserade av vad som händer när man bara använder vissa delar av proteinet: kan man behålla samma funktion om enbart vissa delar används?

# Abbreviations

AD	Alzheimer's disease
ApoA-I	Apolipoprotein A-I
APP	Amyloid precursor protein
A $\beta$	Amyloid- $\beta$
BBB	Blood-brain barrier
CD	Circular dichroism
Cryo-EM	Cryogenic-transmission electron microscopy
CSF	Cerebrospinal fluid
CTD	C-terminal domain of DNAJB6
DLS	Dynamic light scattering
DMPC	1,2-dimyristoyl-sn-glycero-3-phosphocholine
DNA	Deoxyribonucleic acid
DNAJB6	DnaJ homolog subfamily B member 6 isoform b
DTT	Dithiothreitol
EDTA	Ethylenediaminetetraacetic acid
<i>E. coli</i>	<i>Escherichia coli</i>
FAD	Familial Alzheimer's disease
GuHCl	Guanidine hydrochloride
HDL	High-density lipoprotein
HIC	Hydrophobic interaction chromatography
IEC	Ion-exchange chromatography
IMAC	Immobilized metal ion affinity chromatography
MS	Mass spectrometry
PAGE	Polyacrylamide gel electrophoresis
POPC	1-palmitoyl-2-oleoyl-sn-glycero-3-phosphocholine
SDS	Sodium dodecyl sulphate
SEC	Size-exclusion chromatography
ThT	Thioflavin T
UV	Ultraviolet

Abbreviation		Name
A	Ala	Alanine
C	Cys	Cysteine
D	Asp	Aspartic acid
E	Glu	Glutamic acid
F	Phe	Phenylalanine
G	Gly	Glycine
H	His	Histidine
I	Ile	Isoleucine
K	Lys	Lysine
L	Leu	Leucine
M	Met	Methionine
N	Asn	Asparagine
P	Pro	Proline
Q	Gln	Glutamine
R	Arg	Arginine
S	Ser	Serine
T	Thr	Threonine
V	Val	Valine
W	Trp	Tryptophan
Y	Tyr	Tyrosine
O	<i>Pyl</i>	<i>L-Pyrrolysine*</i>
U	<i>Sec</i>	<i>L-Selenocysteine*</i>

*\*not coded by the human genome*



# CHAPTER 1

---

## Introduction

---

The human body is made up of four major types of biomolecules. These are carbohydrates, nucleic acids, proteins, and lipids<sup>1</sup>; however, the two latter kinds are the main focus in this thesis. In the body, proteins are responsible for several functions, including catalysing reactions, replicating DNA, acting as signal molecules, transporting different biomolecules, providing structure in tissues and cells, to mention a few. Proteins are made up of amino acids, i.e. organic compounds containing a carbon atom, with attached side chain (R-group), in between an amino ( $-\text{NH}_2$ ) and a carboxyl ( $-\text{COOH}$ ) end. To link the residues together, the amino group and the carboxyl group will form a covalent bond called the peptide bond. This chain of amino-, hydrocarbon- and carboxyl groups throughout the linked amino acid residues is also called the backbone of the protein. The side chains differ depending on the amino acid, giving rise to a number of different characteristics; often, the side chains are charged, hydrophilic, or hydrophobic<sup>2</sup>. In total, there are 22 different proteinogenic amino acids, 20 of which can be coded from the human genome<sup>3</sup>. Typically, a protein consisting of few ( $<50$ ) amino acids is referred to as a peptide, though the specific definition of a peptide may vary.

The sequence of residues that make up a protein is also called the primary structure of said protein. The secondary structure is the conformation of the backbone, stabilised by interactions between the backbone of the different residues; they can orient into  $\alpha$ -helices,  $\beta$ -sheets, or random coils<sup>2,4,5</sup>. The 3D-structure of the protein is called the tertiary structure; this is also referred to as a protein fold. Finally, if a protein is made up of several different chains, this combination is called the quaternary structure (figure 1.1).

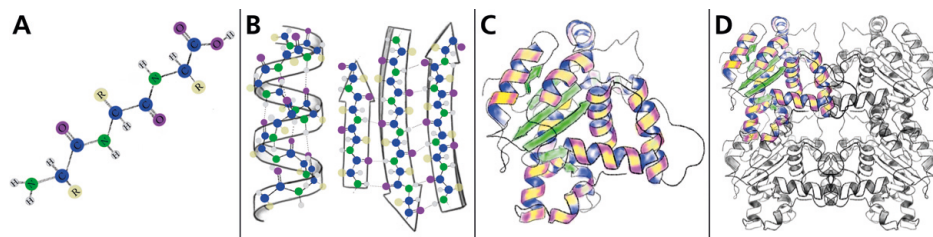


**Figure 1.1:** The different structures of a protein. A) A short chain of amino acids. B) Secondary structures, with an  $\alpha$ -helix to the left and  $\beta$ -sheets to the right. C) A representation of the tertiary structure. D) The quaternary structure of a protein made up of four chains. In A) and B), blue represents carbon, grey is hydrogen, purple is oxygen, and beige is the R-group. In C) and D), these colours are aesthetic choices.

The second kind of biomolecule focused on in this thesis is lipids. There are different kinds of lipids, such as fatty acids, sterols, hydrophobic vitamins, glycerides, and phospholipids. Phospholipids are amphiphilic molecules, meaning that they have one hydrophilic and one hydrophobic part. The hydrophilic part – also called the headgroup – is typically charged and/or polar of different sizes depending on lipid. The hydrophobic part – also called the tail – is comprised of hydrocarbon chains with varying length and saturation. This versatility of the headgroup and tail gives rise to various characteristics of the phospholipids. *In vivo*, they primarily make up the core of all biological membranes, both in cells and organelles. *In vitro*, the ability of phospholipids to self-assemble into different structures is extensively exploited. Some application areas include when creating a model membrane, for instance when studying lipid-interactions or creating a native-like environment for membrane proteins<sup>1,6</sup>, as well as in cosmetics, food industry, and drug delivery (for instance the mRNA vaccine against COVID-19, as reviewed<sup>7</sup>).

Furthermore, in the body, lipids can act as energy reserve through fatty deposits, as hormones, nutrients, and as important parts of axons and dendrites in the brain<sup>1,6</sup>. Lipids are used in the entire body in humans; therefore, the transport of lipids in the body is important, often accomplished through interactions with proteins in lipoprotein particles.

## Lipoprotein particles

The interactions between lipids and proteins *in vivo* is clearly demonstrated in the lipoprotein particles. There are five different kinds of lipoprotein particles in blood plasma and other extracellular fluids, typically classified by their density and protein:lipid ratio<sup>8</sup>: chylomicrons, very-low-density lipoprotein (VLDL), intermediate-density lipoprotein (IDL), low-density lipoprotein (LDL), and high-density lipoprotein (HDL). The latter is the smallest and densest, due to its high protein:lipid ratio. The lipo-

protein particles may either be discoidal (figure 1.2) or spherical, depending on their composition<sup>9–11</sup>. The primary function of all these lipoproteins is to transport lipids – often triglycerides, cholesterol, and phospholipids – either from the liver to the appropriate cells, or to the liver to metabolise. HDL particles – which have been the focus of this thesis – are the only lipoprotein particles present in cerebrospinal fluid (CSF) due to their high density and corresponding smaller size<sup>10,12</sup>. Studies have shown a correlation between the concentration of lipoprotein particles in blood and the disease atherosclerosis, where build-up of plaque in the arteries can lead to coronary artery disease, stroke, peripheral artery disease, or kidney problems<sup>1,8,11</sup>. LDL has sometimes been referred to as the “bad” lipoprotein, as the studies have shown a correlation between increased LDL concentration and the progression of atherosclerosis; HDL, on the other hand, has similarly been referred to as the “good” lipoprotein, as its increased concentration is correlated with the regression of the disease<sup>1,8,11</sup>.

Another feature shared by all classes of lipoproteins is the presence of apolipoproteins, a class of proteins responsible for stabilising the dispersed lipid components of the lipoprotein particles, as well as transporting the particles and acting as ligands for cell-surface receptors. They can also act as co-factors for certain enzymes involved in the lipid transport<sup>13</sup>.

Depending on the class of apolipoprotein the particle contains, their function will be different. Two of these apolipoproteins are apolipoprotein A-I (ApoA-I) and apolipoprotein E (ApoE), both of which are present in the HDL particles. In blood plasma ApoA-I is the major protein component, while in CSF HDL consist of approximately the same amount of both these proteins<sup>10,12,13</sup>. ApoA-I will be further discussed in chapter 2.1.1.

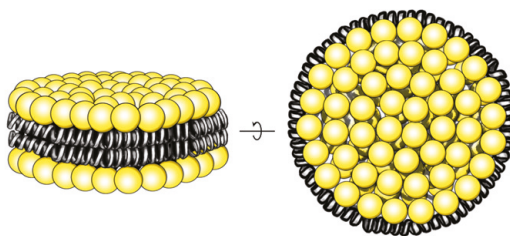


**Figure 1.2:** Schematic model of a lipodisc. The lipids have formed into a circular bilayer, with the hydrophobic hydrocarbon chains shielded from water by the circumference belt of dimeric,  $\alpha$ -helical ApoA-I.

## General objectives of the thesis

The intricate play between self-assembly and co-assembly of biomolecules are in focus in this thesis, with particular interest in the study of protein interactions *in vitro*. Protein interactions were investigated either with other protein molecules – of the same or different kind – or in the presence of lipids. The proteins of particular interest was amyloid- $\beta$  (A $\beta$ ), apolipoprotein A-I (ApoA-I), and DNAJB6. In **paper I**, we investigated the net-effects from interactions of A $\beta$ 42 in the presence of a body fluid,

and whether this “*ex vivo*”-like complex system could be studied. In **paper III** and **V** we sought to investigate the individual components from previous studies – ApoA-I in the presence and absence of lipids, as well as DNAJB6 –, and if the effects seen can be replicated when using as simple system as possible. In **paper II**, we developed a protocol to recombinantly produce ApoA-I. This product was further used in **paper IV** where we investigated ApoA-I’s propensity to aggregate into globular and amyloid aggregates, and how the propensity is influenced by intrinsic and extrinsic factors.

### Studied biomolecules

---

## 2.1 Proteins and peptides

### 2.1.1 Apolipoprotein A-I

ApoA-I is one of the most abundant protein in HDL particles in blood and CSF<sup>14, 15</sup> and mediator for – among other things – its function in the reverse cholesterol transport, i.e. from arteries to the liver for catabolism<sup>16</sup>. Approximately 5% of circulating ApoA-I is found in lipid-free or lipid-poor form<sup>17, 18</sup> while the rest is found bound to lipids in the lipoprotein particles. Moreover, ApoA-I has other protective properties, as displayed through its anti-inflammatory, antioxidant, and anti-thrombotic effects<sup>19</sup>. It also acts as a cofactor to the lecithin:cholesterol acyltransferase (LCAT), allowing for the esterification of free cholesterol and HDL particle remodeling<sup>20, 21</sup>. Additionally, ApoA-I has been found to be a major constituent of the protein corona formed around nanoparticles after addition to blood plasma<sup>22–24</sup>. ApoA-I has also been discussed as a possible protector against neurological diseases<sup>18</sup>, as an increase of ApoA-I was correlated with a decreased risk of dementia<sup>25</sup>, and as it has been found to interact with the A $\beta$  peptide<sup>26, 27</sup> (**paper III**).

ApoA-I consists of 243 amino acid residues, converted from the slightly longer proapoA-I<sup>28</sup>. Mutations in its sequence are related to different forms of amyloidosis – where amyloid plaques are deposited in various organs in the body<sup>17, 29, 30</sup> and further discussed in chapter 4.1 – as well as atherosclerosis<sup>17, 18</sup>. Two of these mutants were used in this thesis work: one where a glycine residue has been substituted for an arginine at position 26 (G26R, also called the Iowa mutation<sup>31</sup>, used in **paper II**),

and one where a lysine residue at position 107 has been deleted (K107 $\Delta$ , also called the Helsinki mutation<sup>32,33</sup>, used in **paper II** and **IV**).

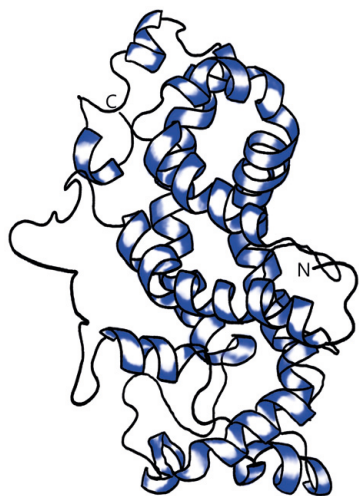


**Figure 2.1:** Model of an ApoA-I monomer, adapted from Zhang *et al.*<sup>34</sup>.

to readily interact with lipids. In HDL particles, ApoA-I is suggested to dimerise and encircle the lipids by forming a belt in contact with the phospholipid tails<sup>41</sup> (figure 1.2).

In this thesis, ApoA-I has been studied, both in terms of its interaction with A $\beta$  when in lipid-free or lipid-rich form (**paper III**), and its self-assembly (**paper IV**). Also, as ApoA-I has been found to be prone to protease degradation<sup>42</sup>, we developed a protocol for the expression of ApoA-I in *E. coli* using the protective tag EDDIE<sup>43</sup> (**paper II**).

### 2.1.2 Amyloid- $\beta$

Another protein circulating in the body is the A $\beta$  peptide, present in body fluids – including cerebrospinal fluid (CSF) and blood serum<sup>44–47</sup> – and neuronal synapses<sup>48</sup>. It is derived from the amyloid precursor protein (APP), a transmembrane glycoprotein expressed from the *APP* gene located on chromosome 21<sup>49</sup>. APP is present in, among other tissues, neuronal synapses, and A $\beta$  is produced from proteolytic cleavage of APP by  $\beta$ - and  $\gamma$ -secretase;  $\beta$ -secretase has its cleavage site at the N-terminus of A $\beta$ , while  $\gamma$ -secretase cleavage will define the C-terminal length of the peptide (figure 2.2). Several length variants of A $\beta$ , of between 37 to 49 amino acid residues, coexist in the body, with A $\beta$ 40 being the most common in healthy individuals<sup>50,51</sup>.

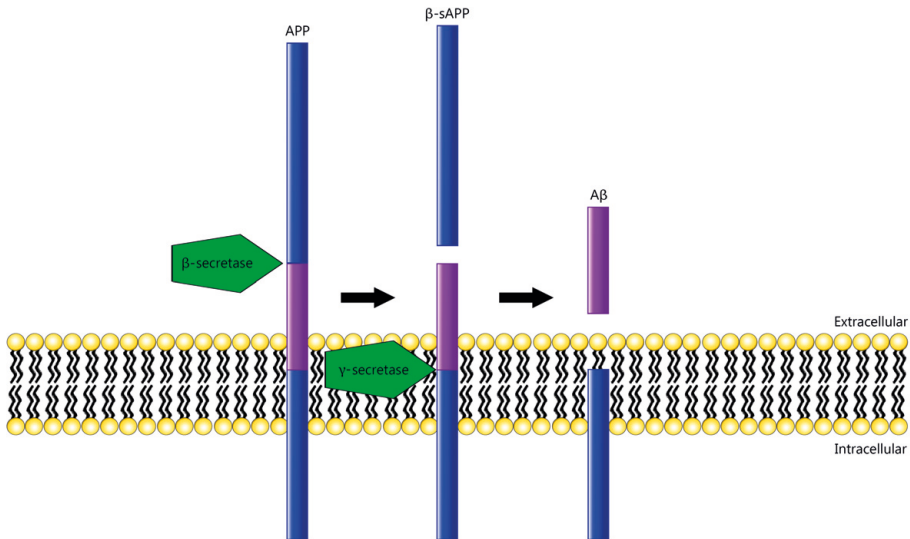


Figure 2.2: The creation of A $\beta$  from APP by cleavage of  $\beta$ - and  $\gamma$ -secretase.

The function of A $\beta$  is still unknown. It has been observed to increase hippocampal long-term potentiation (i.e. a kind of sustained change in synaptic plasticity, suggested to be related to learning and memory<sup>1</sup>); however, this effect was only seen at low concentrations, as higher concentrations of A $\beta$  had the opposite effect. It is thereby implied that A $\beta$  has an effect on synaptic plasticity and memory in a biphasic manner<sup>48,52</sup>. Additionally, it has been shown to have some protective properties, through its antioxidant<sup>53</sup> and anti-microbial activity<sup>54</sup>, and improved recovery after spinal cord injuries in mice<sup>55</sup>.

The dysfunction of A $\beta$  is more known, as it is famously involved in Alzheimer's disease (AD) as amyloidal plaque deposits. Zagoraski *et al.*<sup>56</sup> had this to say regarding A $\beta$ :

The phrase 'the peptide from hell' has been used frequently to describe amyloid- $\beta$ , particularly by the bench chemist or biologist who must endeavor on a day-to-day basis with its ever-changing demeanor. Biophysical and biological studies of the A $\beta$  peptides, especially studies with the less soluble and more pathogenic 42 residue A $\beta$ (1-42), are plagued by many difficulties. The major difficulty relates to the ease in which the A $\beta$  peptides aggregate and precipitate.

AD and amyloids will be further discussed in chapter 4.2 and chapter 3.1.2, respectively.

### 2.1.3 DNAJB6

The final protein studied in this thesis is DNAJB6 isoform b (hereafter referred to as simply DNAJB6), belonging to the DNAJ/Hsp40 heat shock protein family<sup>57,58</sup>. As one of the two major classes of chaperones, the DNAJ family is involved in a wide range of cellular events, including protein folding<sup>59</sup>, Hsp70 activity regulation<sup>60,61</sup>, and protein complex assembly<sup>62</sup>. DNAJB6 has been shown to interact with a variety of proteins, such as polyglutamine (polyQ)<sup>63–66</sup>,  $\alpha$ -synuclein<sup>67,68</sup>, and A $\beta$  length variants 40<sup>69</sup> and 42<sup>70,71</sup>, to mention a few.

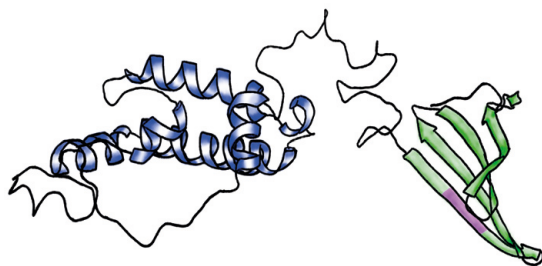


**Figure 2.3:** DNAJB6 monomer, based on PDB entry 6U3R. Blue is the N-terminus, where the J-domain is located. Green is the C-terminus. Purple is the most conserved S/T-rich region.

presented<sup>73</sup>. At the N-terminus, the protein has a highly conserved domain called the J-domain, consisting of approximately 70 amino acids folded into four  $\alpha$ -helices<sup>74</sup>. The C-terminal domain, on the other hand, has been suggested to consist of four  $\beta$ -strands, folded into a  $\beta$ -sandwich (figure 2.3). This region also contains part of the conserved S/T-rich region mentioned. The dimeric structure of DNAJB6 proposes a cleft between the two subunits; this cleft, lined with the S/T-residues, has been suggested as a potential site for peptide binding<sup>73</sup>.

DNAJB6 has been studied in **paper V**, where different constructs of the C-terminal domain (CTD) were designed to investigate the domain's potential effect on A $\beta$  fibril formation, and whether smaller fragments of the domain would interfere with fibrillisation in the same manner as full-length DNAJB6.

## 2.2 Lipids

Three lipids have been used in this thesis: two phospholipids and a sterol, shown in figure 2.4. The first phospholipid is 1,2-dimyristoyl-sn-glycero-3-phosphocholine (DMPC), meaning it consists of a phosphocholine headgroup, with two C14 tetradecanoyl (myristoyl) acyl groups making up the tail. The second phospholipid,

1-palmitoyl-2-oleoyl-glycero-3-phosphocholine (POPC), have the same headgroup as DMPC but different hydrocarbon chains: one C16 palmitoyl acyl group and one C18 oleoyl acyl group. The difference in chain composition can lead to different properties and influence self-assembly, which will be discussed further in chapter 3.2. *In vitro*, both are utilised in biophysical studies requiring model lipid membranes and in lipid disc formation; *in vivo*, POPC has been detected as one of the abundant PC species in the human body<sup>75</sup>.

The sterol included in this thesis is cholesterol. Cholesterol is present in all animal cells, acting as precursor of many important molecules, such as steroids and vitamins. Cholesterol is very hydrophobic, and is therefore insoluble in water. It is, however, solubilised at rather high concentration in phospholipid structures (as reviewed<sup>76</sup>). It is therefore transported in the body by lipoprotein particles, both in plasma and in CSF.

## 2.3 Cerebrospinal fluid

Returning to the role of proteins and lipids in the body; above is described the different proteins and lipids studied in this thesis, but how does this relate to the situation *in vivo*? In addition to the separate components, we have also worked with the complex mixture of molecules that is a body fluid, namely cerebrospinal fluid (CSF). CSF is used in **paper I**, but more on that later.

CSF is a clear, extracellular body fluid surrounding the brain and spinal cord, as well as filling the ventricles in the brain<sup>1,77</sup>. In healthy adults, the CSF volume is 90 to 200 mL<sup>78</sup>, and is derived from blood plasma but has a lower protein content and different electrolyte levels<sup>79</sup>. It is connected to the blood-brain barrier (BBB), which controls which solutes enter CSF, thereby also the brain. CSF contains a variety of biomolecules, such as salts, proteins, lipids, etc. that play critical roles in many physiological processes<sup>79</sup>. It contains approximately 150 to 450 mg/L total proteins<sup>79,80</sup>; most of the proteins in CSF originates from blood plasma<sup>77</sup>, but are lower in concentration. Some of the above-mentioned studied molecules exist in

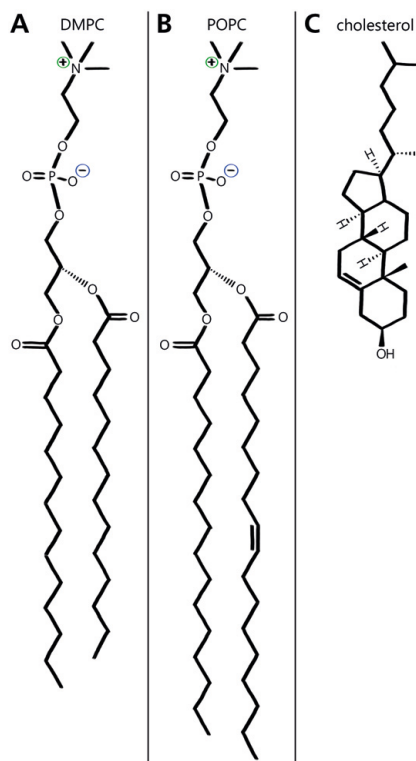


**Figure 2.4:** The structures of the three lipids used in this thesis: A) DMPC, B) POPC, and C) cholesterol

CSF, where it is possible that they interact; studies separating CSF components based on size found that A $\beta$  interacts with apolipoproteins A-I, E and J, as well as cholesterol<sup>81</sup>, all of which are commonly engaged in HDL particles in CSF<sup>10, 82–84</sup>. Regarding DNAJB6, on the other hand, a literature search revealed no record of it being detected in CSF; whether this is because no one has investigated it or that it does not exist in CSF is not certain. However, DNAJB6 is expressed intracellularly in the brain, and therefore its localisation in the brain is not dependent on transport across the BBB.

### Biomolecular assemblies

---

Simplified, biomolecular assemblies can be divided into two categories: self-assemblies and co-assemblies. Both the rate of formation as well as their structures may be of great importance for their function. Self-assembly corresponds to a composite involving one single component, either in terms of folding or aggregation. Co-assembled composites, on the other hand, are made up from several different components. In this chapter, these assemblies will be discussed with focus on the aforementioned biomolecules. The self-assembly will be discussed with particular focus on amyloid structure and formation. Co-assemblies will be discussed either as protein-protein assemblies, or as protein-lipid assemblies.

#### 3.0.1 Protein folding

Most proteins will gain a function that is biologically relevant by adapting a certain conformation. This conformation may include only a single polypeptide chain, or several of either the same or different kinds. The main forces guiding protein stability are the hydrophobic effect and the conformational entropy of the polypeptide chains. The hydrophobic effect is the tendency of nonpolar hydrophobic molecules to cluster together in aqueous solutions. It is governed by the hydrogen bonding network of water: if a hydrophobic molecule is present in an aqueous environment, the hydrogen bonding network of the water will be disrupted, and instead has to form a cage structure around the dissolved hydrophobic molecules, which involves an entropy cost<sup>85</sup>. The hydrophobic effect is considered the major driving force in protein folding<sup>86</sup>. The main opposing force is the protein's conformational entropy. This stems from the fact that folding – and self-assembly – results in a protein becoming more restricted, and

thereby loses conformational energy mostly due to the peptide backbone rigidity<sup>87</sup>. The hydrophobic effect and the entropy, while opposing, are similar in magnitude<sup>88</sup>. While the native state of a protein is often the most thermodynamically stable structure of a protein under physiological conditions<sup>89</sup>, this stability is only marginal, and much weaker than covalent or ionic bonds<sup>88</sup>. Therefore, the protein folding, structure and stability will be noticeably modulated by changes in solution conditions.

How a newly synthesised amino acid chain folds into its native state depends on its amino acid sequence<sup>90</sup>. This discussion was ongoing already in the 1930's, and further developed in the 1960's with the discovery of the reversibility of protein folding and its implication of a thermodynamically stable native state<sup>91</sup>. From this, one can infer that protein folding is a search for the lowest free energy, and a spontaneous process on the sub-second time scale. *In vivo*, the protein folding can also be assisted by chaperones, assuring the correct folding into its native state. The unfolded state of the protein will be in equilibrium with the native state, though the unfolded population may be low in native conditions. Folding and unfolding of proteins are important ways of regulating biological activity.

## 3.1 Protein assembly

### 3.1.1 Protein aggregation

If aggregation occurs depend both on the solubility of the protein and the total concentration of the monomers (thermodynamic stability). The kinetic stability of the the system against aggregation will also depend on the intermolecular interactions, including van der Waals' interactions, electrostatic interactions, and entropic repulsion<sup>85</sup>. Van der Waals' interactions describe the sum of relatively short-ranged attractive forces between dipoles (either polar, or induced/non-polar). These interactions will always be attractive for the same kind of particles. Electrostatic interactions are more long-ranged. They correspond to the interactions between two charged objects, and can be either attractive or repulsive depending on the charge distribution. Finally, an entropic repulsion may arise if the number of accessible configurations of the protein chain is fewer when molecules become more constricted.

As the protein folding process is a search for the lowest free energy state, it is possible that the native state corresponds to a *local* free energy minimum in the free energy surface, considering that assembly may lower the global free energy<sup>92,93</sup>. Protein aggregation may be triggered by alternative folding of the protein, which can affect both its solubility and the intermolecular interactions. If a protein misfolds, it changes its secondary and/or tertiary structure. As the native state of a protein is only

marginally stable, changes in extrinsic or intrinsic factors may have a large impact on the stability of the protein, and on the equilibrium of the folded and unfolded states. These changes may increase the population of unfolded protein, in turn possibly leading to aggregation as the exposed hydrophobic patches of the protein may interact with those of other unfolded proteins<sup>88</sup>. These aggregated states exist in several forms, such as more unstructured and amorphous, but also more structured states such as the amyloid structure.

### 3.1.2 Amyloids

#### Structure

Amyloids are supramolecular and rigid structures, existing both *in vivo* and *in vitro*. In the 1830s, Schleiden introduced the term amyloids – or “starch-like”, from the Latin word for starch *Amylum* – to describe botanical starch fibrils<sup>94</sup>. In the 1850s, Virchow discovered *in vivo* amyloid deposits by iodine staining of liver and spleen samples during autopsy; as iodine staining was thought to exclusively stain starch, Virchow applied Schleiden’s term to these as well<sup>94,95</sup>. Even though the amyloid deposits have been shown to have minimum carbohydrate content, the name stuck<sup>94,96</sup>. In 1922, Congo red was introduced as stain for the tissue containing amyloid deposits, and found to exhibit apple-green birefringence when studied using microscopy with polarised light, and has been used frequently since<sup>96,97</sup>. Additional dyes have also been introduced in order to study amyloids, such as thioflavin T<sup>98</sup> and oligothiophenes<sup>99,100</sup>. Using transmission electron micrographs of amyloids, the fibrillar structure was confirmed<sup>101</sup>.

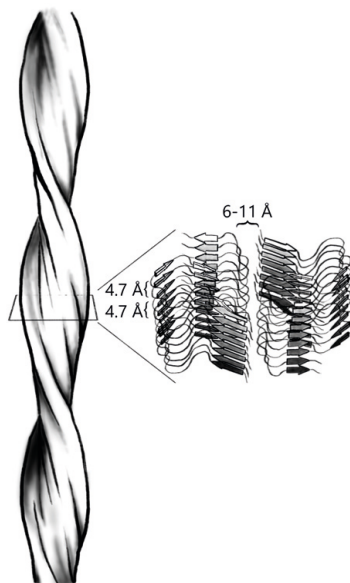


**Figure 3.1:** Schematic of a typical amyloid fibril. From the cross-section of the fibril, the typical cross- $\beta$  structure is demonstrated as well, where two  $\beta$ -sheets are stacked next to each other with the typical distance of 6-11 Å. The distance between the  $\beta$ -sheets stacked on top of each other – 4.7 Å – is also marked.

Today more is known about the fibrillar structure, and the polymorphism existing in amyloid structures of the same protein<sup>102–107</sup>. Generally, amyloid fibrils are defined by their thread-like, twisted structures; they have cross- $\beta$  structure, where  $\beta$ -sheets are stacked with the polypeptide chains perpendicular to the fibril axis<sup>108</sup> in repeating substructure units<sup>109</sup>. From X-ray diffraction, the spacing between  $\beta$ -

strands within a sheet has been determined to be 4.7-4.8 Å<sup>4</sup>, and the spacing between the β-sheets 6-11 Å<sup>110, 111</sup> (figure 3.1). The length of the fibrils differ, but are typically long (>1 μm) and thin (10 nm)<sup>112, 113</sup>.

*In vitro*, a large number of proteins have shown the ability to form amyloids under different conditions, enough to infer it to be a generic feature for all polypeptide chains<sup>90, 114</sup>. As these proteins are non-homologous and are made up of different amino acid sequences, this general feature implies that fibril formation is instead driven by the hydrophobic effect and backbone interactions, and is limited by steric hindrance of side-chains when the protein assumes β-sheet formation<sup>115</sup>.

## Formation

While the ability to form amyloid fibrils may be generic, the propensity to do so under given circumstances vary significantly between different peptides and proteins. It often depends on the physicochemical attributes of the given sequence, such as hydrophobicity, charge, and β-sheet propensity<sup>90, 116, 117</sup>. Therefore, both extrinsic factors – such as pH<sup>118</sup>, ionic strength<sup>119, 120</sup>, and temperature<sup>121, 122</sup> – and intrinsic factors – such as point-mutations<sup>118, 123</sup>, oxidation<sup>124–127</sup>, other post-translational modifications<sup>128–133</sup>, or proteolysis<sup>134, 135</sup> – may have a large effect on the amyloid formation propensity.

Amyloid deposits have been found in several human illnesses. In order to understand how these are formed, it is important to investigate the entire process of formation, not only the start- and end-states. After identification of the different processes, it would hopefully also be possible to detect ways to interfere with the specific steps. So how are the amyloid fibrils formed? The first and slowest phase involve the formation of oligomers, which is monomers coming together to form small aggregates. As the creation of a surface is related to an unfavourable free energy cost – as related to the entropic repulsion described above –, these aggregates are innately unstable<sup>85</sup>. Therefore, the growth of the aggregates will on average be slower than their dissolution<sup>122</sup>. However, if the aggregate reaches a certain critical size, the aggregate will – through one or several conversion steps – switch to form a nucleus and from this on growth is favoured. This creation of a more fast-growing nucleus is referred to as primary nucleation (figure 3.2A). By addition of more monomers to the nucleus, the fibril will grow through elongation (figure 3.2B), which has a lower energy barrier than the primary nucleation and therefore proceeds at a higher rate<sup>122, 136</sup>. It is possible for fibrils to form through only primary nucleation and elongation; however, amyloid formation typically involves a mechanism requiring a more complex model to describe its aggregation pattern.

The initial phase is called the lag phase, where little fibril formation can be detected (above the signal-to-noise ratio of most bulk methods); however, this is followed by a rapid growth acceleration, possibly due to the already formed fibrils catalysing the rate of additional fibril formation. Fragmentation, where the cleavage of a fibril creates new ends where elongation may occur, has been suggested as one such mechanism. Another way to generate new fibril ends is secondary nucleation, where the fibril surface acts as a catalyst for the formation of new fibrils (figure 3.2C). This secondary nucleation process is associated with a much lower energy barrier than primary nucleation and leads to an autocatalytic process with rapid multiplication of the number of aggregates. Through the development of experimental protocols using quiescent (non-shaking) conditions, the secondary nucleation for A $\beta$ 40<sup>137</sup>, A $\beta$ 42<sup>118,119,138</sup>, and  $\alpha$ -synuclein<sup>139</sup> – to mention a few – could be identified. The role of the different processes could be elucidated through kinetic experiments starting from several monomer concentrations, as the monomer concentration dependence will be different depending on the mechanisms.

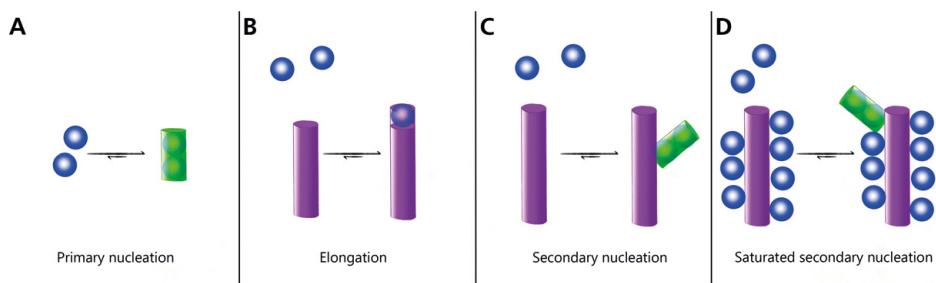


**Figure 3.2:** Sketches of the different mechanistic steps of  $\beta$  fibril formation. A) Primary nucleation. B) Elongation. C) Secondary nucleation. D) Saturated secondary nucleation.

### Rate equations of aggregation kinetics

As the most prevalent peptide in this thesis – A $\beta$ 42 – has been shown to undergo this secondary nucleation process, the following formulation in mathematical terms will focus only on these relevant steps, and not on other secondary processes, such as fragmentation.

During fibril formation, at a given time  $t$ , the system will contain:

$m(t)$  – the concentration of free monomers

$M(t)$  – the mass concentration of fibrils

$P(t)$  – the number concentration of fibrils

Starting from a pure monomer solution, both  $P(t)$  and  $M(t)$  will be zero, and  $m(t)$  will be the initial concentration of free monomers ( $m(0)$ ). The primary nucleation process can then be described through:

$$\frac{\delta P}{\delta t} = k_n m(t)^{n_c} \quad (3.1)$$

where  $k_n$  is the primary nucleation rate constant and  $n_c$  is the primary nucleation reaction order.

While this will conversely reduce the concentration of free monomers and increase the fibril mass, this contribution is small enough to be neglected. Instead, the process mainly contributing to the fibril mass and reducing the concentration of free monomers is elongation, described by:

$$\frac{\delta M}{\delta t} = k_+ m(t) P(t) \quad (3.2)$$

$$\frac{\delta m}{\delta t} = -k_+ m(t) P(t) \quad (3.3)$$

where  $k_+$  is the elongation rate constant.

Finally, the production of new fibrils through secondary nucleation is described as:

$$\frac{\delta P}{\delta t} = k_2 m(t)^{n_2} M(t) \quad (3.4)$$

where  $k_2$  is the secondary nucleation rate constant and  $n_2$  is the secondary nucleation reaction order. These equations all contribute to the fibril formation process over time. By looking at the influence of the different microscopic steps, we can investigate the effect on the overall process. It should be noted that both  $k_+$  and  $k_2$  only report on the net rate of formation of growth competent species; if several stages of oligomerisation and rearrangement occur, it is not detailed in this model.

In the end, in order to quantify the contributions of the different microscopic processes to the time evolution of fibril mass, and in turn determine the individual rate constants, an analytical solution in the form of a single master equation has been derived<sup>140</sup>:

$$\frac{M(t)}{M_\infty} = 1 - \left( \frac{B_+ + C_+}{B_+ + C_+ e^{\kappa t}} \cdot \frac{B_- + C_+ e^{\kappa t}}{B_- + C_+} \right)^{\frac{k_\infty^2}{\kappa k_\infty}} e^{-k_\infty t} \quad (3.5)$$

where

$$\begin{aligned}
\lambda &= \sqrt{2k_+k_n m(0)^{n_c}} \\
\kappa &= \sqrt{2k_+k_2 m(0)^{n_2+1}} \\
B_{\pm} &= (k_{\infty} \pm \tilde{k}_{\infty})/(2\kappa) \\
C_{\pm} &= \pm \lambda^2/(2\kappa^2) \\
k_{\infty} &= \sqrt{2\kappa^2/[n_2(n_2+1)] + 2\lambda^2/n_c} \\
\tilde{k}_{\infty} &= \sqrt{k_{\infty}^2 - 4C_+C_- \kappa^2}
\end{aligned}$$

Individual rate constants can be estimated by fitting this equation and expansions of it, to experimental data. Thereby, it is also possible to investigate how the rate constants change when applying different conditions to the system, or how additives will affect the aggregation mechanism. This is facilitated by the online platform Amylofit, where large data sets can be uploaded and analysed using global fits of the models<sup>141</sup>. Global kinetic analysis will typically reveal changes on the products of the rate constants, i.e. either  $k_+k_n$  (primary nucleation) or  $k_+k_2$  (secondary nucleation). To separate the rate constants, for instance to determine the effect solely on elongation, more experiments are needed. This is done in **paper V**, where heavily seeded experiments – where elongation is prominent – are used to estimate values for  $k_+$  and thereby  $k_2$ .

### Saturated secondary nucleation

There are instances – such as for A $\beta$ 40<sup>137</sup>, and for A $\beta$ 42 at pH 7.4<sup>118</sup> and at high ionic strength<sup>119</sup> – when secondary nucleation has been observed to saturate. One possible explanation is that the rate limiting step is the conversion and dissociation of the oligomers from the fibril surface (figure 3.2D). This will make the rate of secondary nucleation depend on monomer concentration in a manner similar to Michaelis-Menten kinetics, since an enzyme-substrate complex is formed prior to catalysis<sup>142</sup>. In this saturated secondary nucleation case, the effective rate of formation of new aggregates through secondary nucleation is:

$$\frac{\delta P}{\delta t} = k_2 M(t) \frac{m(t)^{n_2}}{1 + \frac{m(t)^{n_2}}{K_M}} \quad (3.6)$$

where  $k_2$  is the secondary nucleation rate constant,  $n_2$  is the secondary nucleation reaction order, and  $K_M$  is the saturation constant for secondary nucleation.

Subsequently, the master equation is adapted to:

$$\frac{M(t)}{M_\infty} = 1 - \left(1 - \frac{M(0)}{M_\infty}\right) \cdot \left(\frac{B_+ + C_+}{B_+ + C_+ e^{\kappa t}} \cdot \frac{B_- + C_+ e^{\kappa t}}{B_- + C_+}\right)^{\frac{k_\infty^2}{\kappa k_\infty}} e^{-k_\infty t} \quad (3.7)$$

where

$$\begin{aligned} \lambda &= \sqrt{2k_+ k_n m(0)^{n_c}} \\ \kappa &= \sqrt{2m(0)k_+ \frac{m(0)^{n_2} k_2}{1 + m(0)^{n_2}/K_M}} \\ B_\pm &= \frac{(k_\infty \pm \tilde{k}_\infty)}{(2\kappa)} \\ C_\pm &= \frac{k_+ P(0)}{\kappa} \pm \frac{k_+ M(0)}{2m(0)k_+} \pm \frac{\lambda^2}{2\kappa^2} \\ k_\infty &= 2k_+ P_\infty \\ \tilde{k}_\infty &= \sqrt{k_\infty^2 - 2C_+ C_- \kappa^2} \end{aligned}$$

In **papers I and III**, this model was found to well describe the fibril formation of A $\beta$ 42 as it occurred in the regime where saturated secondary nucleation is the most prominent nucleation step. Attempts to fit other models (as described elsewhere<sup>140,141</sup>) to the data were also done, but these failed to describe the data as well as the saturated secondary nucleation model.

### 3.1.3 Amyloid formation in the presence of other proteins

When introducing a new component to the system, it might interfere with different steps in the protein aggregation process. This could be due to the added component associating with the aggregating protein, thus forming co-assembled aggregates.

Many proteins have been suggested to inhibit amyloid formation. Examples include some from the apolipoprotein class, where ApoE as well as ApoA-I interact with A $\beta$ <sup>21,143</sup>. When it comes to chaperones, several kinds have been reported to play a role in preventing A $\beta$  aggregation and fibril formation<sup>143</sup>. One that has received increased attention is the chaperone domain Brichos<sup>144</sup>, shown to bind to fibril surfaces, and thereby effectively prevent secondary nucleation in A $\beta$  fibril formation<sup>145,146</sup>. Furthermore, the chaperone DNAJB6 has been shown to prevent both polyQ<sup>63</sup> and A $\beta$  fibrillisation<sup>69,70</sup>. This inhibition by DNAJB6 occurs already at sub-stoichiometric molar ratios of chaperone to peptide, indicating favorable binding to A $\beta$  (as opposed to being free in solution). It has been shown to interact with fibrillar and oligomeric structures rather than monomeric forms of the amyloid peptide.

Furthermore, the largest inhibitory effect by DNAJB6 was demonstrated through a reduced primary nucleation in the fibril formation process, dependent on the previously mentioned S/T-residue motif located in the CTD of the chaperone<sup>69,70</sup>.

In this thesis, protein-amyloid co-assemblies have been studied regarding ApoA-I and the chaperone DNAJB6 and their respective inhibitory effect of A $\beta$ 42 fibril formation (**paper III** and **V**).

## 3.2 Lipid assembly

Phospholipids consist of a polar headgroup and a non-polar hydrocarbon tail. This gives the phospholipids an amphiphilic property, and so they spontaneously self-assemble in aqueous solutions in order to reduce the exposure of the tails to the water. In other words, the self-assembly of lipids in aqueous solutions is driven mainly by hydrophobic interaction<sup>147</sup>. *In vivo*, a typical example of lipid self-assembly is cellular membranes. Here, the lipids form a bilayer that will encapsulate the cells. This will limit the transport of polar and charged molecules, as these molecules cannot easily pass through the nonpolar interior of the bilayer. *In vitro*, the lipid self-assembly can be extensively utilised; examples include to provide model membranes for interaction studies, as native environments for membrane proteins, as well as in drug delivery systems, cosmetics, etc.

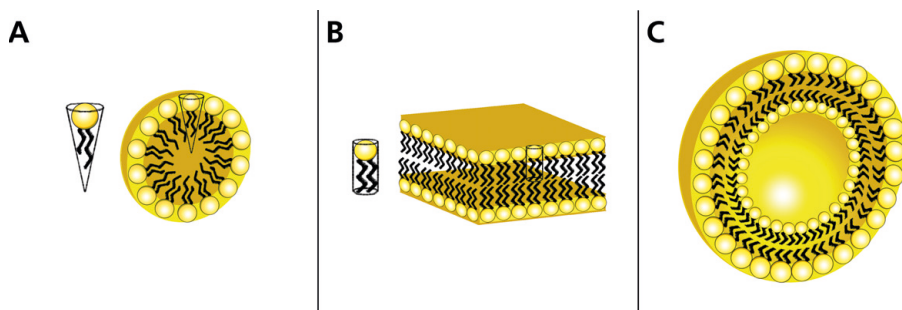


**Figure 3.3:** Schematic of different self-assembled lipid structures. A) A micelle, made up of lipids with a conical shape. B) A planar lipid bilayer, composed of lipids with a cylindrical shape. C) A lipid vesicle with a solvent interior, formed by dispersion of the lamellar phase. Reproduced with permission<sup>148</sup>. Copyright 2014, American Chemical Society.

What the self-assembled structure will look like depend on characteristics of the lipids, such as their size and shape. Typically the so-called surfactant number<sup>85</sup> – approximately “how cone-shaped a lipid molecule is” – is considered, when rationalising over the various self-assembled lipid structures. Low packing parameters indicate that the molecule have a cone-like shape, promoting the formation of non-planar structures, for example spherical micelles (figure 3.3A), while packing parameters close

to one indicate cylindrical shape, promoting the formation of planar bilayers (figure 3.3B). The lamellar phase can further be dispersed into (multilamellar or unilamellar) vesicles (figure 3.3C), a process that requires energy from, for example, sonication. Factors that might affect the surfactant number include temperature, ionic strength, and solution pH<sup>85</sup>, depending on the chemical character of the lipid headgroup. For instance, two of the lipids mentioned in chapter 2.2 – DMPC and POPC – both have surfactant parameters close to one for a wide range of conditions, thus forming bilayers. However, a detergent such as sodium cholate, has conical shape and will by itself form micelles (if above the critical micelle concentration (CMC)). When mixing the PC lipids with sodium cholate, they may co-assemble. The structure of the object formed may be micelles or dispersed vesicles (figure 3.3C), depending on the PC-to-cholate proportions<sup>149</sup>. The mixtures of POPC and cholate are commonly used in protocols for preparing recombinant lipodiscs<sup>150</sup>, as used in **paper III**.

Cholesterol is a very hydrophobic molecules that can be dissolved on a phospholipid membrane at rather high contents, as typically observed in biological membranes<sup>76,151</sup>. Due to its bulky and rather rigid molecular shape, it may cause an ordering of the lipid acyl-chains in a fluid lipid bilayer, and it is therefore referred to as a membrane stabiliser<sup>151</sup>. These changes in lipid chain ordering may in turn lead to changes in the membrane properties in terms of its flexibility<sup>1</sup>. The effect of introducing cholesterol – up to 15%, as to remain in the liquid disordered phase – to lipodiscs, and the effect this would have on A $\beta$ 42 fibril formation was studied in **paper III**.

### 3.3 Co-assembly of proteins and lipids

So far, the assemblies including only proteins or lipids have been discussed. However, *in vivo*, the system is typically more complex and the biomolecules will co-exist in environment with complex composition, thereby opening the possibility of co-assemblies of different types of biomolecules.

In the perspective of amyloid fibril formation, this is of fundamental interest, as fibril formation *in vivo* typically occurs in a lipid-rich environment. Lipids are surface active molecules, which can affect processes driven by hydrophobic interactions. Several studies have reported an effect by the lipids on the amyloid formation process<sup>152–154</sup>, as well as uptake of the lipids in the formed aggregates<sup>155,156</sup>. The precise effect of how the lipid membranes interfere with the amyloid aggregation process depend both on the type of amyloid protein, the lipid composition as well as the lipid to protein ratio. For example, it has been shown that zwitterionic phospholipid membranes may cause an inhibition of A $\beta$  fibrillisation<sup>157</sup>, while incorporation of

cholesterol in membranes can lead to an acceleration of the amyloid formation<sup>157, 158</sup>.

For the formation of lipodiscs serving as recombinant HDL-like particles, one need to control the co-assembly of lipids and protein. For some lipids, it is enough to mix the protein and lipids, and perturb the system through sonication. This was done in **paper II**, **III**, and **paper IV**, when using DMPC. An additional protocol, used in **paper III**, uses a "helper" molecule – sodium cholate – to disperse the lipids into small mixed objects. ApoA-I associate with the lipid structure, and via dialysis, there is finally a selective removal of the "helper" compound with the highest solubility in water (cholate), thus leaving a dispersed lipid bilayer with a ApoA-I belt<sup>150</sup>.

In this thesis, the co-assembly of proteins and lipids – from lipodiscs to amyloid aggregates – was investigated in three systems. The first is the complex, *in vivo*-like environment of a body fluid (CSF), and how this multitude of possible interaction partners would effect the fibril formation of A $\beta$ 42 (**paper I**). The second system includes small, dispersed lipodiscs (**paper III**) and their effect on A $\beta$ 42 fibrillisation. The last system involves large protein-rich structures made up from ApoA-I and how PC can inhibit this aggregation (**paper IV**).



### Misfolding diseases

---

Folding of proteins is essential to ensure their proper function in the body. However, sometimes the proteins can change conformation, and *misfold*. The term misfold typically refers to a harmful state of the protein, where the fold either leads to toxic activity of the protein or loss of function<sup>159, 160</sup>. Therefore, the body has systems to detect incorrectly folded proteins; however, sometimes these misfolded proteins escape this quality-control, which can lead to aggregation and progression of different diseases<sup>90</sup>. Protein misfolding and aggregation formation is the cause of several diseases in humans<sup>112, 159–161</sup>, such as Parkinson's, Huntington's, and Alzheimer's disease, as well as amyloidosis. The two latter are most relevant for this thesis and will be further discussed.

#### 4.1 Amyloidosis

By 2017, 37 proteins had been discovered in insoluble fibrils in humans, only 4 of which have been found intracellularly while the rest are extracellular<sup>113</sup>. When these fibril deposits cause disease, the disease is called amyloidosis<sup>162</sup>, and further specified depending on the amyloidogenic protein involved<sup>163</sup>. The disease can be local – where the deposits and disease are restricted to a specific organ or tissue – or systematic – where the deposits are spread to connective tissue and organs. Furthermore, the instigation of the disease can be either acquired or familial (also called hereditary). In acquired amyloidosis, the disease is caused by the wildtype protein in response to factors such as inflammatory and infectious states or other diseases, resulting in increased amount of amyloidogenic protein. Familial amyloidosis, instead, is due to mutations in specific genes, where the mutations lead to decreased stability of the

native state of the corresponding protein or other factors that make the proteins more amyloidogenic<sup>162</sup>.

In this thesis, great focus is on ApoA-I. ApoA-I is one of the proteins that can cause amyloidosis, both acquired and familial. In acquired ApoA-I amyloidosis, full-length ApoA-I forms fibrils that are deposited in arteries and tissues<sup>17, 18, 164</sup>. Fibril formation *in vitro* is accelerated after oxidation of the methionine residues, which suggest a potential fibrillisation mechanism for ApoA-I in the oxidative environment of atherosclerotic plaques<sup>164, 165</sup>. In familial ApoA-I, the disease instigation is due to fibril deposition by mutant ApoA-I or its proteolytic cleaved fragments, typically 1-83 to 1-93 of the N-terminus<sup>166</sup>. These fibril depositions often occur in different organs depending of the ApoA-I mutant<sup>17, 29, 30</sup>. Mutations associated with amyloid deposits can occur both outside this N-terminal region – such as K107 $\Delta$ <sup>32, 33</sup> – or clustered close to the N-terminus<sup>166</sup> – such as G26R<sup>31</sup>. In total (as of 2017) 19 ApoA-I mutations had been shown related to systematic ApoA-I amyloidosis, likely due to destabilisation of the native fold and exposure of hydrophobic patches of the protein. This in turn also facilitates proteolysis, resulting in the higher concentrations of the more amyloidogenic N-terminal fragments<sup>113, 134, 135</sup>. Some mutations also increase the fibrillisation rate of the fragments<sup>113, 134</sup>; others have been suggested to increase dissociation rate of the full-length protein from HDL particles<sup>113, 135</sup>, though this appears to be a matter of debate<sup>167, 168</sup>.

In **paper IV**, we investigated the aggregation propensity of wildtype ApoA-I as well as the K107 $\Delta$ -variant, and evaluated if there is a morphological difference of the formed aggregates.

## 4.2 Alzheimer's Disease

Another peptide of interest has been the A $\beta$ -peptide, involved in Alzheimer's disease (AD). AD is a devastating neurodegenerative disease, which affects a large and increasing number of individuals world-wide<sup>169–171</sup>. It was first described in 1906 by Alois Alzheimer, and the findings published in 1907<sup>172, 173</sup>, and is now known as the most common form of dementia. The deposition of extracellular plaques is one of the key features in AD, including the formation of neurofibrillary tangles composed of hyperphosphorylated tau<sup>174</sup>. AD is associated with age, with prevalence almost doubling every 5 years after aged 65<sup>175</sup>. As with ApoA-I amyloidosis, there are two forms of AD: sporadic (acquired) and familial. Several risk factors correlate with the sporadic form and are known to accelerate its progression, either life-style related – such as sleep deprivation<sup>176</sup>, low education<sup>177</sup>, smoking<sup>178</sup>, and obesity<sup>179, 180</sup> – or genetic – for instance, the  $\epsilon 4$  allele of the APOE gene<sup>81, 181–183</sup>. The onset of familial

AD (FAD) occurs earlier than the sporadic form, often before age 65 and often with a more aggressive progression<sup>184</sup>. The early onset is associated with A $\beta$  expression, exhibited in people with Down's syndrome due to chromosome 21 trisomy<sup>49,185</sup>, as well as individuals with proteogenic mutations close to the cleavage sites of  $\beta$ - and  $\gamma$ -secretase of APP<sup>186–188</sup>.

As progress in science has increased the life expectancy, this also correlates with an increased occurrence of AD in the world<sup>169,170</sup>. Therefore, an effective treatment is of great need. Currently, few medical options exist, with the antibody Aducanumab being the latest accepted treatment in the US<sup>189,190</sup>. However, while it is possible to retard the progression of AD, it is no cure for ongoing disease. Therefore, there is a massive effort towards understanding the underlying mechanisms of the disease in order to increase the medical options and possible cures, an effort somewhat hampered as the exact cause of the disease is still unknown.

One theory of the propagation of AD is the amyloid cascade hypothesis. Due to the observations made above regarding A $\beta$ 's relation to AD onset and the phosphorylation of tau – which can be induced by A $\beta$ <sup>191</sup> –, the basis of this theory identifies A $\beta$  as a key player in AD<sup>192,193</sup>. It suggests that A $\beta$  self-assembly acts as a disease instigator, followed by truncation, phosphorylation and aggregation of tau, and subsequent neuronal death<sup>192,194,195</sup>. The most common form of A $\beta$  is A $\beta$ 40, while A $\beta$ 42 is more aggregation prone, more cytotoxic<sup>196</sup>, and up until recently thought to be more prevalent in plaques<sup>197</sup>; however, methods with higher resolution have recently started to re-evaluate the A $\beta$  proteoforms in plaques and found the exact length distribution to be more complex, as reviewed<sup>198</sup>.

While the fibrillar products of A $\beta$  seem fairly harmless, the oligomers formed during the fibrillisation process appear more cytotoxic<sup>199</sup>. While the mechanism behind the toxicity of the oligomers is still unknown, different suggestion has been put forth, including cell membrane pore formation<sup>200–203</sup>, nerve receptor binding<sup>204,205</sup>, reactive oxygen species formation<sup>206–208</sup>, and increased membrane permeation<sup>209–212</sup>.

In AD, lipid has been found included in the cerebral amyloid deposits<sup>213,214</sup>. Indeed, complex metabolic changes of membrane lipids are occurring in AD, possibly both as a consequence and promoter of AD pathogenesis, as reviewed<sup>215</sup>. Furthermore, studies have found that higher levels of plasma HDL cholesterol (HDL-C) are correlated with lower risk of AD progression<sup>216,217</sup>, and that AD patients exhibited lower HDL-C<sup>83</sup> and ApoA-I levels<sup>218</sup>. Some contrasting results have been reported<sup>219,220</sup>, though age at which the HDL-C levels are measured as well as the follow-up times of the studies may be of importance for the outcome of the experiments (reviewed by Button *et al*<sup>221</sup>). The role of HDL from an AD perspective has been extensively reviewed<sup>21,221</sup> and while no causality is yet detected, it elucidates the

possible association between HDL, its proteome, and AD. In this thesis, the effect of HDL on A $\beta$ 42 fibril formation is investigated in **paper III**.

---

## Methodologies and experimental techniques

---

### 5.1 Top down versus bottom up

*In vivo*, A $\beta$  aggregation occurs in complex fluids consisting of many thousands of biomolecules. To understand differences in the fibrillisation mechanism in these complex fluids compared to pure buffer systems, at least two approaches are possible: in a *top-down* approach, A $\beta$  aggregation is studied either directly in the complex fluid of interest, or after fractionation of the fluid. This approach is the fastest route towards the aggregation mechanism in a complex environment, but does not provide a clear understanding of the connection between effects and effectors due to multiple simultaneous effects. However, through the fractionation and analysis of their composition, apolipoproteins A-I, E and J, as well as cholesterol – all of which are commonly engaged in HDL particles in CSF – have been identified as putative effectors<sup>81</sup>. In a *bottom-up* approach, components from relevant fluids – purified from a host or chemically synthesised in the absence of the body fluid – are added one at a time and the effect on the A $\beta$  aggregation mechanism and rates are quantified to find the effects on each of the underlying microscopic steps. The bottom-up approach is the fastest route towards a physicochemical understanding of the effects from each component and was recently used to understand the effects of ionic strength<sup>119, 120</sup> and pH<sup>118</sup>.

In this work we have used both; through a top-down approach, we studied A $\beta$  aggregation in CSF and tried to characterise the fibril formation process based on previously determined mechanism (**paper I**). Then, in a bottom-up approach, we purified single components from non-CSF sources and tried to build the examined particles *in vitro* in order to determine the effect of these components on the A $\beta$

aggregation (**paper II** and **III**). We further used a bottom-up approach in **paper V**, to investigate if isolated chaperone domains from DNAJB6 could be used to mimic the effect seen by intact DNAJB6 on A $\beta$ 42 fibril formation.

## 5.2 Protein expression and preparation

To study the interactions of proteins – and other molecules in general – it is essential to have protocols for production of the protein that results in a sample free from contaminants, with the desired amino acid sequence for the protein. There are different ways to attain protein products, for example by extraction from body fluids, chemical synthesis or using a recombinant expression system. Extraction from body fluids may be useful, but since many thousands of biomolecules are also present, the purification can be difficult, and low yielding; chemical synthesis is convenient, but obtaining long homogeneous peptides are difficult; recombinant expression through other hosts – such as the gram-negative bacterium *Escherichia coli* (*E. coli*) or yeast (*Saccharomyces cerevisiae* or *Pichia pastoris*) – may offer high yield and economical production of proteins<sup>2</sup>. In this work, *E. coli* was utilised to produce the proteins, by inserting the DNA encoding the protein of interest into vectors, which in turn allows for the protein to be produced by the bacteria<sup>5</sup>.

Expression in a bacterial host can fail, especially for unfolded proteins and those prone to protease degradation, such as ApoA-I<sup>42</sup>. Therefore, fusion with a protective tag may be needed to obtain sufficient yield. However, the use of tags and sequence extension may affect the physicochemical properties of the protein. The tag must therefore be removed; often this is done using expensive proteases, which requires further purification to eliminate the additives from the system. Therefore, when preparing ApoA-I, the EDDIE mutant of N<sup>Pro</sup> autoprotease was used (**paper II**), as EDDIE will cleave itself off upon refolding, leaving a free target protein with its N-terminus intact and eliminating the need to add more proteases to the system.

## 5.3 Chromatographic methods

Chromatography is typically used to separate components in a mixture. There are different types of chromatography techniques, some of which will be further discussed below (as these were used in **paper II**). However, they employ the same basic principles, and are composed of the same components: the mobile phase – a fluid (liquid or gas) into which the sample (or solute) is dissolved – and the stationary phase – the system through which the mobile phase is carried through. The stationary phase

is often composed of a solid or liquid attached to a tube or surface of beads (resin). The different components will partition differently between the mobile and stationary phase and separate the solutes<sup>222</sup>.

### 5.3.1 Ion-Exchange Chromatography (IEC)

Ion-exchange chromatography (IEC) separates molecules based on the attraction between them and the charged sites on the stationary phase; by selecting columns with either positively or negatively charged ligands, proteins with the opposite charge may be purified from the rest. The proteins are then eluted either by a change in pH or by increasing the salt concentration, thereby interfering with the protein-ligand interactions.<sup>2,222</sup> This is typically done through a gradient, i.e., by altering the pH or salt concentration gradually, to separate the solutes bound to the stationary phase, as different solutes will have different affinity for the resin and be released at different ionic strengths or pH. By using consecutive IEC steps at separate pH values or concentration of a charged ligand – such as a metal ion – the purity of the product can be greatly improved.

### 5.3.2 Immobilized Metal Affinity Chromatography (IMAC)

Immobilized Metal Affinity Chromatography (IMAC) in protein purification utilises histidine's (His) affinity for metal ions that it has through its imidazole side-group. Metal ions (often nickel, copper, or zinc ions) are immobilised by binding to nitrilotriacetic acid (NTA) on the stationary phase. When the protein sample is loaded onto the column, proteins with an affinity for the metal ions – for instance, when having an additional His-tag – bind to metal ions coordinated to the stationary phase, while the remaining protein elutes with the flow-through.<sup>222</sup> Then the bound proteins may be eluted with increasing concentrations of imidazole, i.e. eluted through competitive binding to the resin. It is worth noting that, as His is a naturally occurring amino acid, many proteins have one or multiple His that will bind to the stationary phase in the same manner as the His-tag. Therefore, more proteins than the target protein may bind. Hence IMAC may be regarded more as an isolation step rather than a purification step.

### 5.3.3 Hydrophobic Interaction Chromatography (HIC)

Hydrophobic interaction chromatography (HIC) allows for separation of proteins based on their hydrophobicity.<sup>2</sup> The stationary phase consists of a resin with hydro-

phobic ligands. These will then bind to the hydrophobic patches of the solutes. To ensure solubility, addition of salt to the protein sample is needed (salting in), as this will expose the hydrophobic patches by disrupting the hydration shells of the proteins, and thereby facilitate the binding between the protein and ligands. It is important to ensure, however, that the salt concentration is not too high as this can cause the proteins to precipitate (salting out). In order to elute the proteins after binding, the ionic strength is decreased to allow for the reformation of the hydration shells. This will eventually disturb the protein-ligand interactions. Depending on the hydrophobicity of the protein, the salt gradient may be different; if a protein is very hydrophobic and thereby interacts strongly with the stationary phase, the lower the salt concentration needs to be for the hydration shells to reform.<sup>222</sup>

### 5.3.4 Size-Exclusion Chromatography (SEC)

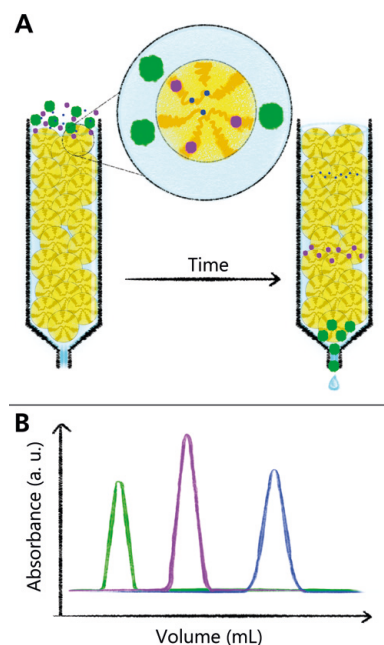


**Figure 5.1:** The principle of SEC. A) shows solutes of different sizes, entering the pores to different extent depending on the size of the species. B) is a theoretical chromatogram obtained from A), assuming the species absorb light at the same wavelength.

Size-exclusion chromatography (SEC) – also called gel filtration or molecular exclusion chromatography – is used in several aspects in a biochemical lab. It is a prominent method for separating species depending on size (Stokes radius),<sup>2,222</sup> for instance when desalting a sample or when requiring a monomeric solution free from oligomers. It can also be used to study protein-protein equilibrium and exchange rates. In SEC, the stationary phase is comprised of a porous gel; when the solutes in the mobile phase pass through the column, particles of smaller size will enter the pores in the beads while the larger ones cannot and passes through without entering the pores. Thereby, the smaller solutes will be retained in the column for longer time, while the larger will be eluted first (figure 5.1).

In this thesis, SEC was used in all experiments involving A $\beta$  and ApoA-I, as these were purified the same day as the experiment was carried out, to ensure homogenous sample.

## 5.4 Sodium Dodecyl Sulphate – PolyacrylAmide Gel Electrophoresis (SDS-PAGE)

Sodium dodecyl sulphate – polyacrylamide gel electrophoresis (SDS-PAGE) is an electrophoretic method where a polymeric gel is used to separate macromolecules such as proteins through sieving. In SDS-PAGE, proteins are first reduced or denatured – through 2-mercaptoethanol (to reduce the disulphide bonds) or through boiling – in the presence of SDS, which will charge the proteins equally according to size by coating hydrophobic regions with a large, negative charge. When placing the gel between two electrodes, and applying the voltage, the charged proteins will migrate through the gel depending on their electrophoretic mobility, which in SDS-PAGE is often mainly governed by size; smaller will migrate more easily through the polymer network and thereby travel further.<sup>2</sup> Exceptions are highly stable proteins which resist denaturation upon boiling in SDS. By staining the gel afterwards, the different proteins may be detected as bands, separated by size. To extract the sizes corresponding to the distance travelled in the gel, a molecular standard – often called a ladder – containing proteins of known sizes must be added, as well. SDS-PAGE was mainly used in **paper II**, to evaluate the elution and purity of ApoA-I throughout the purification procedure.

## 5.5 Mass spectrometry (MS)

Mass spectrometry (MS) is a technique used to analyse the molecular masses of molecules or fragments of molecules in a sample. In this technique, ionised samples are separated based on charge and size, prior to being detected. The first part is accomplished through an ionisation source, of which there are different types. One of the most commonly used sources is electrospray ionisation (ESI), where the liquid sample is dispersed into an aerosol by applying high voltage, solvent evaporation, and eventual droplet dissociation, leaving positive ions behind<sup>223</sup>. The second method is called matrix-assisted laser desorption ionisation (MALDI), where the sample is mixed with a matrix; a laser is then used, as the matrix absorbs energy and transfers protons to the protein. It is important to note, though, that the ionisation will be qualitative – not quantitative – as different samples ionise to different extents. To get a quantitative measure, isotope-labeled samples of known quantities must be included as well.

After ionisation, the ions are accelerated in an electrical or magnetic field, travelling and separating according to their mass/charge ( $m/z$ ) ratios. This can also be accomplished in a variety of ways: one example is time of flight (TOF), where the analyser uses an electric field to accelerate the ions and then measures how long time

it takes for them to arrive at the detector; a second example is the quadrupole, where the analyser has four parallel metal rods conducting oscillating electrical fields to select between ions of certain  $m/z$  ratios, as the ions will have different trajectories depending on their  $m/z$ . Finally, the detector will report the mass spectrum, where the detected signal will be plotted versus the  $m/z$  ratio. It is also possible to combine the different analysers – so called tandem MS –, for instance to first isolate one specific peptide, then fragment it through collision with a gas, and then sort the produced fragments. This can be used to detect, for instance, modifications of specific amino acid residues or to analyse if a mutation is present<sup>222</sup>. In this thesis, MS was used in **paper II**, both as an analysis tool for modifications of ApoA-I, but also to analyse the purity of the samples.

## 5.6 Dynamic Light Scattering (DLS)

Dynamic light scattering (DLS) is a non-destructive technique used to characterise particle sizes in suspensions (figure 5.2). It measures the light scattered by particles in the solution, and calculates their sizes based on the Brownian motion of the particles (assuming spherical geometry). Smaller particles will move faster compared to larger ones as given by the Stokes-Einstein relation:

$$D = \frac{k_B T}{3\pi\eta d_p} \quad (5.1)$$

where  $D$  is the diffusion coefficient,  $k_B$  is Boltzmann constant,  $T$  is the temperature,  $\eta$  the viscosity, and  $d_p$  the hydrodynamic diameter.

To determine  $D$ , a laser is directed to the sample contained in a cuvette and the scattered single frequency light is detected at a certain angle over time to monitor the movement of the particles. The initial intensity is used to generate an autocorrelation function, which describes for how long time a particle is suspended in the same spot. The decay then represents the time needed by the particles to change position. As small particles move more quickly – as stated above – their decay will be faster than larger, and so the decay of their autocorrelation function will be faster than those of larger particles. This can then be related to the lag time, and further calculated to obtain  $D$ <sup>224</sup>.

$$g_2(\tau) = 1 + \beta e^{-2Dq^2\tau} \quad (5.2)$$

where  $g$  is the autocorrelation function,  $\tau$  is the time between the two time-points,  $\beta$  is the coherence factor that depends on detector area, optical alignment, and scattering

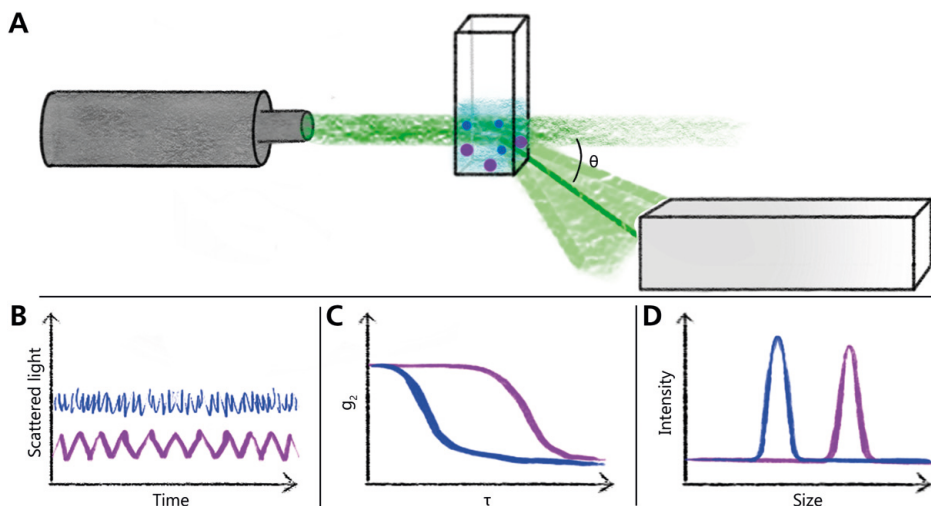


**Figure 5.2:** Dynamic light scattering. A) A laser shining light on a sample, scattering the light to a detector positioned at angle  $\theta$ . B) The scattered light as a function of time. C) The autocorrelation function, showing the faster decay for the smaller particles compared to the large. D) The calculated size distribution. For all, blue is small particles and purple is larger.

properties of macromolecules, and  $q$  is the Bragg wave vector (calculated from the viscosity, wavelength of incident light, and the  $\theta$  angle at which the detector is placed). Typically, the conversion of the autocorrelation function to the corresponding size (assuming spherical particles) is included in the software of the DLS instrument, while analysis according to other shapes has to be done on exported data. In this thesis, the conversions have been done using the software of the DLS instrument, with the assumption of spherical particles (**papers II, III, and IV**). As the measurements were done to observe the change in size after a certain time or addition of a sample – i.e. a qualitative analysis, as opposed to a quantitative – it was deemed adequate, even if some particles are expected to not be precisely spherical.

## 5.7 Circular Dichroism (CD) spectroscopy

Circular dichroism (CD) is a spectroscopic technique for samples in solution. It is based on plane-polarised light, which is a superposition of two circularly polarised components of the same amplitude, one rotating counter-clockwise (L) and the other clockwise (R), and how these two components will interact with the samples<sup>225,226</sup>. Non-chiral molecules will interact with these two polarisations of light to the same extent. Most biomolecules, however, are chiral and will absorb the L- and R-components to different extents. This difference can then be measured at the detector, and presented as a function of the wavelength of the incoming light:

$$\Delta A = A_L - A_R \quad (5.3)$$

or, by applying Beer-Lambert's law:

$$\Delta A = (\epsilon_L - \epsilon_r) * C * l \quad (5.4)$$

as

$$\Delta \epsilon = (\epsilon_L - \epsilon_r) \quad (5.5)$$

where  $\epsilon_L$  and  $\epsilon_r$  are the molar extinction coefficients for L- and R-circularly polarised light,  $C$  is the molar concentration, and  $l$  is the path length in centimeters (cm). Typically it is also reported in terms of the ellipticity ( $\theta$ ) in degrees, where  $\theta = 3298 \Delta A$ , or  $3298.2 \Delta \epsilon$ .

Depending on the spectral regions investigated, different structural information can be obtained. Analyzing the absorption of light at wavelengths 260-320 nm (near-UV) will report on the aromatic amino acid residues and can lead to fingerprints of the tertiary structure of the protein. Absorption at 240 nm down to 180 nm (far-UV) will instead result from the peptide bonds of the protein and give information regarding the secondary structure such as  $\alpha$ -helix,  $\beta$ -sheet, and random coil, as these show characteristic spectral patterns (figure 5.3). In summary, the  $\alpha$ -helix spectrum

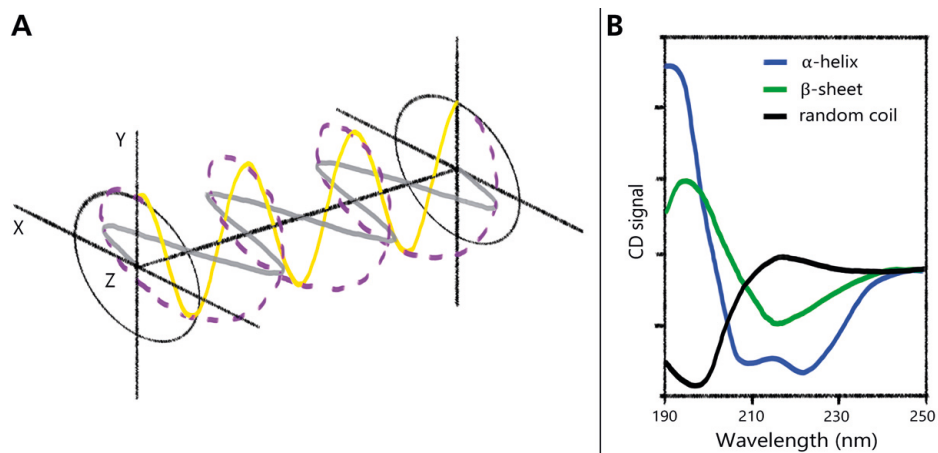


**Figure 5.3:** Circular dichroism. A) Representation of circularly polarised light (purple) – clockwise in this sketch – based on plane polarised light (grey and yellow). B) The characteristic spectral patterns for  $\alpha$ -helix (blue),  $\beta$ -sheet (green), and random coil. B) is adapted with permission from.<sup>227</sup> Copyright 1969, American Chemical Society.

shows two minima at 208 and 222 nm, and a maximum at 193 nm;  $\beta$ -sheet results in one minimum at 215 nm – though the exact position depends on  $\beta$ -sheet curvature and parallelity – and a maximum at 196 nm; random coil shows a small minimum at approximately 198 nm<sup>2</sup>.

The analysis of CD data can be difficult if the sample contains a mixture of various secondary structures, as the acquired spectrum will be a superposition of the different absorptions. The different contributions can be separated through linear decomposition of the spectrum, or by comparison to a reference database<sup>226</sup>. This deconvolution is never better than the accuracy of the protein concentration determination. In addition, signals from disulfide bonds and aromatic side chains may spill over into the far-UV range. It is also important to note that the presence of macroscopic aggregates will distort the CD spectrum due to scattering effects or heterogeneous absorption, in turn also leading to lower observed CD signal<sup>226</sup>.

In this work, CD has mostly been used to investigate the change in secondary structure of ApoA-I due to aggregation (**paper IV**), to possibly detect fibril formation.

## 5.8 Fluorescence spectroscopy

Another type of optical spectroscopy is fluorescence spectroscopy, where the emission of photons is measured after a sample is exposed to electromagnetic radiation. This exposure can cause a molecule to absorb light, leading to some of its electrons changing molecular orbital from a ground state to an excited state. However, this excited state is not energetically favourable, and so the electron will eventually return to the ground state. When doing so, it can either emit heat or a photon. If a photon is emitted, this is called fluorescence and the molecules doing so to a high extent (high quantum yield) are called fluorophores.

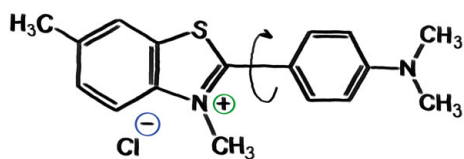


**Figure 5.4:** A Thioflavin T (ThT) molecule. The carbon-carbon around which the two rings can rotate has been marked with an arrow.

One such fluorophore is thioflavin T (ThT). The molecule is comprised of a benzothiazole ring and a benzyl ring connected by a single carbon-carbon bond (figure 5.4). In solution, the fluorescence quantum yield of ThT will be lower as the two rings can rotate freely around this bond, letting energy dissipate. In bound form, however, the molecule will be more rigid – with less ring rotation around the carbon-carbon bond – and an increase of the excitation maximum (at circa 440 nm) and emission maximum (at circa 482 nm) will occur<sup>98, 228</sup> (figure 5.5).

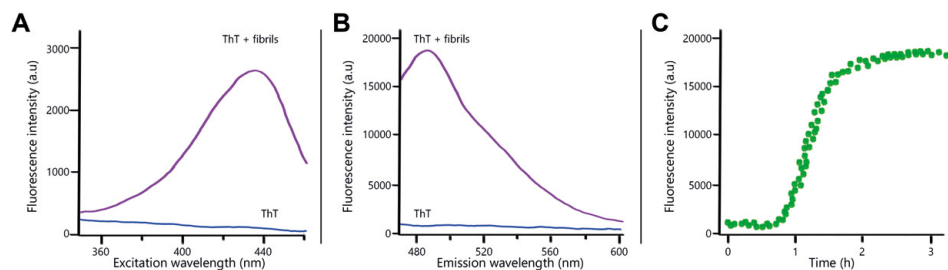


**Figure 5.5:** Fluorescence spectra for ThT in buffer and bound to amyloid fibrils. A) The excitation spectrum of ThT, free in solution and bound to fibrils. B) The emission spectrum of ThT, with and without fibrils. C) Typical fluorescence curve as a function of time, through which the fibril formation over time can be inferred. For A) and B), blue is ThT alone, and purple is ThT in the presence of amyloid fibrils. A) and B) are adapted from<sup>237</sup>.

ThT has been used extensively to study amyloid fibril formation, due to its binding propensity to  $\beta$ -sheets<sup>228,229</sup>; by measuring the fluorescence intensity, the fibril formation can be followed, as more ThT molecules in solution can bind and fluoresce with larger amounts of fibrils formed (if the ThT concentration is optimised to provide a linear response of the fibril concentration). The fluorescence intensity over time can be plotted (figure 5.5C), and mathematical models fitted to it in order to investigate the aggregation mechanism (see Kinetic analysis). However, ThT is not always inert in respect to the aggregation equilibrium and kinetics<sup>230,231</sup> or selective exclusively to amyloid structures<sup>229,232–235</sup>. Therefore, one can use the ThT fluorescence intensity as a reporter of fibril formation - as has been done in **papers I, III, IV and V** - but other complementary methods are needed to confirm it<sup>236</sup>.

## 5.9 Kinetic analysis

The models for the fibrillisation mechanism have been described previously (chapter 3.1.2). After fibril formation of a peptide at a series of monomer concentrations (in the presence of ThT), these models can be fitted to the ThT fluorescence data, to find the minimal set of steps providing an acceptable fit. This is typically evaluated from the error square sum, which will reflect how well a model fits to the data analysed.

In this thesis, the online platform Amylofit<sup>141</sup> was used, allowing for global analysis of a large amount of kinetic data. Thereby, the different models and their different parameters – such as rate constants and saturating concentrations – can be evaluated more easily. This was done in **paper I** – where the global analysis allowed for determination of the A $\beta$ 42 mechanism in CSF –, in **paper III** – where the effect of ApoA-I and rHDL was analysed – and in **paper V** – to investigate the effect from DNAJB6 constructs.

## 5.10 Cryogenic-transmission electron microscopy (cryo-EM)

Cryogenic-transmission electron microscopy (cryo-EM) is another technique, used in all papers of this thesis to get a visual presentation of the different samples. For the EM technique, Aaron Klug was awarded the Nobel Prize in 1982. As the name suggest, it operates based on streams of electrons, whose wavelength can be adjusted down to picometers based on their kinetic energy. The electrons in TEM are accelerated by an applied voltage in vacuum and steered through magnetic lenses to hit the sample, where they are scattered or absorbed. A detector may then create high resolution images of the observed sample based on these interactions<sup>238</sup>. Cryo-EM imaging can be brought down to picometers in resolution easily, and down to atomic level if averaging identical objects of many images<sup>239</sup>. However, increasing the number of electrons bombarding the sample will lead to damages in the sample, and so the number of images that may be acquired for a specific area of the sample is limited<sup>239,240</sup>.

Specific for cryo-EM is the sample preparation. The liquid samples are deposited on sample grids – a thin carbon film full of holes, mounted on a copper grid – and plunged into liquid ethane at  $-180^{\circ}\text{C}$ , vitrifying the samples and acquiring transparent amorphous ice<sup>240,241</sup>. This will trap the samples, frozen in place, and allow snap-shots of the investigated process to be taken without risk of structural rearrangements prior to imaging. The samples are stored and imaged in liquid nitrogen, to prevent thawing. The sample preparation is one of the most crucial steps in cryo-EM, as the presence of crystalline ice will interfere with the images. For the freezing technique, Jacques Dubochet was awarded the Nobel Prize in Chemistry 2017, shared with Joachim Frank and Richard Henderson for the methodology for single particle reconstruction and structure determination.



### Summary of thesis work

---

The intricate play between self-assembly and co-assembly of biomolecules is the focus of this thesis.

In **paper I** we used a top-down approach to study the fibril formation of A $\beta$ 42. As it is very difficult to follow the fibril formation in real time *in vivo* with techniques available today, we strove to create an *ex vivo* environment by using the body fluid CSF, and further investigate the fibrillisation behaviour and mechanism of A $\beta$ 42.

Another protein of interest is ApoA-I, due to its double-faceted property of self- and co-assembly. In **paper II**, the aim was to develop a new protocol for the production of pure ApoA-I, with focus on a stream-line purification to avoid time consuming lyophilisation steps and buffer exchanges.

In **paper III** we used a bottom-up approach to investigate if some candidate components – identified from CSF<sup>81</sup> – would be able to replicate the retarding effect on A $\beta$ 42 fibril formation seen in **paper I**. We combined purified ApoA-I with DMPC and POPC – as well as a mixture of POPC and cholesterol – to investigate the effect these components would have on A $\beta$ 42 fibril formation, either as self-assembled components or as co-assembled composites.

In **paper IV** we investigated the aggregation behaviour of ApoA-I, and how different extrinsic and intrinsic factors would affect the possible amyloid fibril formation.

In **paper V**, we again took a bottom-up approach to investigate a simple model system composed of A $\beta$  and one chaperone to mimic a more complicated scenario. We asked if the chaperone activity demonstrated by DNAJB6 can be reproduced by an isolated chaperone domain and, if so, how small this domain could be.

## 6.1 Paper I

The mechanism of A $\beta$  fibril formation *in vitro* has been extensively studied, and protocols have been developed to obtain accurate and reproducible kinetic data. However, the conditions *in vitro* are typically highly stringent, with few and specifically chosen components to ensure sample control to the greatest extent possible. This is in comparison to the *in vivo* environment, with high concentrations of other biomolecules that may interact with the studied peptide; additionally, ions and other small molecules will be present. Altogether, there is a multitude of possible effects and effectors on the A $\beta$  fibril formation, which are difficult to predict. Therefore, as the mechanism of A $\beta$  fibril formation *in vivo* – while elusive – is of greatest interest, this study was constructed to use the protocols made *in vitro* and apply them to an *in vivo*-like situation. Here, we asked the questions: do A $\beta$  fibrils form in the presence of CSF? If so, can reproducible data amenable to kinetic analysis be obtained in CSF? Is the autocatalytic nature of the process, including a double nucleation mechanism originally found in pure buffer, also present in CSF? Finally, is it possible to identify how the individual microscopic steps are affected by CSF? To answer these questions, a series of experiments were performed where human CSF was spiked with recombinantly expressed and purified human A $\beta$ 42 and the fibril formation kinetics was then followed. The buffer conditions were chosen to mimic the ionic and pH conditions of CSF, thereby allowing for CSF in different concentrations to be investigated without major shifts in conditions (for details, see **paper I**).

We found that A $\beta$ 42 formed ThT-positive fibrils in CSF as well as in buffer. The morphology of the fibrils was confirmed with cryo-EM, and found to resemble those formed in the absence of CSF. Possibly, some small particles could be observed

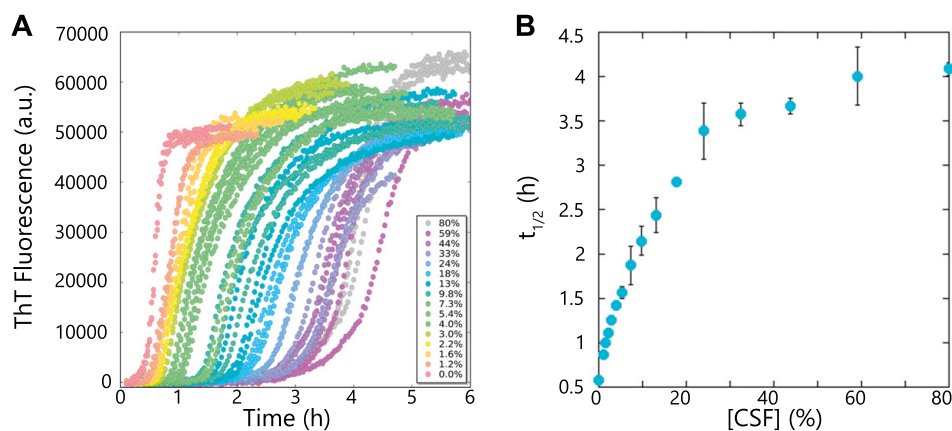


**Figure 6.1:** A) The ThT fluorescence as a function of time for 3  $\mu$ M A $\beta$ 42 in buffer with various concentrations of CSF (0-80%). B) The  $t_{1/2}$  h as estimated from the data in panel A) as a function of CSF concentration.

at the surface of the fibrils; however, the cryo-EM images alone could not identify the possibly bound species. We also found that – despite the various molecular species present in CSF – reproducible kinetic data could be obtained for the A $\beta$ 42 fibrillisation. This was observed both by using several different CSF pools from two different hospitals, as well as within the repeats of the concentrations. Some minor differences in curve shape could be observed between CSF pools, but the overall appearance of retardation and observed  $t_{1/2}$  versus A $\beta$ 42 concentration was remarkably similar.

Furthermore, we found that the presence of CSF delays fibril formation (figure 6.1A), as previously seen<sup>81,242,243</sup>. We observed that the  $t_{1/2}$  of A $\beta$ 42 fibril formation was increased with increased percentage of CSF added, showing the net retarding effect of all effectors in CSF. In some pools of CSF tested, this retarding effect was saturated at higher CSF concentrations – as evident in  $t_{1/2}$  graph in figure 6.1B – while other pools showed no such saturation.

The obtained kinetic data of A $\beta$ 42 at constant CSF concentrations were globally fitted with models as determined previously from aggregation of pure protein. The saturated secondary nucleation model (equation [3.7]) – as determined to agree with A $\beta$ 42 fibril formation in physiological salt concentration<sup>119</sup> – was found to best fit the data at all CSF concentrations. This was further supported by the performed seeding experiments, where the lag phase was shortened by the addition of premade fibrils. However, the primary nucleation reaction order,  $n_c$ , had to be set to effectively 0 in order to fit the data of A $\beta$ 42 in buffer alone. This infers that the primary nucleation is saturated, which has not been seen in previous systems. The reason for this is unknown, though suggested explanations include the ionic strength – though this has previously only been seen to saturate secondary nucleation<sup>119</sup> – or the presence of calcium ions<sup>244</sup>. Furthermore, we found that the rate of secondary nucleation is decreased when adding CSF. Whether this is connected to the previously mentioned molecules on the fibril surface is unknown, but of interest for future work.

In conclusion, our main findings in **paper I** was: A $\beta$ 42 forms fibrils in the presence of CSF, of similar morphology as those formed in buffer. Reproducible kinetic data can be achieved, amenable to global kinetics analysis of the same rate laws as inferred from aggregation in pure buffer. Thereby it is possible to approximate the presence of CSF as a perturbation to the rate constants of aggregation in pure buffer. Most importantly, the autocatalytic nature of the process – which includes a mechanism with secondary nucleation mechanism – is present also in CSF. The main retarding effect of CSF on the aggregation of A $\beta$ 42 stems from a reduction of the rate of secondary nucleation. Our findings illustrate how the analysis of the aggregation kinetics in pure buffer can be used to identify the microscopic steps in the aggregation reaction and then be used to translate these findings to the *in vivo* situation by repeating the aggregation reaction in increasing concentrations of bodily fluids.

## 6.2 Paper II

ApoA-I is involved in lipid transport *in vivo*, being the major protein constituent of HDL particles. It has also been found to form amyloid deposits, involved in amyloidosis. Thus it is of interest both to study the multifaceted interactions of ApoA-I, and to investigate if the effector observed in **paper I** could be HDL-particles (as suggested<sup>81</sup>). ApoA-I therefore needs to be reconstructed from a non-CSF host, to ensure only constituents of interest are present in the sample. In this study we developed an expression and purification strategy for the production of high-purity ApoA-I.

ApoA-I constitutes of 243 residues; as chemical synthesis is only suited for relatively short peptides<sup>245</sup>, we chose to recombinantly express it through the gram-negative bacterium *Escherichia coli* (*E. coli*). ApoA-I has been found prone to protease degradation<sup>42</sup>, thus we elected to co-express it with a protective tag called EDDIE. EDDIE is a mutant form of the N<sup>Pro</sup> autoprotease from classical swine fever virus, forming inclusion bodies in the bacterial cells and then upon refolding cleaves itself off from the target protein. This serves two purposes: firstly, it protects ApoA-I from proteolysis; secondly, it eliminates the need to add additional proteases after purification. An additional advantage with EDDIE is that, after cleavage, the target protein is left with its N-terminus intact.

The used chromatographic methods have been described in chapter 5.3. These were selected, as ApoA-I is negatively charged in neutral pH and with hydrophobicity shown through its interactions with lipids. Additionally, we added a His-tag to EDDIE in order to use IMAC to remove it after cleavage. Then, as this was insufficient to ensure proper purity, the thermostability of ApoA-I<sup>246,247</sup> was exploited through boiling. Finally, SEC was performed prior to further experiments, to ensure homogeneity of the sample. To create as efficient purification as possible, the order of the different chromatographic steps was investigated. The optimal order was determined to be IEC-IMAC-HIC-boil-storage/SEC: IEC will remove the DTT added when cleaving His-EDDIE from ApoA-I as well as increasing the ionic strength slightly; IMAC removed the uncleaved construct and the cleaved His-EDDIE and concentrated the sample, as most of the ApoA-I was eluted with the water front when changing mobile phase; HIC was placed next, as the elution resulted in low ionic strength, optimal for buffer changes in coming experiments; boiling was added as the first three chromatographic steps still contained contaminating proteins; SEC was placed last, after lyophilisation and storage of the protein, to ensure homogeneous sample prior to further experiments.

Several factors was investigated in order to optimise the protocol, both in terms of increased EDDIE cleavage and purification (for details, see **paper II**). The final

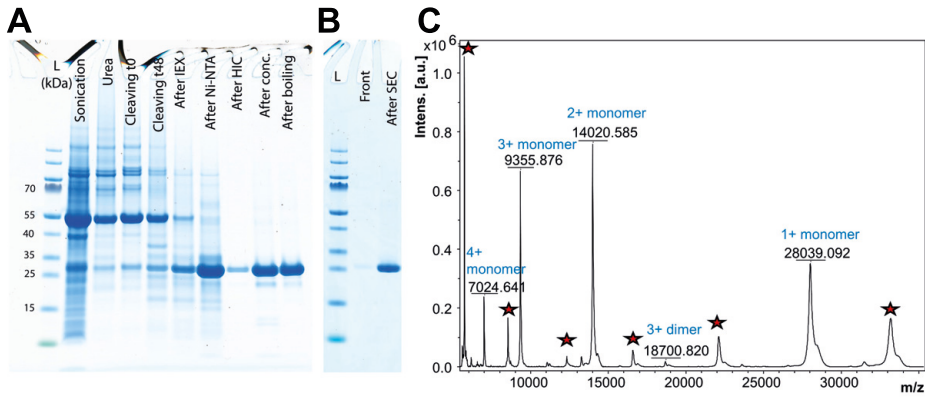


**Figure 6.2:** A) Samples taken throughout the purification, visualised through SDS-PAGE. B) SDS-PAGE of a typical example of an aliquot of the purified sample, after SEC. The “front” fraction is the beginning of the peak, while the “After SEC” fraction is typically used for further experiments. The molecular standard ladder contains the same sizes in A) and B). C) Intact weight MALDI-MS of purified ApoA-I, internally calibrated using BSA+Bruker Protein Std I. The signals corresponding to the calibrants are marked with a star. The signals at 28 039 Da, 14 021 Da, 9356 Da, and 7025 Da correspond to the 1+, 2+, 3+, and 4+ charged ApoA-I monomer respectively; the signal at 18701 Da corresponds to the 3+ dimer.

strategy led to samples with high purity as confirmed with SDS-PAGE and mass spectrometry (figure 6.2), and a yield of 5 mg/L for wildtype ApoA-I. Two more aggregation-prone ApoA-I mutants – G26R and K107Δ – were also expressed and purified with the protocol, resulting in a 3 mg/L and 16 mg/L yield for respective mutant. The reason for the increased yield for K107Δ is unknown, but possibly the mutation lead to simplified elution, particularly from the HIC column as K107Δ eluted at higher salt concentration compared to wildtype ApoA-I. Still, the ability to express and purify mutants using the same protocol demonstrates its robustness; also the protocol was a prudent strategy to eliminate the need of extrinsic proteases as well as imidazole.

In conclusion, in **paper II**, we found that we could develop a protocol through which human ApoA-I may be recombinantly expressed in *E. coli*. This was facilitated by the autocleavable tag EDDIE. The protocol results in is very pure, tag-free ApoA-I with authentic N-terminus. The protocol could be used to express and purify two mutants of ApoA-I, further showing the robustness of the protocol.

### 6.3 Paper III

As mentioned, in **paper I** a top-down approach was used to study A $\beta$ 42 fibril formation in an *ex vivo* situation. In **paper III**, we instead used a bottom-up approach to investigate if we could achieve a similar retarding effect on A $\beta$ 42 fibril formation in a simpler system. We ask therefore ask if lipoprotein particles – rHDL – interfere with A $\beta$  aggregation processes? If so, are lipids required, or can the ApoA-I alone cause the same effect? Is there a lipid specificity? Does the fibril morphology change due to co-aggregation with lipids?

To avoid possible contamination of unknown minor components from CSF, we used samples prepared from CSF-free hosts. We produced ApoA-I as described in **paper II**, along with synthetic lipid molecules. We reconstituted rHDL particles from ApoA-I and either single phospholipids with a PC headgroup, or a mixture of PC and cholesterol (of concentrations corresponding to a liquid disordered bilayer phase). We then investigated the effect the rHDL particles – as well as protein alone and lipid vesicles alone – had on the fibrillisation of A $\beta$ 42.

Through the ThT fluorescence assay, we noted that both lipid-free ApoA-I and rHDL particles retard A $\beta$ 42 fibril formation, while no retardation was observed after addition of lipid vesicles. This retardation effect was more pronounced for lipid-free ApoA-I compared to rHDL. It is still unknown whether the effect we see with rHDL is due to free ApoA-I in the sample; however, from the NMR experiment, no population of free ApoA-I could be detected. It should however be noted that the exchange between free and rHDL-bound ApoA-I occurs the same time scale as the fibrillisation experiment<sup>248</sup>. Thereby, it is possible that ApoA-I may redistribute between lipid-bound and A $\beta$ 42-bound, if the affinity for A $\beta$ 42 is higher than the affinity for lipids. Interesting though is that, the co-assembly of protein-lipids seem to have a smaller effect on the A $\beta$ 42 fibril formation compared to the lipid-free ApoA-I.

From the global kinetic analysis, we found that the effect from both lipid-free ApoA-I and rHDL can best be described as affecting the secondary nucleation pathway, demonstrated through a change in  $k_+k_2$  (equation [3.7]). For lipid-free ApoA-I, however, it was inferred that it might also enhance the primary nucleation process; improved fits to the kinetic curves could be achieved by fitting individual  $k_+k_n$  – along with individual  $k_+k_2$  – to each curve, where the resulting  $k_+k_n$  was higher after addition of ApoA-I compared to A $\beta$ 42 alone. The seeding experiments resulted in shorter lag-time for A $\beta$ 42 alone; however, no such shortening could be detected for neither ApoA-I or rHDL particles, confirming the effect on the secondary nucleation pathway. Two explanations for this effect seem possible: a competition with A $\beta$ 42 monomers for the interaction with the fibrils surface, or an interaction between the

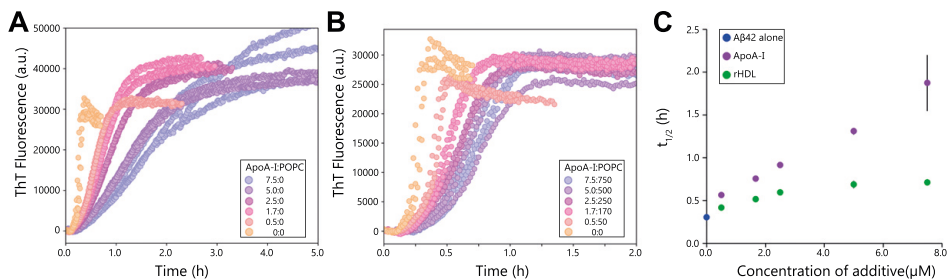


**Figure 6.3:** The ThT fluorescence as a function of time for 5  $\mu$ M A $\beta$ 42 in buffer with addition of A) ApoA-I, or B) rHDL particles. C) is the extracted  $t_{1/2}$  h plots of A) and B).

additives and nucleating species and thereby a hindrance of the conversion to fibrillar structure<sup>249</sup>. More experiments are needed in order to determine which explanation is more likely.

Furthermore, the fibrils formed after ThT fluorescence plateau was reached was visualised using cryo-EM. Through this, we found that the A $\beta$ 42 fibrils formed after addition of ApoA-I and rHDL are longer compared to the control sample of A $\beta$ 42 alone, possibly due to an increased use of monomers through elongation after inhibition of the dominant secondary nucleation step. It is also interesting to note that the morphology of the fibrils formed after addition of lipid-free ApoA-I seem to be less twisted, with a longer node-to-node distance, implying interaction of ApoA-I with A $\beta$ 42. For the images of the samples with added rHDL particles, a very low number of free rHDL particles can be observed. Additionally, the visualised fibrils are more similar to those formed from A $\beta$ 42 alone than those formed from A $\beta$ 42 in the presence of lipid-free ApoA-I (at least concerning the twist of the fibrils but not the length distribution). Considering that the molar ratio of rHDL:fibril was high enough to have the fibrils decorated by rHDL particles – is such interactions are favorable – the absence of rHDL in the images would suggest that no such association exist.

In conclusion, in **paper III** we found that the retardation of A $\beta$ 42 fibril formation observed in CSF can be largely reproduced by ApoA-I or rHDL. In CSF, the retarding effect is more pronounced; given the multitude of components in CSF, this difference is expected. Still, it is remarkable that much of the effect observed in CSF is captured by the very simple systems used here. Through the bottom-up approach we thus identified ApoA-I and HDL-like particles as components interfering more specifically with secondary nucleation.

## 6.4 Paper IV

In **paper IV**, we investigated ApoA-I and its aggregation propensity. We asked whether ApoA-I would readily aggregate in a lipid-free environment. If so, what is the morphology of the aggregates? Would it be possible to shift the aggregation from more  $\alpha$ -helical content to  $\beta$ -sheet (figure 6.4)? Finally, would the possible aggregation be effected by addition of lipids to the system?

To answer these questions, we investigated the aggregation of ApoA-I *in vitro*, and the effect of different factors on the morphology of the aggregates. For wild-type ApoA-I at pH 7.4, we find it readily forms large, globular condensates, with an  $\alpha$ -helical conformation retained from the monomeric state. These aggregates were formed after approximately 4-5 days after incubation in quiescent conditions.

As discussed in chapter 4.1, ApoA-I can form fibrils, related to ApoA-I amyloidosis. Therefore, we explored several extrinsic and intrinsic factors of the system to identify conditions when ApoA-I form globular condensates versus amyloid fibrils. The full list can be found in Table 1 in **paper IV**. To summarise, we investigated the effect of decreasing the pH, oxidising the methionine residues with  $\text{H}_2\text{O}_2$ , using the ApoA-I mutant K107 $\Delta$ , and agitation, or a combination of all. We followed the increase in ThT fluorescence for all systems, as this has previously been used as

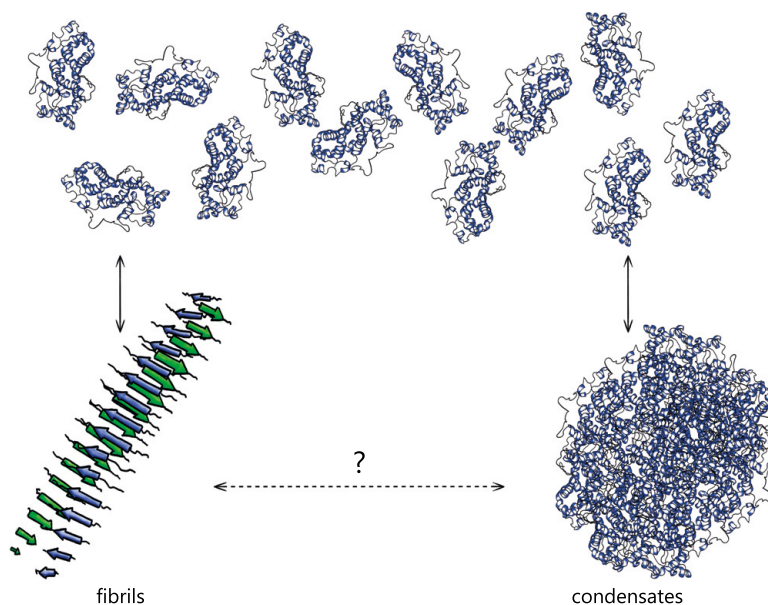


**Figure 6.4:** Possible forms of aggregated ApoA-I, where  $\alpha$ -helical, monomeric ApoA-I interact to form either globular condensate – with no large change in secondary conformation – or amyloid fibril structure with cross- $\beta$  characteristics.

indicator of ApoA-I fibril formation<sup>18,165,250,251</sup>.

Out of all the systems investigated, we observe clear amyloid formation for only one set of conditions, and that is for the K107 $\Delta$  mutation at decreased pH and after oxidation of the methionine residues. As changes in the protein charge – either through altering pH or introduced mutations – can affect the intramolecular electrostatic interactions, as well as the hydrophobicity of the protein, it may alter both the secondary structures in the protein as well as the colloidal stability. We hypothesise that, since ApoA-I has a pI of approximately 5.5 depending on isoform<sup>252</sup>, lowering the pH would reduce the net repulsion between the different protein molecules, as well as between the side chains within the protein. This could possibly give rise to a conformational change, either of the aggregates, or of the secondary structure (or both). The deletion of a lysine in the K107 $\Delta$  can further reduce the net repulsion; it may also introduce a structural change in the secondary structure, as it is located in an amphipathic  $\alpha$ -helix and, when removed, the helix has to change conformation slightly to compensate. The oxidation of the methionine can further introduce steric effects on the residues, all or which are located in different helices in wildtype ApoA-I<sup>167,253</sup>. Oxidation could further affect the system due to a shift in polarity and possibly the pKa of surrounding amino acid residues. All these modifications lead to a cumulative destabilisation of the native state, shifting the fold to a larger population with  $\beta$ -sheet secondary structure. It is also worth to note that there seem to be a co-existence of globular condensates and fibrillar structures in this sample. It is highly unlikely that the co-existence of both these types of aggregates represent the equilibrium state, whereby it is possible that further conformational conversion will occur within already formed aggregates if the energy barrier is low enough. This, however, could not be observed in our experiments.

*In vivo*, most of the ApoA-I is co-assembled with lipids in different lipoprotein particles<sup>1,17</sup>. By addition of phospholipids to the system, this will reduce the free protein concentration in solution and is thereby one way of preventing protein aggregation. This is observed in our experiments as well, where no aggregation is detected in the time scale measured, for the system containing ApoA-I and DMPC.

In conclusion, our main findings in **paper IV** was that, for most conditions investigated, ApoA-I readily form globular protein-only condensates, with retained  $\alpha$ -helical conformation. Further, the conversion to ThT positive aggregates with higher  $\beta$ -sheet content can be achieved by destabilisation of the native structure through mutation, oxidation, and decreasing the pH. Still, even after several days of incubation, we observe a mixture of  $\beta$ -sheet rich amyloid fibrils and  $\alpha$ -helix-rich condensates. Finally, the addition of lipids to the system resulted in no detectable aggregation.

## 6.5 Paper V

In **paper V**, we ask the question: can chaperone activity be reproduced by isolated chaperone domains? This is furthering the bottom-up strategy, by not only seeing if a single component can reproduce a certain effect, but by separating this component into further sub-parts.

The anti-amyloid activity of DNAJB6 has previously been inferred, and the conserved S/T-stretch established as important for this inhibition of fibril formation. In **paper V**, we investigated the effect of the C-terminal domain (CTD) – in which the S/T region is located – on A $\beta$ 42 fibril formation, and what effect is seen when including different sizes of the domain. Different constructs were created and purified: one consisted of the entire CTD; a second consisted of the four  $\beta$ -strands that make up part of the CTD; and a third, consisting of two of the  $\beta$ -strands from the CTD. The  $\beta$ -strands of the second and third constructs were also grafted onto a scaffold protein, in order to ensure that the structure was still intact (figure 6.6). For these three constructs, corresponding controls were designed where the S/T residues were substituted with alanine; for the full-length protein, these S/T to A substitutions have previously resulted in a 50% less active chaperone<sup>71</sup>. These substitution constructs were therefore included to investigate if the S/T-residues would be responsible for the possible effects of the constructs.

Our results show that, while some anti-amyloid activity is retained in the six constructs, it is less pronounced than for the intact DNAJB6 (figure 6.6). Full-length

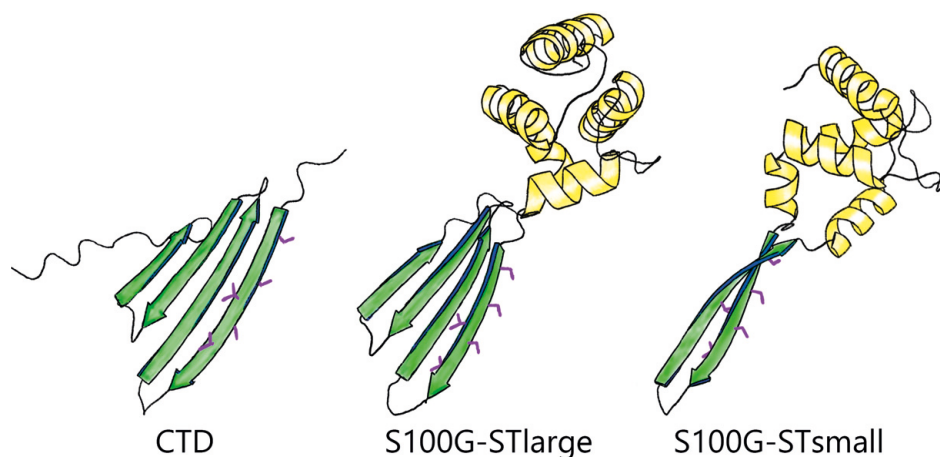


**Figure 6.5:** The different constructs of DNAJB6, adapted from their predicted AlphaFold-structure (for details, see **paper V**). To the left is CTD, middle is S100G-STlarge, and S100G-STsmall. Green indicates the  $\beta$ -sheets, present in the CTD (also indicated in 2.3; magenta is the S/T-residues, substituted in the STA controls; yellow is the S100G-graft.

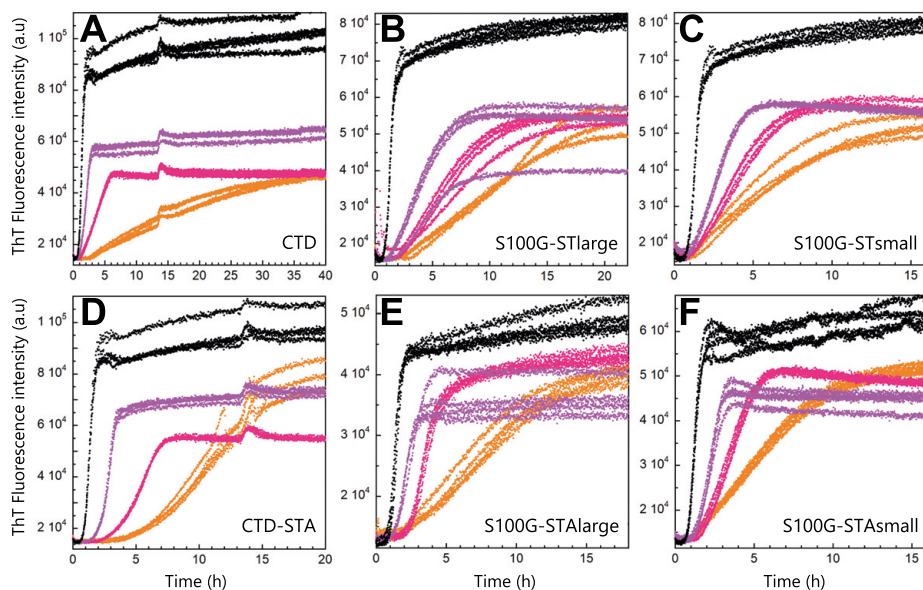


**Figure 6.6:** Examples of aggregation kinetics starting from 3  $\mu$ M A $\beta$ 42 monomer in the absence (black) and presence of A) CTD, B) S100G-STlarge, C) S100G-STsmall, D) CTD-STA, E) S100G-STAlarge, F) S100G-STAsmall at 187 nM (purple), 750 nM (pink) and 3  $\mu$ M (orange).

DNAJB6 effectively inhibit the primary nucleation of A $\beta$ 42 fibril formation, clearly seen through an extended lag phase; the constructs, on the other hand, seem to mainly affect the secondary nucleation pathway, as inferred through global kinetic analysis (equation [3.5]). These results indicate that, while some binding to A $\beta$  is still retained in the constructs – confirmed by SPR –, other parts outside the CTD of DNAJB6 are required to retain the same inhibition mechanism as seen for full-length DNAJB6. Thereby, it is not enough that the conserved S/T-residues are included in the constructs, but the other domains are required as well. Further experiments are ongoing to investigate this further.

In conclusion, our main findings in **paper V** was that none of the tested constructs affect the aggregation mechanism of A $\beta$ 42 in the same manner as full-length DNAJB6. All six constructs is instead suggested to have a prominent effect on secondary nucleation with none or a small additional effect on elongation.



### Concluding remarks

---

This thesis has focused on the intricate play between self-assembly and co-assembly of biomolecules, with particular interest in protein-protein and protein-lipid interactions. The amyloid fibril formation has been of primary interest, and the effect on the mechanism that certain additives may have. The main findings from the five papers that constitutes this thesis are listed below.

- A $\beta$ 42 forms fibrils in the presence of CSF, through the same autocatalytic pathway – including the secondary nucleation mechanism – as inferred from buffer.
- The main retarding effect of CSF on the aggregation of A $\beta$ 42 stems from a reduction of the rate of secondary nucleation, which is can be largely reproduced by ApoA-I or rHDL. While it is more pronounced in CSF, it is remarkably captured by a very simple system.
- Our findings illustrate how aggregation kinetics in pure buffer can identify the microscopic steps in the aggregation reaction and then be used to translate these findings to the *in vivo* situation by repeating the aggregation reaction in increasing concentrations of bodily fluids.
- Through the bottom-up approach we thus identified ApoA-I and HDL-like particles as components interfering more specifically with secondary nucleation.
- The protocol developed for the recombinant expression and purification of ApoA-I provides a robust strategy that may be used for both wildtype protein as well as additional, more aggregation prone ApoA-I mutants.

- ApoA-I readily form globular protein-only condensates, with retained  $\alpha$ -helical conformation. The conversion to ThT positive aggregates with higher  $\beta$ -sheet content can be achieved through mutation, oxidation, and decreasing the pH.
- The addition of lipids to ApoA-I resulted in no detectable protein-rich aggregation.
- None of the tested DNAJB6 constructs affect the aggregation mechanism of A $\beta$ 42 in the same manner as full-length DNAJB6. All six constructs is instead suggested to have a prominent effect on secondary nucleation with none or a small additional effect on elongation.

## 7.1 Outlook

While these conclusions can be drawn from the work of this thesis, by no means are we running out of new questions to investigate and answer. Through the work with CSF we can see that the protocols developed *in vitro* can be used to describe a more complex environment. We can then start adding on components to the rHDL particles. The next step would be to involve more proteins – such as ApoE – to investigate the effect of A $\beta$  fibril formation, and hopefully investigate the differences in CSF from individuals with and without AD. This, in the end, could potentially help identify further factors either enhancing or retarding the fibrillisation.

This addition of biomolecules to the system is of interest also regarding ApoA-I aggregation. By investigating the interplay between proteins and lipids, though *in vitro*, it will hopefully provide more answers regarding how ApoA-I can proceed from a lipid-rich composite to a protein-rich aggregate.

Finally, the work with DNAJB6 gives further insights into how changes in the same protein can change which mechanistic step in the fibril formation process it may inhibit. This can provide valuable insight in how the different structural forms of A $\beta$  may interact with its binding partners. This can provide information for targeting a specific aggregation event, and may be useful in the development of the therapies for misfolding diseases.

---

## References

---

- [1] D. U. Silverthorn and B. R. Johnson, *Human Physiology An Integrated Approach*. San Francisco: Pearson /Benjamin Cummings, 5th ed., 2010.
- [2] N. C. Price and J. Nairn, *Exploring Proteins: A Student's Guide to Experimental Skills and Methods*. Oxford: Oxford University Press, 2009.
- [3] A. Ambrogelly, S. Palioura, and D. Söll, "Natural expansion of the genetic code.," *Nat. Chem. Biol.*, vol. 3, no. 1, pp. 29–35, 2007.
- [4] L. Pauling, R. B. Corey, and H. R. Branson, "The structure of proteins: Two hydrogen-bonded helical configurations of the polypeptide chain," *Proc. Natl. Acad. Sci.*, vol. 37, no. 4, pp. 205 LP – 211, 1951.
- [5] D. U. o. L. Whitford, *Proteins: Structure and Function*. Chichester: John Wiley & Sons, Ltd, 2005.
- [6] B. Alberts, A. Johnson, J. Lewis, M. Raff, K. Roberts, and P. Walter, *Molecular Biology of the Cell*. New York: Garland Science, 5th ed., 2008.
- [7] X. Hou, T. Zaks, R. Langer, and Y. Dong, "Lipid nanoparticles for mRNA delivery," *Nat. Rev. Mater.*, 2021.
- [8] J. M. Berg, J. L. Tymoczko, and L. Stryer, *Biochemistry*. New York: W. H. Freeman, 2012.
- [9] D. L. Sparks, S. Lund-Katz, and M. C. Phillips, "The charge and structural stability of apolipoprotein A-I in discoidal and spherical recombinant high density lipoprotein particles.," *J. Biol. Chem.*, vol. 267, no. 36, pp. 25839–25847, 1992.
- [10] C. Vitali, C. L. Wellington, and L. Calabresi, "HDL and cholesterol handling in the brain," *Cardiovasc. Res.*, vol. 103, no. 3, pp. 405–413, 2014.
- [11] A. von Eckardstein and D. Kardassis, *High Density Lipoproteins: From Biological Understanding to Clinical Exploitation*, vol. 224. Springer International Publishing, 1 ed., 2015.
- [12] H. Wang and R. H. Eckel, "What are lipoproteins doing in the brain $\alpha$ ," *Trends Endocrinol. Metab.*, vol. 25, no. 1, pp. 8–14, 2014.

- [13] I. Ramasamy, "Recent advances in physiological lipoprotein metabolism.," *Clin. Chem. Lab. Med.*, vol. 52, no. 12, pp. 1695–1727, 2014.
- [14] M. N. Oda, "Lipid-free apoA-I structure - Origins of model diversity," *Biochim. Biophys. Acta - Mol. Cell Biol. Lipids*, vol. 1862, no. 2, pp. 221–233, 2017.
- [15] M. Ouimet, T. J. Barrett, and E. A. Fisher, "HDL and Reverse Cholesterol Transport.," *Circ. Res.*, vol. 124, no. 10, pp. 1505–1518, 2019.
- [16] A. R. Tall, P. Costet, N. Wang, A. R. Tall, P. Costet, and N. Wang, "Regulation and mechanisms of macrophage cholesterol efflux," *J. Clin. Invest.*, vol. 110, no. 7, pp. 899–904, 2002.
- [17] L. Obici, G. Franceschini, L. Calabresi, S. Giorgetti, M. Stoppini, G. Merlini, and V. Bellotti, "Structure, function and amyloidogenic propensity of apolipoprotein A-I," *Amyloid*, vol. 13, no. 4, pp. 191–205, 2006.
- [18] N. A. Ramella, O. J. Rimoldi, E. D. Prieto, G. R. Schinella, S. A. Sanchez, M. S. Jaureguiberry, M. E. Vela, S. T. Ferreira, and M. A. Tricerri, "Human apolipoprotein A-I-derived amyloid: Its association with atherosclerosis," *PLoS One*, vol. 6, no. 7, 2011.
- [19] V. Narasimhan Janakiraman, A. Noubhani, K. Venkataraman, M. Vijayalakshmi, and X. Santarelli, "High yield of recombinant human Apolipoprotein A-I expressed in *Pichia pastoris* by using mixed-mode chromatography," *Biotechnol. J.*, vol. 11, no. 1, pp. 117–126, 2016.
- [20] P. G. Frank and Y. L. Marcel, "Apolipoprotein A-I : structure – function relationships," *J. Lipid Res.*, vol. 41, pp. 853–872, 2000.
- [21] J. Marsillach, M. P. Adorni, F. Zimetti, B. Papotti, G. Zuliani, and C. Cervellati, "Hdl proteome and alzheimer's disease: Evidence of a link," *Antioxidants*, vol. 9, no. 12, pp. 1–24, 2020.
- [22] T. Cedervall, I. Lynch, M. Foy, T. Berggård, S. C. Donnelly, G. Cagney, S. Linse, and K. A. Dawson, "Detailed identification of plasma proteins adsorbed on copolymer nanoparticles," *Angew. Chemie - Int. Ed.*, vol. 46, no. 30, pp. 5754–5756, 2007.
- [23] T. Cedervall, I. Lynch, S. Lindman, T. Berggård, E. Thulin, H. Nilsson, K. A. Dawson, and S. Linse, "Understanding the nanoparticle-protein corona using methods to quantify exchange rates and affinities of proteins for nanoparticles," *Proc. Natl. Acad. Sci. U. S. A.*, vol. 104, no. 7, pp. 2050–2055, 2007.
- [24] E. Hellstrand, I. Lynch, A. Andersson, T. Drakenberg, B. Dahlbäck, K. A. Dawson, S. Linse, and T. Cedervall, "Complete high-density lipoproteins in nanoparticle corona," *FEBS J.*, vol. 276, no. 12, pp. 3372–3381, 2009.
- [25] J. S. Saczynski, L. White, R. L. Peila, B. L. Rodriguez, and L. J. Launer, "The relation between apolipoprotein A-I and dementia: The honolulu-asia aging study," *Am. J. Epidemiol.*, vol. 165, no. 9, pp. 985–992, 2007.

- 
- [26] A. C. Paula-Lima, M. A. Tricerri, J. Brito-Moreira, T. R. Bomfim, F. F. Oliveira, M. H. Magdesian, L. T. Grinberg, R. Panizzutti, and S. T. Ferreira, "Human apolipoprotein A-I binds amyloid- $\beta$  and prevents A $\beta$ -induced neurotoxicity," *Int. J. Biochem. Cell Biol.*, vol. 41, no. 6, pp. 1361–1370, 2009.
- [27] M. M. Rahman, H. Zetterberg, C. Lendel, and T. Hard, "Binding of human proteins to amyloid- $\beta$  protofibrils," *ACS Chem. Biol.*, vol. 10, no. 3, pp. 766–774, 2015.
- [28] G. Ghiselli, A. M. Gotto, S. Tanenbaum, and B. C. Sherrill, "Proapolipoprotein A-I Conversion Kinetics in vivo in Human and in Rat," *Proc. Natl. Acad. Sci. U. S. A.*, vol. 82, no. 3, pp. 874–878, 1985.
- [29] N. A. Ramella, G. R. Schinella, S. T. Ferreira, E. D. Prieto, M. E. Vela, J. L. Ríos, M. A. Tricerri, and O. J. Rimoldi, "Human Apolipoprotein A-I Natural Variants: Molecular Mechanisms Underlying Amyloidogenic Propensity," *PLoS One*, vol. 7, no. 8, 2012.
- [30] D. Rowczenio, A. Dogan, J. D. Theis, J. A. Vrana, H. J. Lachmann, A. D. Wechalekar, J. A. Gilbertson, T. Hunt, S. D. J. Gibbs, P. T. Sattianayagam, J. H. Pinney, P. N. Hawkins, and J. D. Gillmore, "Amyloidogenicity and clinical phenotype associated with five novel mutations in apolipoprotein A-I," *Am. J. Pathol.*, vol. 179, no. 4, pp. 1978–1987, 2011.
- [31] W. C. Nichols, F. E. Dwulet, J. Liepnieks, and M. D. Benson, "Variant apolipoprotein AI as a major constituent of a human hereditary amyloid," *Biochem. Biophys. Res. Commun.*, vol. 156, no. 2, pp. 762–768, 1988.
- [32] M. Amarzguioui, G. Mucchiano, B. Häggqvist, P. Westermark, A. Kavlie, K. Sletten, and H. Prydz, "Extensive Intimal Apolipoprotein A1-Derived Amyloid Deposits in a Patient with an Apolipoprotein A1 Mutation," *Biochem. Biophys. Res. Commun.*, vol. 242, no. 3, pp. 534–539, 1998.
- [33] G. I. Mucchiano, B. Häggqvist, K. Sletten, and P. Westermark, "Apolipoprotein A-1-derived amyloid in atherosclerotic plaques of the human aorta," *J. Pathol.*, vol. 193, no. 2, pp. 270–275, 2001.
- [34] X. Zhang, D. Lei, L. Zhang, M. Rames, and S. Zhang, "A Model of Lipid-Free Apolipoprotein A-I Revealed by Iterative Molecular Dynamics Simulation," *PLoS One*, vol. 10, no. 3, p. e0120233, 2015.
- [35] C. G. Brouillette, G. M. Anantharamaiah, J. A. Engler, and D. W. Borhani, "Structural models of human apolipoprotein A-I: A critical analysis and review," *Biochim. Biophys. Acta - Mol. Cell Biol. Lipids*, vol. 1531, no. 1-2, pp. 4–46, 2001.
- [36] W. S. Davidson, T. Hazlett, W. W. Mantulin, and A. Jonas, "The role of apolipoprotein AI domains in lipid binding," *Proc. Natl. Acad. Sci. U. S. A.*, vol. 93, no. 24, pp. 13605–13610, 1996.
- [37] J. T. Melchior, R. G. Walker, A. L. Cooke, J. Morris, M. Castleberry, T. B. Thompson, M. K. Jones, H. D. Song, K. A. Rye, M. N. Oda, M. G. Sorci-Thomas, M. J. Thomas, J. W. Heinecke, X. Mei, D. Atkinson, J. P. Segrest, S. Lund-Katz, M. C. Phillips, and W. S. Davidson, "A consensus model of human apolipoprotein A-I in its monomeric and lipid-free state," *Nat. Struct. Mol. Biol.*, vol. 24, no. 12, pp. 1093–1099, 2017.

- [38] J. P. Segrest, M. K. Jones, B. Shao, and J. W. Heinecke, "An Experimentally Robust Model of Monomeric Apolipoprotein A-I Created from a Chimera of Two X-ray Structures and Molecular Dynamics Simulations," *Biochemistry*, vol. 53, no. 48, pp. 7625–7640, 2014.
- [39] R. A. G. D. Silva, G. M. Hilliard, J. Fang, S. Macha, and W. S. Davidson, "A three-dimensional molecular model of lipid-free apolipoprotein A-I determined by cross-linking/mass spectrometry and sequence threading," *Biochemistry*, vol. 44, no. 8, pp. 2759–2769, 2005.
- [40] R. D. Pollard, B. Fulp, M. P. Samuel, M. G. Sorci-Thomas, and M. J. Thomas, "The conformation of lipid-free human apolipoprotein A-I in solution," *Biochemistry*, vol. 52, no. 52, pp. 9470–9481, 2013.
- [41] J. P. Segrest, M. K. Jones, A. E. Klon, C. J. Sheldahl, M. Hellinger, H. De Loof, and S. C. Harvey, "A Detailed Molecular Belt Model for Apolipoprotein A-I in Discoidal High Density Lipoprotein \*," *J. Biol. Chem.*, vol. 274, no. 45, pp. 31755–31758, 1999.
- [42] S. E. Panagotopoulos, S. R. Witting, E. M. Horace, J. Nicholas Maiorano, and W. Sean Davidson, "Bacterial expression and characterization of mature apolipoprotein A-I," *Protein Expr. Purif.*, vol. 25, no. 2, pp. 353–361, 2002.
- [43] R. Ueberbacher, A. Dürauer, K. Ahrer, S. Mayer, W. Sprinzl, A. Jungbauer, and R. Hahn, "EDDIE fusion proteins: Triggering autoproteolytic cleavage," *Process Biochem.*, vol. 44, no. 11, pp. 1217–1224, 2009.
- [44] E. Portelius, H. Zetterberg, U. Andreasson, G. Brinkmalm, N. Andreasen, A. Wallin, A. Westman-Brinkmalm, and K. Blennow, "An Alzheimer's disease-specific  $\beta$ -amyloid fragment signature in cerebrospinal fluid," *Neurosci. Lett.*, vol. 409, no. 3, pp. 215–219, 2006.
- [45] N. Kaneko, R. Yamamoto, T.-A. Sato, and K. Tanaka, "Identification and quantification of amyloid beta-related peptides in human plasma using matrix-assisted laser desorption/ionization time-of-flight mass spectrometry," *Proc. Jpn. Acad. Ser. B. Phys. Biol. Sci.*, vol. 90, no. 3, pp. 104–117, 2014.
- [46] A. T. Welzel, J. E. Maggio, G. M. Shankar, D. E. Walker, B. L. Ostaszewski, S. Li, I. Klyubin, M. J. Rowan, P. Seubert, D. M. Walsh, and D. J. Selkoe, "Secreted amyloid  $\beta$ -proteins in a cell culture model include N-terminally extended peptides that impair synaptic plasticity," *Biochemistry*, vol. 53, no. 24, pp. 3908–3921, 2014.
- [47] B. Olsson, R. Lautner, U. Andreasson, A. Öhrfelt, E. Portelius, M. Bjerke, M. Hölttä, C. Rosén, C. Olsson, G. Strobel, E. Wu, K. Dakin, M. Petzold, K. Blennow, and H. Zetterberg, "CSF and blood biomarkers for the diagnosis of Alzheimer's disease: a systematic review and meta-analysis," *Lancet. Neurol.*, vol. 15, no. 7, pp. 673–684, 2016.
- [48] D. Puzzo, L. Privitera, E. Leznik, M. Fà, A. Staniszewski, A. Palmeri, and O. Arancio, "Picomolar amyloid-beta positively modulates synaptic plasticity and memory in hippocampus," *J. Neurosci.*, vol. 28, no. 53, pp. 14537–14545, 2008.

- 
- [49] B. Rumble, R. Retallack, C. Hilbich, G. Simms, G. Multhaup, R. Martins, A. Hockey, P. Montgomery, K. Beyreuther, and C. L. Masters, "Amyloid A4 protein and its precursor in Down's syndrome and Alzheimer's disease.," *N. Engl. J. Med.*, vol. 320, no. 22, pp. 1446–1452, 1989.
- [50] D. R. Gustafson, I. Skoog, L. Rosengren, H. Zetterberg, and K. Blennow, "Cerebrospinal fluid beta-amyloid 1-42 concentration may predict cognitive decline in older women.," *J. Neurol. Neurosurg. Psychiatry*, vol. 78, no. 5, pp. 461–464, 2007.
- [51] R. Lautner, P. S. Insel, T. Skillbäck, B. Olsson, M. Landén, G. B. Frisoni, S.-K. Herukka, H. Hampel, A. Wallin, L. Minthon, O. Hansson, K. Blennow, N. Mattsson, and H. Zetterberg, "Preclinical effects of APOE  $\epsilon$ 4 on cerebrospinal fluid A $\beta$ 42 concentrations," *Alzheimers. Res. Ther.*, vol. 9, no. 1, p. 87, 2017.
- [52] D. Puzzo, L. Privitera, and A. Palmeri, "Hormetic effect of amyloid- $\beta$  peptide in synaptic plasticity and memory.," *Neurobiol. Aging*, vol. 33, no. 7, pp. 1484.e15–24, 2012.
- [53] K. Zou, J.-S. Gong, K. Yanagisawa, and M. Michikawa, "A novel function of monomeric amyloid beta-protein serving as an antioxidant molecule against metal-induced oxidative damage," *J. Neurosci.*, vol. 22, no. 12, pp. 4833–4841, 2002.
- [54] S. J. Soscia, J. E. Kirby, K. J. Washicosky, S. M. Tucker, M. Ingelsson, B. Hyman, M. A. Burton, L. E. Goldstein, S. Duong, R. E. Tanzi, and R. D. Moir, "The Alzheimer's disease-associated amyloid beta-protein is an antimicrobial peptide.," *PLoS One*, vol. 5, no. 3, p. e9505, 2010.
- [55] A. Pajoohesh-Ganji, M. P. Burns, S. Pal-Ghosh, G. Tadvalkar, N. G. Hokenbury, M. A. Stepp, and A. I. Faden, "Inhibition of amyloid precursor protein secretases reduces recovery after spinal cord injury," *Brain Res.*, vol. 1560, pp. 73–82, 2014.
- [56] M. G. Zagorski, J. Yang, H. Shao, K. Ma, H. Zeng, and A. Hong, "Methodological and chemical factors affecting amyloid beta peptide amyloidogenicity.," *Methods Enzymol.*, vol. 309, pp. 189–204, 1999.
- [57] P. Walsh, D. Bursac, Y. C. Law, D. Cyr, and T. Lithgow, "The J-protein family: modulating protein assembly, disassembly and translocation.," *EMBO Rep.*, vol. 5, no. 6, pp. 567–571, 2004.
- [58] X.-B. Qiu, Y.-M. Shao, S. Miao, and L. Wang, "The diversity of the DnaJ/Hsp40 family, the crucial partners for Hsp70 chaperones.," *Cell. Mol. Life Sci.*, vol. 63, no. 22, pp. 2560–2570, 2006.
- [59] J.-Z. Chuang, H. Zhou, M. Zhu, S.-H. Li, X.-J. Li, and C.-H. Sung, "Characterization of a Brain-enriched Chaperone, MRJ, That Inhibits Huntingtin Aggregation and Toxicity Independently\*," *J. Biol. Chem.*, vol. 277, no. 22, pp. 19831–19838, 2002.
- [60] C.-Y. Fan, S. Lee, and D. M. Cyr, "Mechanisms for regulation of Hsp70 function by Hsp40.," *Cell Stress Chaperones*, vol. 8, no. 4, pp. 309–316, 2003.
- [61] K. Ohtsuka and M. Hata, "Molecular chaperone function of mammalian Hsp70 and Hsp40—a review.," *Int. J. Hyperth. Off. J. Eur. Soc. Hyperthermic Oncol. North Am. Hyperth. Gr.*, vol. 16, no. 3, pp. 231–245, 2000.

- [62] J. Hageman, M. A. Rujano, M. A. W. H. van Waarde, V. Kakkar, R. P. Dirks, N. Govorukhina, H. M. J. Oosterveld-Hut, N. H. Lubsen, and H. H. Kampinga, "A DNAJB chaperone subfamily with HDAC-dependent activities suppresses toxic protein aggregation.," *Mol. Cell*, vol. 37, no. 3, pp. 355–369, 2010.
- [63] C. Månsson, V. Kakkar, E. Monsellier, Y. Sourigues, J. Härmark, H. H. Kampinga, R. Melki, and C. Emanuelsson, "DNAJB6 is a peptide-binding chaperone which can suppress amyloid fibrillation of polyglutamine peptides at substoichiometric molar ratios.," *Cell Stress Chaperones*, vol. 19, no. 2, pp. 227–239, 2014.
- [64] V. Kakkar, C. Månsson, E. P. de Mattos, S. Bergink, M. van der Zwaag, M. A. W. H. van Waarde, N. J. Kloosterhuis, R. Melki, R. T. P. van Cruchten, S. Al-Karadaghi, P. Arosio, C. M. Dobson, T. P. J. Knowles, G. P. Bates, J. M. van Deursen, S. Linse, B. van de Sluis, C. Emanuelsson, and H. H. Kampinga, "The S/T-Rich Motif in the DNAJB6 Chaperone Delays Polyglutamine Aggregation and the Onset of Disease in a Mouse Model," *Mol. Cell*, vol. 62, no. 2, pp. 272–283, 2016.
- [65] C. Rodríguez-González, S. Lin, S. Arkan, and C. Hansen, "Co-chaperones DNAJA1 and DNAJB6 are critical for regulation of polyglutamine aggregation," *Sci. Rep.*, vol. 10, no. 1, p. 8130, 2020.
- [66] A. Thiruvalluvan, E. P. de Mattos, J. F. Brunsting, R. Bakels, D. Serlidaki, L. Barazzuol, P. Conforti, A. Fatima, S. Koyuncu, E. Cattaneo, D. Vilchez, S. Bergink, E. H. W. G. Boddeke, S. Copray, and H. H. Kampinga, "DNAJB6, a Key Factor in Neuronal Sensitivity to Amyloidogenesis.," *Mol. Cell*, vol. 78, no. 2, pp. 346–358.e9, 2020.
- [67] F. A. Aprile, E. Källstig, G. Limorenko, M. Vendruscolo, D. Ron, and C. Hansen, "The molecular chaperones DNAJB6 and Hsp70 cooperate to suppress  $\alpha$ -synuclein aggregation," *Sci. Rep.*, vol. 7, no. 1, p. 9039, 2017.
- [68] N. Deshayes, S. Arkan, and C. Hansen, "The Molecular Chaperone DNAJB6, but Not DNAJB1, Suppresses the Seeded Aggregation of Alpha-Synuclein in Cells," *Int. J. Mol. Sci.*, vol. 20, no. 18, p. 4495, 2019.
- [69] N. Österlund, M. Lundqvist, L. L. Ilag, A. Gräslund, and C. Emanuelsson, "Amyloid- $\beta$  oligomers are captured by the DNAJB6 chaperone: Direct detection of interactions that can prevent primary nucleation," *J. Biol. Chem.*, vol. 295, no. 24, pp. 8135–8144, 2020.
- [70] C. Månsson, P. Arosio, R. Hussein, H. H. Kampinga, R. M. Hashem, W. C. Boelens, C. M. Dobson, T. P. J. Knowles, S. Linse, and C. Emanuelsson, "Interaction of the molecular chaperone DNAJB6 with growing amyloid-beta 42 (A $\beta$ 42) aggregates leads to sub-stoichiometric inhibition of amyloid formation.," *J. Biol. Chem.*, vol. 289, no. 45, pp. 31066–31076, 2014.
- [71] C. Månsson, R. T. P. van Cruchten, U. Weininger, X. Yang, R. Cukalevski, P. Arosio, C. M. Dobson, T. Knowles, M. Akke, S. Linse, and C. Emanuelsson, "Conserved S/T Residues of the Human Chaperone DNAJB6 Are Required for Effective Inhibition of A $\beta$ 42 Amyloid Fibril Formation," *Biochemistry*, vol. 57, no. 32, pp. 4891–4902, 2018.

- 
- [72] T. K. Karamanos, V. Tugarinov, and G. M. Clore, "Unraveling the structure and dynamics of the human DNAJB6b chaperone by NMR reveals insights into Hsp40-mediated proteostasis," *Proc. Natl. Acad. Sci.*, vol. 116, no. 43, pp. 21529–21538, 2019.
- [73] C. A. G. Söderberg, C. Månsson, K. Bernfur, G. Rutsdottir, J. Härmark, S. Rajan, S. Al-Karadaghi, M. Rasmussen, P. Höjrup, H. Hebert, and C. Emanuelsson, "Structural modelling of the DNAJB6 oligomeric chaperone shows a peptide-binding cleft lined with conserved S/T-residues at the dimer interface," *Sci. Rep.*, vol. 8, no. 1, p. 5199, 2018.
- [74] M. Pellecchia, T. Szyperski, D. Wall, C. Georgopoulos, and K. Wüthrich, "NMR Structure of the J-domain and the Gly/Phe-rich Region of the Escherichia coli DnaJ Chaperone," *J. Mol. Biol.*, vol. 260, no. 2, pp. 236–250, 1996.
- [75] R. B. Chan, T. G. Oliveira, E. P. Cortes, L. S. Honig, K. E. Duff, S. A. Small, M. R. Wenk, G. Shui, and G. Di Paolo, "Comparative Lipidomic Analysis of Mouse and Human Brain with Alzheimer Disease \*," *J. Biol. Chem.*, vol. 287, no. 4, pp. 2678–2688, 2012.
- [76] G. W. Feigenson, "Phase diagrams and lipid domains in multicomponent lipid bilayer mixtures," *Biochim. Biophys. Acta - Biomembr.*, vol. 1788, no. 1, pp. 47–52, 2009.
- [77] H. Reiber, "Proteins in cerebrospinal fluid and blood: barriers, CSF flow rate and source-related dynamics," *Restor. Neurol. Neurosci.*, vol. 21, no. 3-4, pp. 79–96, 2003.
- [78] V. Leinonen, R. Vanninen, and T. Rauramaa, "Cerebrospinal fluid circulation and hydrocephalus," *Handb. Clin. Neurol.*, vol. 145, pp. 39–50, 2017.
- [79] D. N. Irani, "Properties and Composition of Normal Cerebrospinal Fluid," *Cerebrospinal Fluid Clin. Pract.*, pp. 69–89, 2009.
- [80] R. Frankel, M. Törnquist, G. Meisl, O. Hansson, U. Andreasson, H. Zetterberg, K. Blennow, B. Frohm, T. Cedervall, T. P. Knowles, T. Leiding, and S. Linse, "Autocatalytic amplification of Alzheimer-associated A $\beta$ 42 peptide aggregation in human cerebrospinal fluid," *Commun. Biol.*, vol. 2, no. 1, pp. 1–11, 2019.
- [81] E. R. Padayachee, H. Zetterberg, E. Portelius, J. Borén, J. L. Molinuevo, N. Andreasen, R. Cukalevski, S. Linse, K. Blennow, and U. Andreasson, "Cerebrospinal fluid-induced retardation of amyloid  $\beta$  aggregation correlates with Alzheimer's disease and the APOE  $\epsilon$ 4 allele," *Brain Res.*, vol. 1651, pp. 11–16, 2016.
- [82] A. R. Koudinov, N. V. Koudinova, A. Kumar, R. C. Beavis, and J. Ghiso, "Biochemical characterization of Alzheimer's soluble amyloid beta protein in human cerebrospinal fluid: Association with high density lipoproteins," *Biochem. Biophys. Res. Commun.*, vol. 223, no. 3, pp. 592–597, 1996.
- [83] A. Merched, Y. Xia, S. Visvikis, J. M. Serot, and G. Siest, "Decreased high-density lipoprotein cholesterol and serum apolipoprotein AI concentrations are highly correlated with the severity of Alzheimer's disease," *Neurobiol. Aging*, vol. 21, no. 1, pp. 27–30, 2000.

- [84] S. Stukas, J. Robert, and C. L. Wellington, "High-density lipoproteins and cerebrovascular integrity in Alzheimer's disease," *Cell Metab.*, vol. 19, no. 4, pp. 574–591, 2014.
- [85] D. F. Evans and H. Wennerström, *The Colloidal Domain: Where Physics, Chemistry, Biology, and Technology Meet*. New York: Wiley-VCH, 2nd editio ed., 1999.
- [86] K. A. Dill, "Dominant forces in protein folding,," *Biochemistry*, vol. 29, no. 31, pp. 7133–7155, 1990.
- [87] R. L. Baldwin, "Energetics of Protein Folding," *J. Mol. Biol.*, vol. 371, no. 2, pp. 283–301, 2007.
- [88] E. Y. Chi, S. Krishnan, T. W. Randolph, and J. F. Carpenter, "Physical stability of proteins in aqueous solution: mechanism and driving forces in nonnative protein aggregation,," *Pharm. Res.*, vol. 20, no. 9, pp. 1325–1336, 2003.
- [89] C. M. Dobson, A. Šali, and M. Karplus, "Protein Folding: A Perspective from Theory and Experiment,," *Angew. Chem. Int. Ed. Engl.*, vol. 37, no. 7, pp. 868–893, 1998.
- [90] C. M. Dobson, "Protein folding and misfolding," *Nature*, vol. 426, no. 6968, pp. 884–890, 2003.
- [91] C. B. Anfinsen, "Principles that govern the folding of protein chains,," *Science*, vol. 181, no. 4096, pp. 223–230, 1973.
- [92] A. J. Baldwin, T. P. J. Knowles, G. G. Tartaglia, A. W. Fitzpatrick, G. L. Devlin, S. L. Shammass, C. A. Waudby, M. F. Mossuto, S. Meehan, S. L. Gras, J. Christodoulou, S. J. Anthony-Cahill, P. D. Barker, M. Vendruscolo, and C. M. Dobson, "Metastability of native proteins and the phenomenon of amyloid formation,," *J. Am. Chem. Soc.*, vol. 133, no. 36, pp. 14160–14163, 2011.
- [93] E. Gazit, "The "Correctly Folded" state of proteins: is it a metastable state?," *Angew. Chem. Int. Ed. Engl.*, vol. 41, no. 2, pp. 257–259, 2002.
- [94] R. N. Rambaran and L. C. Serpell, "Amyloid fibrils: abnormal protein assembly,," *Prion*, vol. 2, no. 3, pp. 112–117, 2008.
- [95] J. D. Sipe and A. S. Cohen, "Review: history of the amyloid fibril,," *J. Struct. Biol.*, vol. 130, no. 2-3, pp. 88–98, 2000.
- [96] R. Wetzel, "Amyloid," *Encycl. Biol. Chem. Second Ed.*, vol. 1, pp. 100–104, 2013.
- [97] J. N. Buxbaum and R. P. Linke, "A molecular history of the amyloidoses,," *J. Mol. Biol.*, vol. 421, no. 2-3, pp. 142–159, 2012.
- [98] H. Naiki, K. Higuchi, M. Hosokawa, and T. Takeda, "Fluorometric determination of amyloid fibrils in vitro using the fluorescent dye, thioflavin T1,," *Anal. Biochem.*, vol. 177, no. 2, pp. 244–249, 1989.
- [99] T. Klingstedt, A. Aslund, R. A. Simon, L. B. G. Johansson, J. J. Mason, S. Nyström, P. Hammarström, and K. P. R. Nilsson, "Synthesis of a library of oligothiophenes and their utilization as fluorescent ligands for spectral assignment of protein aggregates,," *Org. Biomol. Chem.*, vol. 9, no. 24, pp. 8356–8370, 2011.

- 
- [100] K. P. R. Nilsson, M. Lindgren, and P. Hammarström, "Luminescent-Conjugated Oligothiophene Probe Applications for Fluorescence Imaging of Pure Amyloid Fibrils and Protein Aggregates in Tissues.," *Methods Mol. Biol.*, vol. 1779, pp. 485–496, 2018.
- [101] E. D. Eanes and G. G. Glenner, "X-ray diffraction studies on amyloid filaments.," *J. Histochem. Cytochem.*, vol. 16, no. 11, pp. 673–677, 1968.
- [102] K. Klement, K. Wieligmann, J. Meinhardt, P. Hortschansky, W. Richter, and M. Fändrich, "Effect of different salt ions on the propensity of aggregation and on the structure of Alzheimer's abeta(1-40) amyloid fibrils.," *J. Mol. Biol.*, vol. 373, no. 5, pp. 1321–1333, 2007.
- [103] T. P. J. Knowles, J. F. Smith, A. Craig, C. M. Dobson, and M. E. Welland, "Spatial Persistence of Angular Correlations in Amyloid Fibrils," *Phys. Rev. Lett.*, vol. 96, no. 23, p. 238301, 2006.
- [104] H. H. Bauer, U. Aebi, M. Häner, R. Hermann, M. Müller, and H. P. Merkle, "Architecture and polymorphism of fibrillar supramolecular assemblies produced by in vitro aggregation of human calcitonin.," *J. Struct. Biol.*, vol. 115, no. 1, pp. 1–15, 1995.
- [105] T. Watanabe-Nakayama, K. Ono, M. Itami, R. Takahashi, D. B. Teplow, and M. Yamada, "High-speed atomic force microscopy reveals structural dynamics of amyloid  $\beta$ 1-42 aggregates.," *Proc. Natl. Acad. Sci. U. S. A.*, vol. 113, no. 21, pp. 5835–5840, 2016.
- [106] J. Meinhardt, C. Sachse, P. Hortschansky, N. Grigorieff, and M. Fändrich, "Abeta(1-40) fibril polymorphism implies diverse interaction patterns in amyloid fibrils.," *J. Mol. Biol.*, vol. 386, no. 3, pp. 869–877, 2009.
- [107] M. Fändrich, J. Meinhardt, and N. Grigorieff, "Structural polymorphism of Alzheimer Abeta and other amyloid fibrils.," *Prion*, vol. 3, no. 2, pp. 89–93, 2009.
- [108] A. J. Geddes, K. D. Parker, E. D. T. Atkins, and E. Beighton, "'Cross- $\beta$ ' conformation in proteins," *J. Mol. Biol.*, vol. 32, no. 2, pp. 343–358, 1968.
- [109] A. V. Kajava, J. M. Squire, and D. A. D. Parry, "Beta-structures in fibrous proteins.," *Adv. Protein Chem.*, vol. 73, pp. 1–15, 2006.
- [110] J. L. Jiménez, E. J. Nettleton, M. Bouchard, C. V. Robinson, C. M. Dobson, and H. R. Saibil, "The protofilament structure of insulin amyloid fibrils," *Proc. Natl. Acad. Sci. U. S. A.*, vol. 99, no. 14, pp. 9196–9201, 2002.
- [111] B. H. Toyama and J. S. Weissman, "Amyloid structure: conformational diversity and consequences.," *Annu. Rev. Biochem.*, vol. 80, pp. 557–585, 2011.
- [112] F. Chiti and C. M. Dobson, "Protein Misfolding, Functional Amyloid, and Human Disease," *Annu. Rev. Biochem.*, vol. 75, no. 1, pp. 333–366, 2006.
- [113] F. Chiti and C. M. Dobson, "Protein Misfolding, Amyloid Formation, and Human Disease: A Summary of Progress Over the Last Decade," *Annu. Rev. Biochem.*, vol. 86, no. 1, pp. 27–68, 2017.

- [114] M. Fändrich and C. M. Dobson, "The behaviour of polyamino acids reveals an inverse side chain effect in amyloid structure formation," *EMBO J.*, vol. 21, no. 21, pp. 5682–5690, 2002.
- [115] C. M. Dobson, "Protein misfolding, evolution and disease," *Trends Biochem. Sci.*, vol. 24, no. 9, pp. 329–332, 1999.
- [116] F. Chiti, M. Stefani, N. Taddei, G. Ramponi, and C. M. Dobson, "Rationalization of the effects of mutations on peptide and protein aggregation rates," *Nature*, vol. 424, no. 6950, pp. 805–808, 2003.
- [117] C. M. Dobson, "The structural basis of protein folding and its links with human disease," *Philos. Trans. R. Soc. Lond. B. Biol. Sci.*, vol. 356, no. 1406, pp. 133–145, 2001.
- [118] G. Meisl, X. Yang, B. Frohm, T. P. J. Knowles, and S. Linse, "Quantitative analysis of intrinsic and extrinsic factors in the aggregation mechanism of Alzheimer-associated A $\beta$ -peptide," *Sci. Rep.*, vol. 6, no. 1, p. 18728, 2016.
- [119] G. Meisl, X. Yang, C. M. Dobson, S. Linse, and T. P. J. Knowles, "Modulation of electrostatic interactions to reveal a reaction network unifying the aggregation behaviour of the A $\beta$ 42 peptide and its variants," *Chem. Sci.*, vol. 8, no. 6, pp. 4352–4362, 2017.
- [120] A. Abelein, J. Jarvet, A. Barth, A. Gräslund, and J. Danielsson, "Ionic Strength Modulation of the Free Energy Landscape of A $\beta$ 40 Peptide Fibril Formation," *J. Am. Chem. Soc.*, vol. 138, no. 21, pp. 6893–6902, 2016.
- [121] Y. Kusumoto, A. Lomakin, D. B. Teplow, and G. B. Benedek, "Temperature dependence of amyloid  $\beta$ -protein fibrillization," *Proc. Natl. Acad. Sci.*, vol. 95, no. 21, pp. 12277 LP – 12282, 1998.
- [122] S. I. A. Cohen, R. Cukalevski, T. C. T. Michaels, A. Šarić, M. Törnquist, M. Vendruscolo, C. M. Dobson, A. K. Buell, T. P. J. Knowles, and S. Linse, "Distinct thermodynamic signatures of oligomer generation in the aggregation of the amyloid- $\beta$  peptide," *Nat. Chem.*, vol. 10, no. 5, pp. 523–531, 2018.
- [123] X. Yang, G. Meisl, B. Frohm, E. Thulin, T. P. J. Knowles, and S. Linse, "On the role of sidechain size and charge in the aggregation of A $\beta$ 42 with familial mutations," *Proc. Natl. Acad. Sci.*, vol. 115, no. 26, pp. E5849 LP – E5858, 2018.
- [124] L. Hou, I. Kang, R. E. Marchant, and M. G. Zagorski, "Methionine 35 oxidation reduces fibril assembly of the amyloid abeta-(1-42) peptide of Alzheimer's disease," *J. Biol. Chem.*, vol. 277, no. 43, pp. 40173–40176, 2002.
- [125] M. Palmblad, A. Westlind-Danielsson, and J. Bergquist, "Oxidation of methionine 35 attenuates formation of amyloid beta -peptide 1-40 oligomers," *J. Biol. Chem.*, vol. 277, no. 22, pp. 19506–19510, 2002.
- [126] F. Misiti, M. E. Clementi, and B. Giardina, "Oxidation of methionine 35 reduces toxicity of the amyloid beta-peptide(1-42) in neuroblastoma cells (IMR-32) via enzyme methionine sulfoxide reductase A expression and function," *Neurochem. Int.*, vol. 56, no. 4, pp. 597–602, 2010.

- 
- [127] P. Maiti, R. Piacentini, C. Ripoli, C. Grassi, and G. Bitan, "Surprising toxicity and assembly behaviour of amyloid  $\beta$ -protein oxidized to sulfone.," *Biochem. J.*, vol. 433, no. 2, pp. 323–332, 2011.
- [128] S. Kumar, N. Rezaei-Ghaleh, D. Terwel, D. R. Thal, M. Richard, M. Hoch, J. M. McDonald, U. Wüllner, K. Glebov, M. T. Heneka, D. M. Walsh, M. Zweckstetter, and J. Walter, "Extracellular phosphorylation of the amyloid  $\beta$ -peptide promotes formation of toxic aggregates during the pathogenesis of Alzheimer's disease.," *EMBO J.*, vol. 30, no. 11, pp. 2255–2265, 2011.
- [129] Y. Bouter, K. Dietrich, J. L. Wittnam, N. Rezaei-Ghaleh, T. Pillot, S. Papot-Couturier, T. Lefebvre, F. Sprenger, O. Wirths, M. Zweckstetter, and T. A. Bayer, "N-truncated amyloid  $\beta$  (A $\beta$ ) 4–42 forms stable aggregates and induces acute and long-lasting behavioral deficits.," *Acta Neuropathol.*, vol. 126, no. 2, pp. 189–205, 2013.
- [130] T. Weiffert, G. Meisl, P. Flagmeier, S. De, C. J. R. Dunning, B. Frohm, H. Zetterberg, K. Blennow, E. Portelius, D. Klenerman, C. M. Dobson, T. P. J. Knowles, and S. Linse, "Increased Secondary Nucleation Underlies Accelerated Aggregation of the Four-Residue N-Terminally Truncated A $\beta$ 42 Species A $\beta$ 5–42.," *ACS Chem. Neurosci.*, vol. 10, no. 5, pp. 2374–2384, 2019.
- [131] M. P. Kummer, M. Hermes, A. Delekarte, T. Hammerschmidt, S. Kumar, D. Terwel, J. Walter, H.-C. Pape, S. König, S. Roeber, F. Jessen, T. Klockgether, M. Korte, and M. T. Heneka, "Nitration of tyrosine 10 critically enhances amyloid  $\beta$  aggregation and plaque formation.," *Neuron*, vol. 71, no. 5, pp. 833–844, 2011.
- [132] R. L. Williamson, K. Laulagnier, A. M. Miranda, M. A. Fernandez, M. S. Wolfe, R. Sadoul, and G. Di Paolo, "Disruption of amyloid precursor protein ubiquitination selectively increases amyloid  $\beta$  (A $\beta$ ) 40 levels via presenilin 2-mediated cleavage.," *J. Biol. Chem.*, vol. 292, no. 48, pp. 19873–19889, 2017.
- [133] Y.-Q. Zhang and K. D. Sarge, "Sumoylation of amyloid precursor protein negatively regulates Abeta aggregate levels.," *Biochem. Biophys. Res. Commun.*, vol. 374, no. 4, pp. 673–678, 2008.
- [134] S. Raimondi, F. Guglielmi, S. Giorgetti, S. Di Gaetano, A. Arciello, D. M. Monti, A. Relini, D. Nichino, S. M. Doglia, A. Natalello, P. Pucci, P. Mangione, L. Obici, G. Merlini, M. Stoppini, P. Robustelli, G. G. Tartaglia, M. Vendruscolo, C. M. Dobson, R. Piccoli, and V. Bellotti, "Effects of the known pathogenic mutations on the aggregation pathway of the amyloidogenic peptide of apolipoprotein A-I.," *J. Mol. Biol.*, vol. 407, no. 3, pp. 465–476, 2011.
- [135] O. Gursky, X. Mei, and D. Atkinson, "The crystal structure of the C-terminal truncated apolipoprotein A-I sheds new light on amyloid formation by the N-terminal fragment," *Biochemistry*, vol. 51, no. 1, pp. 10–18, 2012.
- [136] J. J. De Yoreo and P. G. Vekilov, "Principles of Crystal Nucleation and Growth," *Rev. Mineral. Geochemistry*, vol. 54, no. 1, pp. 57–93, 2003.
- [137] G. Meisl, X. Yang, E. Hellstrand, B. Frohm, J. B. Kirkegaard, S. I. Cohen, C. M. Dobson, S. Linse, and T. P. Knowles, "Differences in nucleation behavior underlie the

- contrasting aggregation kinetics of the A $\beta$ 40 and A $\beta$ 42 peptides,” *Proc. Natl. Acad. Sci. U. S. A.*, vol. 111, no. 26, pp. 9384–9389, 2014.
- [138] S. I. Cohen, S. Linse, L. M. Luheshi, E. Hellstrand, D. A. White, L. Rajah, D. E. Otzen, M. Vendruscolo, C. M. Dobson, and T. P. Knowles, “Proliferation of amyloid- $\beta$ 42 aggregates occurs through a secondary nucleation mechanism,” *Proc. Natl. Acad. Sci. U. S. A.*, vol. 110, no. 24, pp. 9758–9763, 2013.
- [139] R. Gaspar, G. Meisl, A. K. Buell, L. Young, C. F. Kaminski, T. P. J. Knowles, E. Sparr, and S. Linse, “Secondary nucleation of monomers on fibril surface dominates  $\alpha$ -synuclein aggregation and provides autocatalytic amyloid amplification,” *Q. Rev. Biophys.*, vol. 50, p. e6, 2017.
- [140] S. I. Cohen, M. Vendruscolo, C. M. Dobson, and T. P. Knowles, “Nucleated polymerization with secondary pathways. II. Determination of self-consistent solutions to growth processes described by non-linear master equations,” *J. Chem. Phys.*, vol. 135, no. 6, 2011.
- [141] G. Meisl, J. B. Kirkegaard, P. Arosio, T. C. Michaels, M. Vendruscolo, C. M. Dobson, S. Linse, and T. P. Knowles, “Molecular mechanisms of protein aggregation from global fitting of kinetic models,” *Nat. Protoc.*, vol. 11, no. 2, pp. 252–272, 2016.
- [142] L. Michaelis and M. L. Menten, “Die Kinetik der Invertinwirkung,” *Biochem. Z.*, vol. 49, pp. 333–369, 1913.
- [143] M. M. M. Wilhelmus, R. M. W. de Waal, and M. M. Verbeek, “Heat shock proteins and amateur chaperones in amyloid-Beta accumulation and clearance in Alzheimer’s disease,” *Mol. Neurobiol.*, vol. 35, no. 3, pp. 203–216, 2007.
- [144] H. Willander, E. Hermansson, J. Johansson, and J. Presto, “BRICHOS domain associated with lung fibrosis, dementia and cancer—a chaperone that prevents amyloid fibril formation?,” *FEBS J.*, vol. 278, no. 20, pp. 3893–3904, 2011.
- [145] H. Willander, J. Presto, G. Askarieh, H. Biverstål, B. Frohm, S. D. Knight, J. Johansson, and S. Linse, “BRICHOS Domains Efficiently Delay Fibrillation of Amyloid  $\beta$ -Peptide \*,” *J. Biol. Chem.*, vol. 287, no. 37, pp. 31608–31617, 2012.
- [146] S. I. A. Cohen, P. Arosio, J. Presto, F. R. Kurudenkandy, H. Biverstål, L. Dölfe, C. Dunning, X. Yang, B. Frohm, M. Vendruscolo, J. Johansson, C. M. Dobson, A. Fisahn, T. P. J. Knowles, and S. Linse, “A molecular chaperone breaks the catalytic cycle that generates toxic A $\beta$  oligomers,” *Nat. Struct. Mol. Biol.*, vol. 22, no. 3, pp. 207–213, 2015.
- [147] D. Chandler, “Interfaces and the driving force of hydrophobic assembly,” *Nature*, vol. 437, no. 7059, pp. 640–647, 2005.
- [148] M. Langecker, V. Arnaut, J. List, and F. C. Simmel, “DNA nanostructures interacting with lipid bilayer membranes,” *Acc. Chem. Res.*, vol. 47, no. 6, pp. 1807–1815, 2014.
- [149] O. Zumbuehl and H. G. Weder, “Liposomes of controllable size in the range of 40 to 180 nm by defined dialysis of lipid/detergent mixed micelles,” *Biochim. Biophys. Acta*, vol. 640, no. 1, pp. 252–262, 1981.

- 
- [150] C. E. Matz and A. Jonas, "Micellar complexes of human apolipoprotein A-I with phosphatidylcholines and cholesterol prepared from cholate-lipid dispersions.," *J. Biol. Chem.*, vol. 257, no. 8, pp. 4535–4540, 1982.
- [151] J. H. Ipsen, G. Karlström, O. G. Mouritsen, H. Wennerström, and M. J. Zuckermann, "Phase equilibria in the phosphatidylcholine-cholesterol system.," *Biochim. Biophys. Acta*, vol. 905, no. 1, pp. 162–172, 1987.
- [152] C. Galvagnion, A. K. Buell, G. Meisl, T. C. T. Michaels, M. Vendruscolo, T. P. J. Knowles, and C. M. Dobson, "Lipid vesicles trigger  $\alpha$ -synuclein aggregation by stimulating primary nucleation.," *Nat. Chem. Biol.*, vol. 11, no. 3, pp. 229–234, 2015.
- [153] M. Grey, C. J. Dunning, R. Gaspar, C. Grey, P. Brundin, E. Sparr, and S. Linse, "Acceleration of  $\alpha$ -synuclein aggregation by exosomes.," *J. Biol. Chem.*, vol. 290, no. 5, pp. 2969–2982, 2015.
- [154] G. P. Gorbenko and P. K. J. Kinnunen, "The role of lipid-protein interactions in amyloid-type protein fibril formation.," *Chem. Phys. Lipids*, vol. 141, no. 1-2, pp. 72–82, 2006.
- [155] E. Hellstrand, A. Nowacka, D. Topgaard, S. Linse, and E. Sparr, "Membrane Lipid Co-Aggregation with  $\alpha$ -Synuclein Fibrils," *PLoS One*, vol. 8, no. 10, 2013.
- [156] C. Galvagnion, D. Topgaard, K. Makasewicz, A. K. Buell, S. Linse, E. Sparr, and C. M. Dobson, "Lipid Dynamics and Phase Transition within  $\alpha$ -Synuclein Amyloid Fibrils.," *J. Phys. Chem. Lett.*, vol. 10, pp. 7872–7877, dec 2019.
- [157] E. Hellstrand, E. Sparr, and S. Linse, "Retardation of A $\beta$  fibril formation by phospholipid vesicles depends on membrane phase behavior," *Biophys. J.*, vol. 98, no. 10, pp. 2206–2214, 2010.
- [158] J. Habchi, S. Chia, C. Galvagnion, T. C. Michaels, M. M. Bellaiche, F. S. Ruggeri, M. Sanguanini, I. Idini, J. R. Kumita, E. Sparr, S. Linse, C. M. Dobson, T. P. Knowles, and M. Vendruscolo, "Cholesterol catalyses A $\beta$ 42 aggregation through a heterogeneous nucleation pathway in the presence of lipid membranes," *Nat. Chem.*, vol. 10, no. 6, pp. 673–683, 2018.
- [159] C. Soto, "Protein misfolding and disease; protein refolding and therapy.," *FEBS Lett.*, vol. 498, no. 2-3, pp. 204–207, 2001.
- [160] J. Pettersson-Kastberg, S. Aits, L. Gustafsson, A. Mossberg, P. Storm, M. Trulsson, F. Persson, K. H. Mok, and C. Svanborg, "Can misfolded proteins be beneficial? The HAMLET case.," *Ann. Med.*, vol. 41, no. 3, pp. 162–176, 2009.
- [161] P. Westermark, M. D. Benson, J. N. Buxbaum, A. S. Cohen, B. Frangione, S.-I. Ikeda, C. L. Masters, G. Merlini, M. J. Saraiva, and J. D. Sipe, "Amyloid: toward terminology clarification. Report from the Nomenclature Committee of the International Society of Amyloidosis.," *Amyloid Int. J. Exp. Clin. Investig. Off. J. Int. Soc. Amyloidosis*, vol. 12, no. 1, pp. 1–4, 2005.
- [162] M. B. Pepys, "Amyloidosis.," *Annu. Rev. Med.*, vol. 57, pp. 223–241, 2006.

- [163] J. D. Sipe, M. D. Benson, J. N. Buxbaum, S.-i. Ikeda, G. Merlini, M. J. M. Saraiva, and P. Westermark, "Nomenclature 2014: Amyloid fibril proteins and clinical classification of the amyloidosis," *Amyloid*, vol. 21, no. 4, pp. 221–224, 2014.
- [164] O. Gursky, "Structural stability and functional remodeling of high-density lipoproteins," *FEBS Lett.*, vol. 589, no. 19, pp. 2627–2639, 2015.
- [165] Y. Q. Wong, K. J. Binger, G. J. Howlett, and M. D. Griffin, "Methionine oxidation induces amyloid fibril formation by full-length apolipoprotein A-I," *Proc. Natl. Acad. Sci. U. S. A.*, vol. 107, no. 5, pp. 1977–1982, 2010.
- [166] M. G. Sorci-Thomas and M. J. Thomas, "The effects of altered apolipoprotein A-I structure on plasma HDL concentration," *Trends Cardiovasc. Med.*, vol. 12, no. 3, pp. 121–128, 2002.
- [167] M. Das, X. Mei, S. Jayaraman, D. Atkinson, and O. Gursky, "Amyloidogenic mutations in human apolipoprotein A-I are not necessarily destabilizing - a common mechanism of apolipoprotein A-I misfolding in familial amyloidosis and atherosclerosis," *FEBS J.*, vol. 281, no. 11, pp. 2525–2542, 2014.
- [168] A. Arciello, R. Piccoli, and D. M. Monti, "Apolipoprotein A-I: the dual face of a protein," *FEBS Lett.*, vol. 590, no. 23, pp. 4171–4179, 2016.
- [169] P. Scheltens, K. Blennow, M. M. B. Breteler, B. de Strooper, G. B. Frisoni, S. Salloway, and W. M. Van der Flier, "Alzheimer's disease," *Lancet (London, England)*, vol. 388, no. 10043, pp. 505–517, 2016.
- [170] H. Niu, I. Álvarez-Álvarez, F. Guillén-Grima, and I. Aguinaga-Ontoso, "Prevalence and incidence of Alzheimer's disease in Europe: A meta-analysis," *Neurol. (English Ed.)*, vol. 32, no. 8, pp. 523–532, 2017.
- [171] R. Brookmeyer, E. Johnson, K. Ziegler-Graham, and H. M. Arrighi, "Forecasting the global burden of Alzheimer's disease," *Alzheimer's Dement.*, vol. 3, no. 3, pp. 186–191, 2007.
- [172] A. Alzheimer, "Über eine eigenartige Erkrankung der Hirnrinde," *Allg. Zeitschrift für Psychiatr. und Psych. Medizin*, vol. 64, pp. 146–148, 1907.
- [173] R. A. Stelzmann, H. Norman Schnitzlein, and F. Reed Murtagh, "An english translation of alzheimer's 1907 paper, "über eine eigenartige erkankung der hirnrinde", " *Clin. Anat.*, vol. 8, no. 6, pp. 429–431, 1995.
- [174] C. Bancher, C. Brunner, H. Lassmann, H. Budka, K. Jellinger, G. Wiche, F. Seitelberger, I. Grundke-Iqbal, K. Iqbal, and H. M. Wisniewski, "Accumulation of abnormally phosphorylated tau precedes the formation of neurofibrillary tangles in Alzheimer's disease," *Brain Res.*, vol. 477, no. 1-2, pp. 90–99, 1989.
- [175] C. Qiu, M. Kivipelto, and E. von Strauss, "Epidemiology of Alzheimer's disease: occurrence, determinants, and strategies toward intervention," *Dialogues Clin. Neurosci.*, vol. 11, no. 2, pp. 111–128, 2009.
- [176] M. Hoore, S. Khailaie, G. Montaseri, T. Mitra, and M. Meyer-Hermann, "Mathematical Model Shows How Sleep May Affect Amyloid- $\beta$  Fibrillization," *Biophys. J.*, vol. 119, no. 4, pp. 862–872, 2020.

- 
- [177] J.-Y. Lee, S. M. Chang, H.-S. Jang, J. S. Chang, G.-H. Suh, H.-Y. Jung, H.-J. Jeon, and M. J. Cho, "Illiteracy and the incidence of Alzheimer's disease in the Yonchon County survey, Korea.," *Int. psychogeriatrics*, vol. 20, no. 5, pp. 976–985, 2008.
- [178] J. K. Cataldo, J. J. Prochaska, and S. A. Glantz, "Cigarette smoking is a risk factor for Alzheimer's Disease: an analysis controlling for tobacco industry affiliation.," *J. Alzheimers. Dis.*, vol. 19, no. 2, pp. 465–480, 2010.
- [179] M. A. Beydoun, H. A. Beydoun, and Y. Wang, "Obesity and central obesity as risk factors for incident dementia and its subtypes: a systematic review and meta-analysis.," *Obes. Rev.*, vol. 9, no. 3, pp. 204–218, 2008.
- [180] M. Kivipelto, T. Ngandu, L. Fratiglioni, M. Viitanen, I. K  reholt, B. Winblad, E.-L. Helkala, J. Tuomilehto, H. Soininen, and A. Nissinen, "Obesity and vascular risk factors at midlife and the risk of dementia and Alzheimer disease.," *Arch. Neurol.*, vol. 62, no. 10, pp. 1556–1560, 2005.
- [181] J. Poirier, J. Davignon, D. Bouthillier, S. Kogan, P. Bertrand, and S. Gauthier, "Apolipoprotein E polymorphism and Alzheimer's disease.," *Lancet (London, England)*, vol. 342, no. 8873, pp. 697–699, 1993.
- [182] E. H. Corder, A. M. Saunders, W. J. Strittmatter, D. E. Schmechel, P. C. Gaskell, G. W. Small, A. D. Roses, J. L. Haines, and M. A. Pericak-Vance, "Gene dose of apolipoprotein E type 4 allele and the risk of Alzheimer's disease in late onset families.," *Science*, vol. 261, no. 5123, pp. 921–923, 1993.
- [183] C.-C. Liu, T. Kanekiyo, H. Xu, and G. Bu, "Apolipoprotein E and Alzheimer disease: risk, mechanisms and therapy.," 2013.
- [184] R. G. Feldman, K. A. Chandler, L. L. Levy, and G. H. Glaser, "Familial Alzheimer's Disease," *Neurology*, vol. 13, pp. 811–824, 1963.
- [185] E. Head and I. T. Lott, "Down syndrome and beta-amyloid deposition.," *Curr. Opin. Neurol.*, vol. 17, no. 2, pp. 95–100, 2004.
- [186] M. Mullan, F. Crawford, K. Axelman, H. Houlden, L. Lilius, B. Winblad, and L. Lannfelt, "A pathogenic mutation for probable Alzheimer's disease in the APP gene at the N-terminus of beta-amyloid.," *Nat. Genet.*, vol. 1, no. 5, pp. 345–347, 1992.
- [187] M. C. Chartier-Harlin, F. Crawford, H. Houlden, A. Warren, D. Hughes, L. Fidani, A. Goate, M. Rossor, P. Roques, and J. Hardy, "Early-onset Alzheimer's disease caused by mutations at codon 717 of the beta-amyloid precursor protein gene.," *Nature*, vol. 353, no. 6347, pp. 844–846, 1991.
- [188] J. Murrell, M. Farlow, B. Ghetti, and M. D. Benson, "A mutation in the amyloid precursor protein associated with hereditary Alzheimer's disease.," *Science*, vol. 254, no. 5028, pp. 97–99, 1991.
- [189] J. Sevigny, P. Chiao, T. Bussiere, P. H. Weinreb, L. Williams, M. Maier, R. Dunstan, S. Salloway, T. Chen, Y. Ling, J. O'Gorman, F. Qian, M. Arastu, M. Li, S. Chollate, M. S. Brennan, O. Quintero-Monzon, R. H. Scannevin, H. M. Arnold, T. Engber, K. Rhodes, J. Ferrero, Y. Hang, A. Mikulskis, J. Grimm, C. Hock, R. M. Nitsch, and A. Sandrock, "The antibody aducanumab reduces A $\beta$  plaques in Alzheimer's disease," *Nature*, vol. 537, no. 7618, pp. 50–56, 2016.

- [190] P. Cavazzon, "FDA's decision to approve new treatment for Alzheimer's disease.," 2021.
- [191] A. Takashima, T. Honda, K. Yasutake, G. Michel, O. Murayama, M. Murayama, K. Ishiguro, and H. Yamaguchi, "Activation of tau protein kinase I/glycogen synthase kinase-3 $\beta$  by amyloid  $\beta$  peptide (25–35) enhances phosphorylation of tau in hippocampal neurons," *Neurosci. Res.*, vol. 31, no. 4, pp. 317–323, 1998.
- [192] J. A. Hardy and G. A. Higgins, "Alzheimer's disease: the amyloid cascade hypothesis.," *Science*, vol. 256, no. 5054, pp. 184–185, 1992.
- [193] J. Hardy, "The amyloid hypothesis for Alzheimer's disease: a critical reappraisal.," *J. Neurochem.*, vol. 110, no. 4, pp. 1129–1134, 2009.
- [194] J. M. Rozemuller, P. Eikelenboom, F. C. Stam, K. Beyreuther, and C. L. Masters, "A $\beta$  protein in Alzheimer's disease: primary and secondary cellular events in extracellular amyloid deposition.," *J. Neuropathol. Exp. Neurol.*, vol. 48, no. 6, pp. 674–691, 1989.
- [195] J. Hardy and D. Allsop, "Amyloid deposition as the central event in the aetiology of Alzheimer's disease.," *Trends Pharmacol. Sci.*, vol. 12, no. 10, pp. 383–388, 1991.
- [196] A. M. Klein, N. W. Kowall, and R. J. Ferrante, "Neurotoxicity and oxidative damage of beta amyloid 1-42 versus beta amyloid 1-40 in the mouse cerebral cortex.," *Ann. N. Y. Acad. Sci.*, vol. 893, pp. 314–320, 1999.
- [197] T. Iwatsubo, A. Odaka, N. Suzuki, H. Mizusawa, N. Nukina, and Y. Ihara, "Visualization of A beta 42(43) and A beta 40 in senile plaques with end-specific A beta monoclonals: evidence that an initially deposited species is A beta 42(43).," *Neuron*, vol. 13, no. 1, pp. 45–53, 1994.
- [198] W. Michno, K. Blennow, H. Zetterberg, and G. Brinkmalm, "Refining the amyloid  $\beta$  peptide and oligomer fingerprint ambiguities in Alzheimer's disease: Mass spectrometric molecular characterization in brain, cerebrospinal fluid, blood, and plasma," *J. Neurochem.*, vol. n/a, no. n/a, 2021.
- [199] M. P. Lambert, A. K. Barlow, B. A. Chromy, C. Edwards, R. Freed, M. Liosatos, T. E. Morgan, I. Rozovsky, B. Trommer, K. L. Viola, P. Wals, C. Zhang, C. E. Finch, G. A. Krafft, and W. L. Klein, "Diffusible, nonfibrillar ligands derived from A $\beta$ 1-42 are potent central nervous system neurotoxins.," *Proc. Natl. Acad. Sci. U. S. A.*, vol. 95, no. 11, pp. 6448–6453, 1998.
- [200] H. A. Lashuel, D. Hartley, B. M. Petre, T. Walz, and P. T. J. Lansbury, "Neurodegenerative disease: amyloid pores from pathogenic mutations.," *Nature*, vol. 418, no. 6895, p. 291, 2002.
- [201] H. A. Lashuel and P. T. J. Lansbury, "Are amyloid diseases caused by protein aggregates that mimic bacterial pore-forming toxins?," *Q. Rev. Biophys.*, vol. 39, no. 2, pp. 167–201, 2006.
- [202] B. Caughey and P. T. Lansbury, "Protofibrils, pores, fibrils, and neurodegeneration: separating the responsible protein aggregates from the innocent bystanders.," *Annu. Rev. Neurosci.*, vol. 26, pp. 267–298, 2003.

- 
- [203] G. Bitan, M. D. Kirkitadze, A. Lomakin, S. S. Vollers, G. B. Benedek, and D. B. Teplow, "Amyloid beta -protein (Abeta) assembly: Abeta 40 and Abeta 42 oligomerize through distinct pathways.," *Proc. Natl. Acad. Sci. U. S. A.*, vol. 100, no. 1, pp. 330–335, 2003.
- [204] N. Yamamoto, E. Matsubara, S. Maeda, H. Minagawa, A. Takashima, W. Maruyama, M. Michikawa, and K. Yanagisawa, "A ganglioside-induced toxic soluble Abeta assembly. Its enhanced formation from Abeta bearing the Arctic mutation.," *J. Biol. Chem.*, vol. 282, no. 4, pp. 2646–2655, 2007.
- [205] B. A. Chromy, R. J. Nowak, M. P. Lambert, K. L. Viola, L. Chang, P. T. Velasco, B. W. Jones, S. J. Fernandez, P. N. Lacor, P. Horowitz, C. E. Finch, G. A. Krafft, and W. L. Klein, "Self-assembly of Abeta(1-42) into globular neurotoxins.," *Biochemistry*, vol. 42, no. 44, pp. 12749–12760, 2003.
- [206] C. Behl, J. B. Davis, R. Lesley, and D. Schubert, "Hydrogen peroxide mediates amyloid beta protein toxicity.," *Cell*, vol. 77, no. 6, pp. 817–827, 1994.
- [207] C. Behl, "Amyloid beta-protein toxicity and oxidative stress in Alzheimer's disease.," *Cell Tissue Res.*, vol. 290, no. 3, pp. 471–480, 1997.
- [208] J. N. Keller, F. A. Schmitt, S. W. Scheff, Q. Ding, Q. Chen, D. A. Butterfield, and W. R. Markesbery, "Evidence of increased oxidative damage in subjects with mild cognitive impairment.," *Neurology*, vol. 64, no. 7, pp. 1152–1156, 2005.
- [209] R. Kaye, Y. Sokolov, B. Edmonds, T. M. McIntire, S. C. Milton, J. E. Hall, and C. G. Glabe, "Permeabilization of Lipid Bilayers Is a Common Conformation-dependent Activity of Soluble Amyloid Oligomers in Protein Misfolding Diseases\*," *J. Biol. Chem.*, vol. 279, no. 45, pp. 46363–46366, 2004.
- [210] P. T. Wong, J. A. Schauerte, K. C. Wisser, H. Ding, E. L. Lee, D. G. Steel, and A. Gafni, "Amyloid- $\beta$  Membrane Binding and Permeabilization are Distinct Processes Influenced Separately by Membrane Charge and Fluidity," *J. Mol. Biol.*, vol. 386, no. 1, pp. 81–96, 2009.
- [211] R. Friedman, R. Pellarin, and A. Caffisch, "Amyloid Aggregation on Lipid Bilayers and Its Impact on Membrane Permeability," *J. Mol. Biol.*, vol. 387, no. 2, pp. 407–415, 2009.
- [212] M. R. R. de Planque, V. Raussens, S. A. Contera, D. T. S. Rijkers, R. M. J. Liskamp, J.-M. Ruysschaert, J. F. Ryan, F. Separovic, and A. Watts, " $\beta$ -Sheet Structured  $\beta$ -Amyloid(1-40) Perturbs Phosphatidylcholine Model Membranes," *J. Mol. Biol.*, vol. 368, no. 4, pp. 982–997, 2007.
- [213] E. Sparr and S. Linse, "Lipid-protein interactions in amyloid formation," *Biochim. Biophys. Acta - Proteins Proteomics*, vol. 1867, no. 5, pp. 455–457, 2019.
- [214] W. Michno, P. M. Wehrli, H. Zetterberg, K. Blennow, and J. Hanrieder, "GM1 locates to mature amyloid structures implicating a prominent role for glycolipid-protein interactions in Alzheimer pathology.," *Biochim. Biophys. acta. Proteins proteomics*, vol. 1867, no. 5, pp. 458–467, 2019.

- [215] J. Walter and G. van Echten-Deckert, "Cross-talk of membrane lipids and Alzheimer-related proteins," *Mol. Neurodegener.*, vol. 8, no. 1, p. 34, 2013.
- [216] G. Zuliani, M. Cavalieri, M. Galvani, S. Volpato, A. Cherubini, S. Bandinelli, A. M. Corsi, F. Lauretani, J. M. Guralnik, R. Fellin, and L. Ferrucci, "Relationship between low levels of high-density lipoprotein cholesterol and dementia in the elderly. The InChianti study," *J. Gerontol. A. Biol. Sci. Med. Sci.*, vol. 65, no. 5, pp. 559–564, 2010.
- [217] N. M. Armstrong, Y. An, L. Beason-Held, J. Doshi, G. Erus, L. Ferrucci, C. Davatzikos, and S. M. Resnick, "Predictors of neurodegeneration differ between cognitively normal and subsequently impaired older adults," *Neurobiol. Aging*, vol. 75, pp. 178–186, 2019.
- [218] P. Johansson, E. G. Almqvist, M. Bjerke, A. Wallin, J. O. Johansson, U. Andreasson, K. Blennow, H. Zetterberg, and J. Svensson, "Reduced Cerebrospinal Fluid Concentration of Apolipoprotein A-I in Patients with Alzheimer's Disease," *J. Alzheimer's Dis.*, vol. 59, no. 3, pp. 1017–1026, 2017.
- [219] K. Yaffe, E. Barrett-Connor, F. Lin, and D. Grady, "Serum lipoprotein levels, statin use, and cognitive function in older women.," *Arch. Neurol.*, vol. 59, no. 3, pp. 378–384, 2002.
- [220] G. Li, J. B. Shofer, W. A. Kukull, E. R. Peskind, D. W. Tsuang, J. C. S. Breitner, W. McCormick, J. D. Bowen, L. Teri, G. D. Schellenberg, and E. B. Larson, "Serum cholesterol and risk of Alzheimer disease: a community-based cohort study," *Neurology*, vol. 65, no. 7, pp. 1045–1050, 2005.
- [221] E. B. Button, J. Robert, T. M. Caffrey, J. Fan, W. Zhao, and C. L. Wellington, "HDL from an Alzheimer's disease perspective," *Curr. Opin. Lipidol.*, vol. 30, no. 3, pp. 224–234, 2019.
- [222] D. C. Harris, *Quantitative chemical analysis*. New York: W. H. Freeman and Company, 8th ed., 2010.
- [223] C. S. Ho, C. W. K. Lam, M. H. M. Chan, R. C. K. Cheung, L. K. Law, L. C. W. Lit, K. F. Ng, M. W. M. Suen, and H. L. Tai, "Electrospray ionisation mass spectrometry: principles and clinical applications," *Clin. Biochem. Rev.*, vol. 24, no. 1, pp. 3–12, 2003.
- [224] J. Stetefeld, S. A. McKenna, and T. R. Patel, "Dynamic light scattering: a practical guide and applications in biomedical sciences," *Biophys. Rev.*, vol. 8, no. 4, pp. 409–427, 2016.
- [225] S. Brahms and J. Brahms, "Determination of protein secondary structure in solution by vacuum ultraviolet circular dichroism," *J. Mol. Biol.*, vol. 138, no. 2, pp. 149–178, 1980.
- [226] S. M. Kelly, T. J. Jess, and N. C. Price, "How to study proteins by circular dichroism," *Biochim. Biophys. Acta - Proteins Proteomics*, vol. 1751, no. 2, pp. 119–139, 2005.
- [227] N. Greenfield and G. D. Fasman, "Computed Circular Dichroism Spectra for the Evaluation of Protein Conformation," *Biochemistry*, vol. 8, no. 10, pp. 4108–4116, 1969.

- 
- [228] H. LeVine 3rd, "Thioflavine T interaction with synthetic Alzheimer's disease beta-amyloid peptides: detection of amyloid aggregation in solution," *Protein Sci.*, vol. 2, no. 3, pp. 404–410, 1993.
- [229] G. Keliényi, "On the histochemistry of azo group-free thiazole dyes," *J. Histochem. Cytochem.*, vol. 15, no. 3, pp. 172–180, 1967.
- [230] E. Coelho-Cerqueira, A. S. Pinheiro, and C. Follmer, "Pitfalls associated with the use of Thioflavin-T to monitor anti-fibrillogenic activity," *Bioorg. Med. Chem. Lett.*, vol. 24, no. 14, pp. 3194–3198, 2014.
- [231] D. J. Lindberg, A. Wenger, E. Sundin, E. Wesén, F. Westerlund, and E. K. Esbjörner, "Binding of Thioflavin-T to Amyloid Fibrils Leads to Fluorescence Self-Quenching and Fibril Compaction," *Biochemistry*, vol. 56, no. 16, pp. 2170–2174, 2017.
- [232] A. Biancardi, T. Biver, A. Burgalassi, M. Mattonai, F. Secco, and M. Venturini, "Mechanistic aspects of thioflavin-T self-aggregation and DNA binding: evidence for dimer attack on DNA grooves," *Phys. Chem. Chem. Phys.*, vol. 16, no. 37, pp. 20061–20072, 2014.
- [233] G. V. De Ferrari, W. D. Mallender, N. C. Inestrosa, and T. L. Rosenberry, "Thioflavin T is a fluorescent probe of the acetylcholinesterase peripheral site that reveals conformational interactions between the peripheral and acylation sites," *J. Biol. Chem.*, vol. 276, no. 26, pp. 23282–23287, 2001.
- [234] S. Kumar, A. K. Singh, G. Krishnamoorthy, and R. Swaminathan, "Thioflavin T displays enhanced fluorescence selectively inside anionic micelles and mammalian cells," *J. Fluoresc.*, vol. 18, no. 6, pp. 1199–1205, 2008.
- [235] P. K. Singh, S. Murudkar, A. K. Mora, and S. Nath, "Ultrafast torsional dynamics of Thioflavin-T in an anionic cyclodextrin cavity," *J. Photochem. Photobiol. A Chem.*, vol. 298, pp. 40–48, 2015.
- [236] K. Gade Malmos, L. M. Blancas-Mejia, B. Weber, J. Buchner, M. Ramirez-Alvarado, H. Naiki, and D. Otzen, "ThT 101: a primer on the use of thioflavin T to investigate amyloid formation," *Amyloid Int. J. Exp. Clin. Investig. Off. J. Int. Soc. Amyloidosis*, vol. 24, no. 1, pp. 1–16, 2017.
- [237] E. J. Danoff and K. G. Fleming, "Aqueous, Unfolded OmpA Forms Amyloid-Like Fibrils upon Self-Association," *PLoS One*, vol. 10, no. 7, p. e0132301, 2015.
- [238] C. Colliex, "Seeing and measuring with electrons: Transmission electron microscopy today and tomorrow – An introduction," *Comptes Rendus Phys.*, vol. 15, no. 2, pp. 101–109, 2014.
- [239] R. F. Thompson, M. Walker, C. A. Siebert, S. P. Muench, and N. A. Ranson, "An introduction to sample preparation and imaging by cryo-electron microscopy for structural biology," *Methods*, vol. 100, pp. 3–15, 2016.
- [240] J. Dubochet, M. Adrian, J. J. Chang, J. C. Homo, J. Lepault, A. W. McDowell, and P. Schultz, "Cryo-electron microscopy of vitrified specimens," *Q. Rev. Biophys.*, vol. 21, no. 2, pp. 129–228, 1988.

- [241] J. Dubochet and A. W. McDowell, "Vitrification of pure water for electron microscopy," *J. Microsc.*, vol. 124, pp. RP3–RP4, 1981.
- [242] A. Chauhan, T. Pirttilä, P. Mehta, V. P. Chauhan, and H. M. Wisniewski, "Effect of cerebrospinal fluid from normal and Alzheimer's patients with different apolipoprotein E phenotypes on in vitro aggregation of amyloid beta-protein.," *J. Neurol. Sci.*, vol. 141, no. 1-2, pp. 54–58, 1996.
- [243] T. Wisniewski, E. Castano, J. Ghiso, and B. Frangione, "Cerebrospinal fluid inhibits Alzheimer  $\beta$ -amyloid fibril formation in vitro," *Ann. Neurol.*, vol. 34, no. 4, pp. 631–633, 1993.
- [244] A. M. Isaacs, D. B. Senn, M. Yuan, J. P. Shine, and B. A. Yankner, "Acceleration of amyloid beta-peptide aggregation by physiological concentrations of calcium.," *J. Biol. Chem.*, vol. 281, no. 38, pp. 27916–27923, 2006.
- [245] R. Gaglione, K. Pane, E. Dell'Olmo, V. Cafaro, E. Pizzo, G. Olivieri, E. Notomista, and A. Arciello, "Cost-effective production of recombinant peptides in *Escherichia coli*," *N. Biotechnol.*, vol. 51, pp. 39–48, 2019.
- [246] O. Gursky and D. Atkinson, "Thermal unfolding of human high-density apolipoprotein A-1: Implications for a lipid-free molten globular state," *Proc. Natl. Acad. Sci. U. S. A.*, vol. 93, no. 7, pp. 2991–2995, 1996.
- [247] N. Ikon, J. Shearer, J. Liu, J. J. Tran, S. B. Feng, A. Kamei, J. A. Beckstead, R. S. Kiss, P. M. Weers, G. Ren, and R. O. Ryan, "A facile method for isolation of recombinant human apolipoprotein A-I from *E. coli*," *Protein Expr. Purif.*, vol. 134, pp. 18–24, 2017.
- [248] G. Cavigliolo, E. G. Geier, B. Shao, J. W. Heinecke, and M. N. Oda, "Exchange of apolipoprotein A-I between lipid-associated and lipid-free states: a potential target for oxidative generation of dysfunctional high density lipoproteins.," *J. Biol. Chem.*, vol. 285, no. 24, pp. 18847–18857, 2010.
- [249] P. Arosio, T. C. T. Michaels, S. Linse, C. Månsson, C. Emanuelsson, J. Presto, J. Johansson, M. Vendruscolo, C. M. Dobson, and T. P. J. Knowles, "Kinetic analysis reveals the diversity of microscopic mechanisms through which molecular chaperones suppress amyloid formation," *Nat. Commun.*, vol. 7, p. 10948, 2016.
- [250] S. A. Rosú, O. J. Rimoldi, E. D. Prieto, L. M. Curto, J. M. Delfino, N. A. Ramella, and M. A. Tricerri, "Amyloidogenic propensity of a natural variant of human apolipoprotein A-I: Stability and interaction with ligands," *PLoS One*, vol. 10, no. 5, pp. 1–17, 2015.
- [251] A. Witkowski, G. K. Chan, J. C. Boatz, N. J. Li, A. P. Inoue, J. C. Wong, P. C. Van Der Wel, and G. Cavigliolo, "Methionine oxidized apolipoprotein A-I at the crossroads of HDL biogenesis and amyloid formation," *FASEB J.*, vol. 32, no. 6, pp. 3149–3165, 2018.
- [252] A. C. Nestruck, G. Suzue, and Y. L. Marcel, "Studies on the polymorphism of human apolipoprotein A-I," *Biochim. Biophys. Acta (BBA)/Lipids Lipid Metab.*, vol. 617, no. 1, pp. 110–121, 1980.

- 
- [253] J. Genschel, R. Haas, M. J. Pröpsting, and H. H. Schmidt, "Apolipoprotein A-I induced amyloidosis," *FEBS Lett.*, vol. 430, no. 3, pp. 145–149, 1998.



---

**Scientific publications**

---

